Studies of the solution chemistry in the oxidation reaction to produce the one-dimensional partially oxidized bis (oxalato) platinate polymers
by Barbara Jo Keller

A thesis submitted in partial fulfillment of the requirements for the degree of Doctor of Philosophy in Chemistry
Montana State University

Abstract:
When acidic aqueous solutions of bis(oxalato)platinate(l I), [Pt(Ox)2]2", are subjected to oxidation, polymeric chains of the partially oxidized bis(oxalato)platinate salts form. These polymeric chains are one-dimensional conductors with metal-metal bonded platinum atoms. Examination of the solution chemistry involved in this polymerization reaction has been studied. Four distinct solution species have been identified. The average Pt oxidation states in each of these four species are (formula not captured in OCR), respectively. The four species have been assigned chemical formulae. A reaction scheme has been proposed to explain the solution chemistry that occurs to produce each of the four solution species and finally, the polymer itself. The Pt3+ species has been investigated with 195Pt NMR and UV-Vis spectroscopies and been determined to be a dimeric Pt3+ complex,(formula not captured in OCR). An extinction coefficient for the(formula not captured in OCR) complex absorbing at 426 nm has been determined. Verification of this extinction coefficient came from the UV-Vis absorbance data obtained of a solution of polymer, (formula not captured in OCR), dissolved in H2O. An extinction coefficient and a formation constant for the (formula not captured in OCR)- complex absorbing at 510 nm were determined. The observance of consistent formation constants under various reaction conditions support the proposed reaction scheme. The dissolution of the polymer also confirmed the presence of the dimeric Pt3+ species through UV-Vis spectroscopy and 195Pt NMR spectroscopy. Base titrations of the dissolved polymer were utilized to determine pKa values for the dimeric Pt3 complex, (formula not captured in OCR) The values are pKa1 = 3.9 and pKa2 = 5.2. The role of the acid in the polymerization reaction was investigated. pH measurements confirmed that each of the four solution species have different proton requirements. Ranges of proton requirements have been determined for each of the four solution species. In addition, FT-IR spectroscopy has confirmed that protonation of the carbonyl group on the oxalate ligand is occurring. Finally, attempts were made to oxidize bis(malonato)platinate(ll), (formula not captured in OCR) to form a partially oxidized bis(malonato)platinate polymer. The attempts were unsuccessful due to the instability of the dimeric Pt3+ malonate complex.

STUDIES OF THE SOLUTION CHEMISTRY IN THE OXIDATION REACTION TO PRODUCE THE ONE-DIMENSIONAL PARTIALLY OXIDIZED BIS(OXALATO)PLATINATE POLYMERS

by

Barbara Jo Keller

A thesis submitted in partial fulfillment
of the requirements for the degree

of

Doctor of Philosophy

in

Chemistry

MONTANA STATE UNIVERSITY
Bozeman, Montana

August 1995

APPROVAL

of a thesis submitted by

Barbara Jo Keller

This thesis has been read by each member of the thesis committee and has been found to be satisfactory regarding content, English usage, format, citations, bibliographic style, and consistency, and is ready for submission to the College of Graduate Studies.

Dr. Edwin H. Abbott — Edwin H. Abbott (Signature) — 8/25/95 Date

Approved for the Department of Chemistry

Dr. David M. Dooley — David M. Dooley (Signature) — 8/30/95 Date

Approved for the College of Graduate Studies

Dr. Robert Brown — R L Brown (Signature) — 9/8/95 Date

STATEMENT OF PERMISSION TO USE

In presenting this thesis in partial fulfillment of the requirements for a doctoral degree at Montana State University-Bozeman, I agree that the Library shall make it available to borrowers under rules of the Library. I further agree that copying of this thesis is allowable only for scholarly purposes, consistent with "fair use" as prescribed in the U.S. Copyright Law. Requests for extensive copying or reproduction of this thesis should be referred to University Microfilms International, 300 North Zeeb Road, Ann Arbor, Michigan 48106, to whom I have granted "the exclusive right to reproduce and distribute my dissertation in and from microform along with the non-exclusive right to reproduce and distribute my abstract in any format in whole or in part."

Signature Barbara Jo Keller

Date 9/9/95

ACKNOWLEDGEMENTS

I gratefully acknowledge support for this work from funding received as fellowships from the Associated Western Universities and the State of Montana/Department of Energy EPsCOR program. In addition, laboratory space and equipment were provided by the Department of Energy at the Idaho National Engineering Laboratory under the direction of Dr. Eric S. Peterson. I am also grateful for a generous loan of platinum from the Johnson Matthey Corp.

TABLE OF CONTENTS

TABLE OF CONTENTS (continued)

TABLE OF CONTENTS

LIST OF TABLES

LIST OF FIGURES

LIST OF FIGURES (continued)

LIST OF FIGURES (continued)

ABSTRACT

When acidic aqueous solutions of bis(oxalato)platinate(II), $[Pt(ox)_2]^{2-}$, are subjected to oxidation, polymeric chains of the partially oxidized bis(oxalato)platinate salts form. These polymeric chains are one-dimensional conductors with metal-metal bonded platinum atoms. Examination of the solution chemistry involved in this polymerization reaction has been studied. Four distinct solution species have been identified. The average Pt oxidation states in each of these four species are Pt^{3+}, $Pt^{2.67+}$, $Pt^{2.5+}$ and $Pt^{2.4+}$, respectively. The four species have been assigned chemical formulae. A reaction scheme has been proposed to explain the solution chemistry that occurs to produce each of the four solution species and finally, the polymer itself. The Pt^{3+} species has been investigated with ^{195}Pt NMR and UV-Vis spectroscopies and been determined to be a dimeric Pt^{3+} complex, $[Pt(ox)_2]_2^{2-}$. An extinction coefficient for the $[Pt(ox)_2]_2^{2-}$ complex absorbing at 426 nm has been determined. Verification of this extinction coefficient came from the UV-Vis absorbance data obtained of a solution of polymer, $K_{1.6}[Pt(ox)_2]\cdot 2H_2O$, dissolved in H_2O. An extinction coefficient and a formation constant for the $[Pt^{2.67+}(ox)_2]_3^{4-}$ complex absorbing at 510 nm were determined. The observance of consistent formation constants under various reaction conditions support the proposed reaction scheme. The dissolution of the polymer also confirmed the presence of the dimeric Pt^{3+} species through UV-Vis spectroscopy and ^{195}Pt NMR spectroscopy. Base titrations of the dissolved polymer were utilized to determine pK_a values for the dimeric Pt^{3+} complex, $[Pt^{3+}(ox)_2(OH_2)]_2^{2-}$. The values are $pK_{a1} = 3.9$ and $pK_{a2} = 5.2$. The role of the acid in the polymerization reaction was investigated. pH measurements confirmed that each of the four solution species have different proton requirements. Ranges of proton requirements have been determined for each of the four solution species. In addition, FT-IR spectroscopy has confirmed that protonation of the carbonyl group on the oxalate ligand is occurring. Finally, attempts were made to oxidize bis(malonato)platinate(II), $[Pt(mal)_2]^{2-}$, to form a partially oxidized bis(malonato)platinate polymer. The attempts were unsuccessful due to the instability of the dimeric Pt^{3+} malonate complex.

INTRODUCTION

The interest in the one-dimensional partially oxidized platinum complexes has recently increased dramatically. These materials exhibit unique electrical properties in that they conduct electricity in one direction along the Pt-Pt metal chain that extends down the backbone of these materials. It appears that conditions can be found whereby chain length can be controlled. If so, these new polymers could lead to new materials with unique electrical properties. It may also be possible, in the future, to form electrical circuits via chemical reactions and thereby provide an entry into the further miniaturization of electrical circuitry.

To date, only two types of one-dimensional partially oxidized platinum materials have been characterized; the linear chain bis(oxalato)platinate salts and the linear chain tetracyanoplatinate salts (1). A possible third type, partially oxidized bis(squarato)platinate has been reported by Toftlund *et al.* (2, 3) although relatively little has been done to characterize this complex. The properties of these materials in solution have received relatively little attention. This is not surprising since dissolution of the one-dimensional polymeric chains breaks up the chains into much smaller segments which do not necessarily possess the unique properties associated with the long chains. Since metal-metal bonds are quite stable it is reasonable to assume that they will persist in solution. The extent to which they persist, however, is unknown. The colors of the solutions from which these one-dimensional platinum complexes precipitate suggest that a complex

array of materials are present in both the formation of the polymer and in the dissolution of the polymer. A study of these solution species, then, could possibly provide great insight into the reactions that occur in the polymer formation. The purpose of this study is to investigate the solution reactions leading to the formation of the partially oxidized bis(oxalato)platinate salts. It is hoped that an understanding of the solution chemistry will eventually lead to ways of controlling the polymerization and thus initiate the formation of electrical circuits via chemical reactions.

Description of Pt Metal-Metal Bond Formation

Dimeric Pt Complexes

The interaction of d orbitals plays the dominant role in transition metal bonding. Platinum is no exception to this. The electronic interaction between two metal atoms is directly related to the amount of d orbital overlap between the two metal atoms. A large metal overlap will delocalize the individual metal orbitals (MO's) such that new unique molecular orbitals will occur. When only two metal atoms are interacting a metal-metal dimer is the result. Two types of metal-metal bonded dimers are known. In one type the metals are bonded directly to each other and bridged by an appropriate ligand along the metal-metal axis. Examples of this type include $K_2[Pt_2(\mu\text{-}SO_4)_4(H_2O)_2]$ (9) and $K_2[Pt_2(\mu\text{-}HPO_4)_4(H_2O)_2]$ (16). In

the second type the metals are directly bonded to each other but there is no bridging of ligands. An example of this type is $[Pt_2Cl_6(NH{=}C(OH)C(CH_3)_3)_4]$ (30). It is the direct bonding without bridging ligands that is of interest in this work since the partially oxidized bis(oxalato)platinate polymer contains many metal-metal bonds but no apparent bridging ligands.

A simplified MO diagram shown in Figure 1 can be utilized to depict the interaction of the two platinum atoms in a dimeric species (4). This MO is the result of two platinum atoms in square planar complexes approaching each other along the z-axis. The d_{z2} orbitals combine directly to form d_σ and d_{σ^*} bonding and antibonding molecular orbitals. The d_{xz} and d_{yz} orbitals combine to form two degenerate d_π bonding and d_{π^*} antibonding molecular orbitals. The d_{xy} orbitals form two degenerate d_δ bonding and d_{δ^*} antibonding molecular orbitals. The $d_{x2\text{-}y2}$ orbital interactions are not depicted in the MO diagram. These orbitals interact with the ligands of the square planar complex to form σ bonds and the relative energy is much lower than any of the other d orbitals. The antibonding orbital, $d_{x2\text{-}y2^*}$, will be a d_δ orbital. It can be seen then, using this simple MO, that two transition metals must have less than sixteen electrons total in their combined d orbitals to form a metal-metal bond. The Pt(II) atoms in the square planar complexes have a d^8 configuration. In order for Pt(II) complexes to form metal-metal bonded structures, they must undergo oxidation. In dimeric Pt complexes, each Pt(II) must lose one electron before metal-metal bonding can occur.

This simple MO for the dimeric complex has the disadvantage that it does

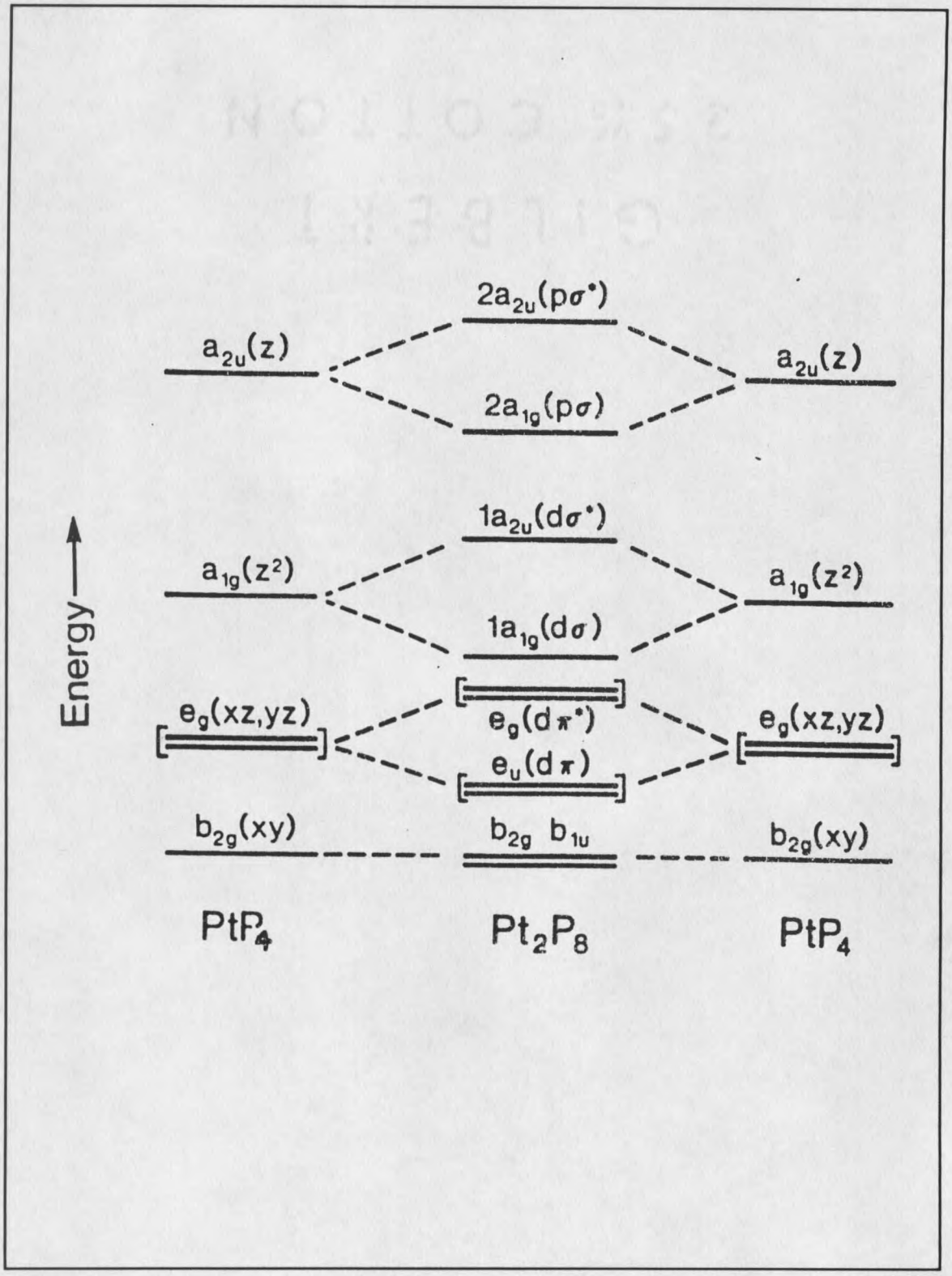

Figure 1. A simplified MO depicting the interaction of two platinum atoms (4).

not show the configuration interaction of the two adjacent complex platinum nuclei. An MO depicting this interaction is shown in Figure 2 (5). As shown before, the two $5d_{z2}$ atomic orbitals have split to form bonding and antibonding orbitals, a_{1g} and a_{2u}. The $6p_z$ atomic orbitals have also split to form bonding and antibonding orbitals, a_{1g} and a_{2u}. The symmetry of the molecular orbitals is the same in both cases. Since nondegenerate MO's of the same symmetry "repel" each other a configuration interaction occurs and the resultant MO is depicted in Figure 2b (5). The MO's derived from the $5d_{z2}$ orbitals obtain some *p* character, and those derived from the $6p_z$ orbitals acquire some *d* character. It is of interest then that two Pt(II) atoms could interact somewhat with each other, even though their d orbitals are filled, due to configuration interaction.

Polynuclear Platinum Complexes

When more than two platinum atoms are joined together in a single complex the MO's retain the same general splitting pattern as depicted in Figures 1 and 2 only the number of MO's obtained is increased. When a chain of platinum atoms is involved band theory is commonly used to describe the electron configurations. As more and more platinum atoms are added to the chain the number of bands become larger and larger. Figure 3 depicts the MO of a chain complex. The shorter the distance between atoms, the broader the band becomes and the shorter is the distance between the highest occupied level in the d_{z2} band and the

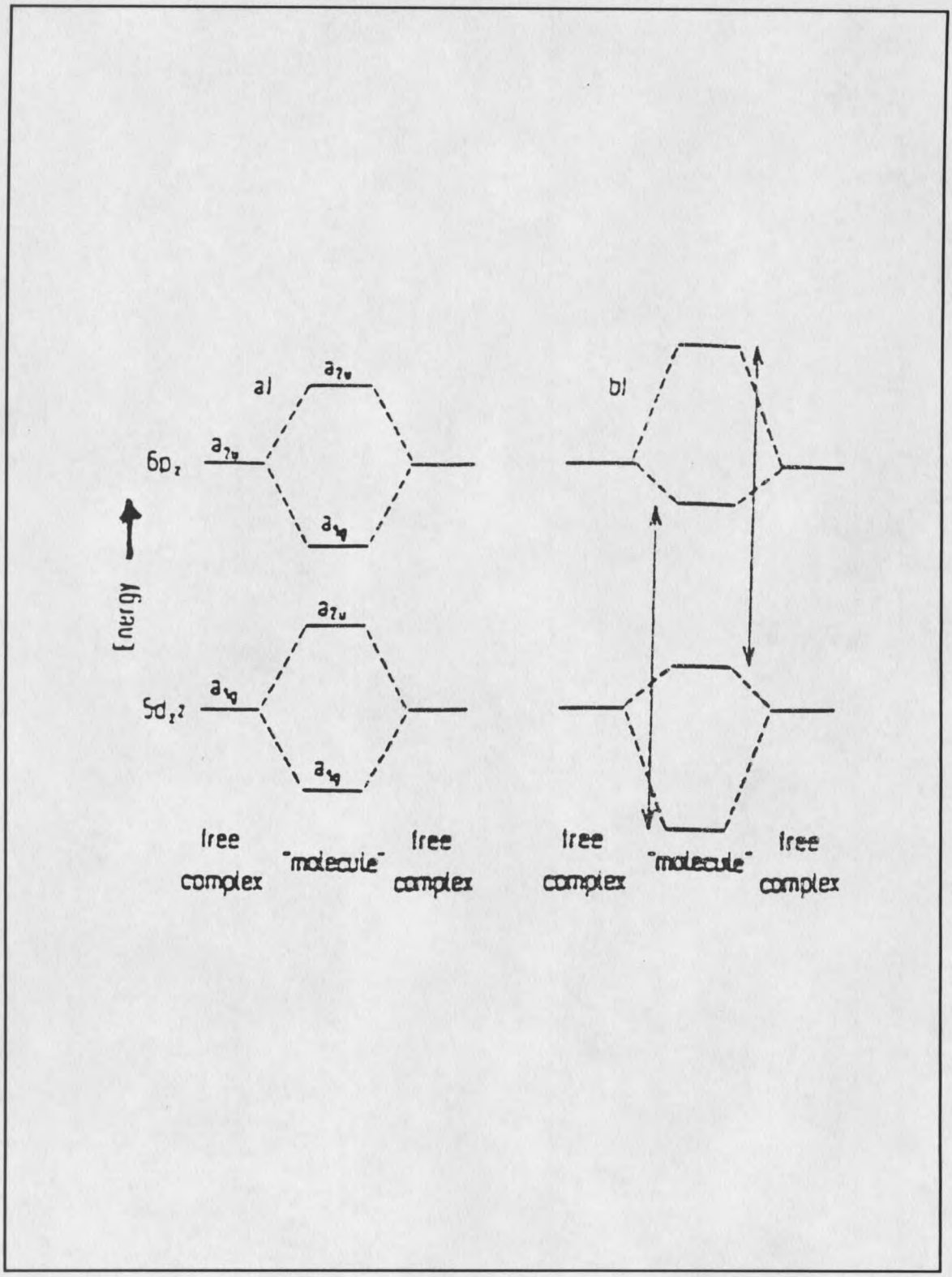

Figure 2. MO depicting configuration interaction of a dimeric Pt complex (5).

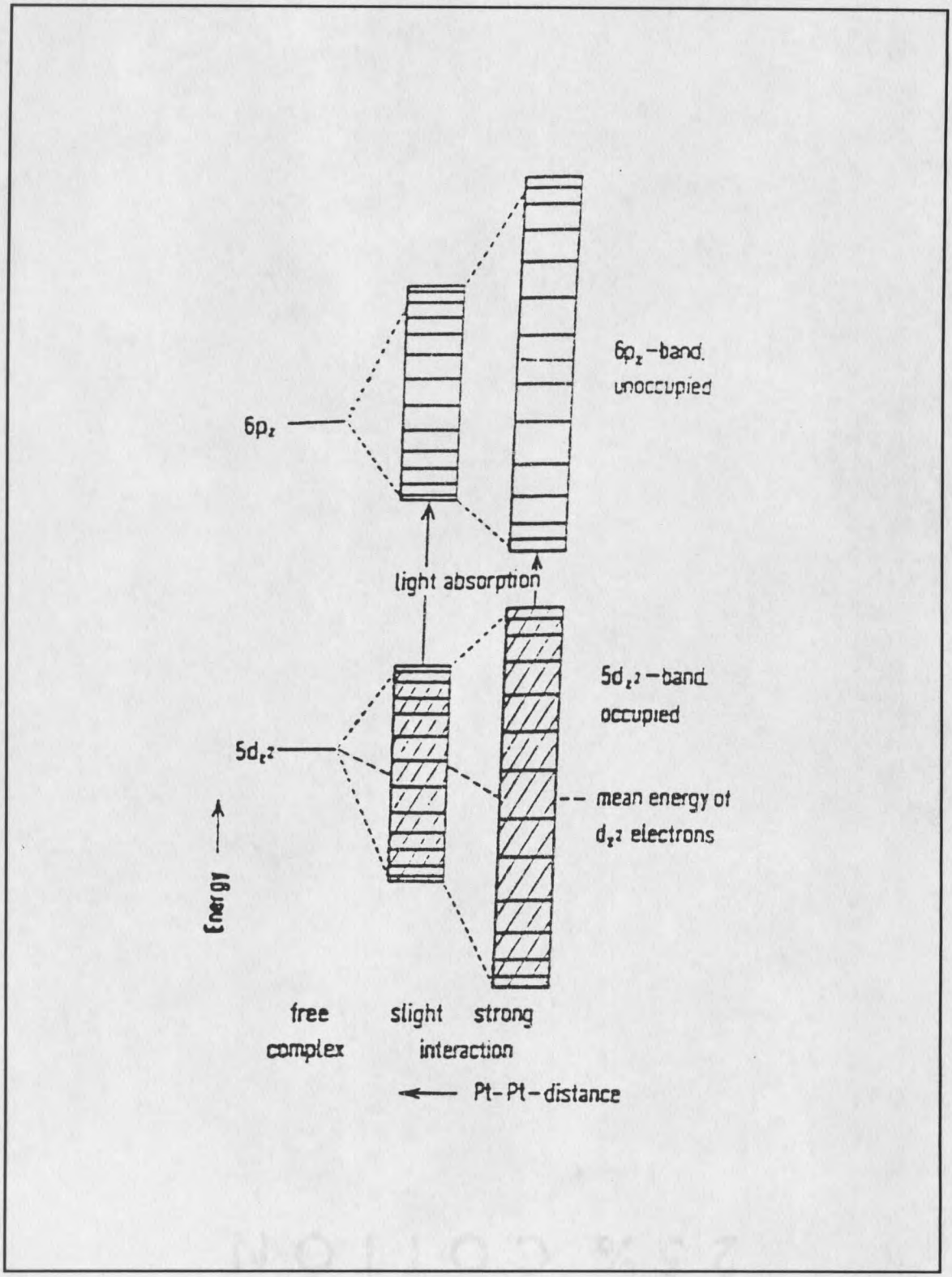

Figure 3. MO of a platinum chain complex complex (5).

lowest unoccupied level in the p_z band. The shorter the distance between Pt atoms, the smaller is the energy required to promote an electron from the highest occupied molecular orbital (HOMO) to the lowest unoccupied molecular orbital (LUMO).

Partially Oxidized Chain Complexes

The d_{z2} orbital is filled in Pt(II) ions. A chain of Pt(II) ions then would have a filled d_{z2} band. If multiple Pt(II) atoms are brought together in a chain then metal-metal bonding would not be expected to occur since the bonding and antibonding orbitals are filled. Even if configuration interaction is considered (Figure 4) the upper orbitals of this band would have an antibonding effect on the chain, since these are situated above the d_{z2} level of the free complex. Strengthening the bonding in the chain could be achieved by removing electrons from the filled orbitals. Figure 4 shows how the Pt-Pt distance decreases (and therefore the strength of the metal-metal bond increases) as electrons are removed (5). The partially oxidized complexes of Pt undergo just such an oxidation as described here. The average oxidation state of the Pt in these complexes is nonintegral.

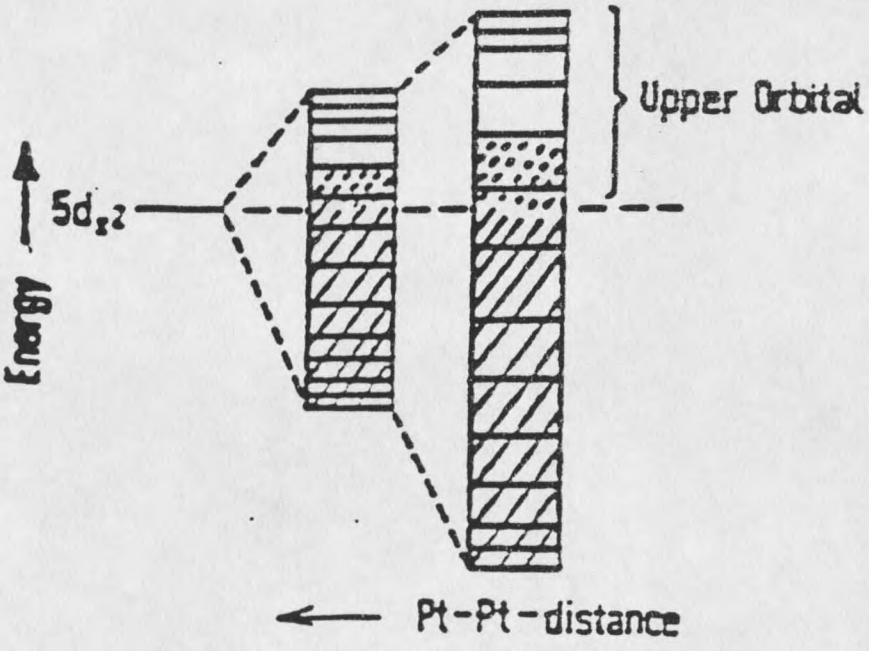

Figure 4. MO of the partially oxidized platinum chain complexes (5).

Mononuclear Platinum(III) Complexes

Mononuclear platinum(III) complexes, in which the formal oxidation state of the platinum metal center is +3, are rare. The first complex of this type to be fully characterized is $(NH_4)[Pt^{III}(C_6Cl_5)_4]$ (6). It is prepared by adding Cl_2 or Br_2 (dissolved in CCl_4) to a solution of $(NH_4)_2[Pt^{II}(C_6Cl_5)_4]$. This complex is paramagnetic since the platinum has a d^7 electron configuration. Figure 5 shows the crystal structure of this blue complex. The molecule has a square planar geometry, and the closest Pt-Pt distance is 9.7 Å. Since the molecule is paramagnetic no ^{195}Pt NMR resonances are observed. One other mononuclear Pt(III) complex that has been reported is $[Pt^{III}L_2]$ where L = 1,4,7-trizacyclononane (7). This complex is formed by room temperature oxidation of $[Pt^{II}L_2]$ where L = 1,4,7-triazacyclononane at 0.5V under nitrogen in acetonitrile. This complex is also paramagnetic. Finally, Boucher *et al.* have reported the complex $[Pt^{III}(diamsar)]^{3+}$ where diamsar = 1,8-diamino-3,6,10,13,16,19-hexaazabicyclo[6.6.6]icosane (8). This complex is generated by the γ-radiolysis of $[Pt^{IV}(diamsar)]^{4+}$ at 77K. Other mononuclear platinum(III) complexes have been reported but exist only as short-lived transients in various reactions.

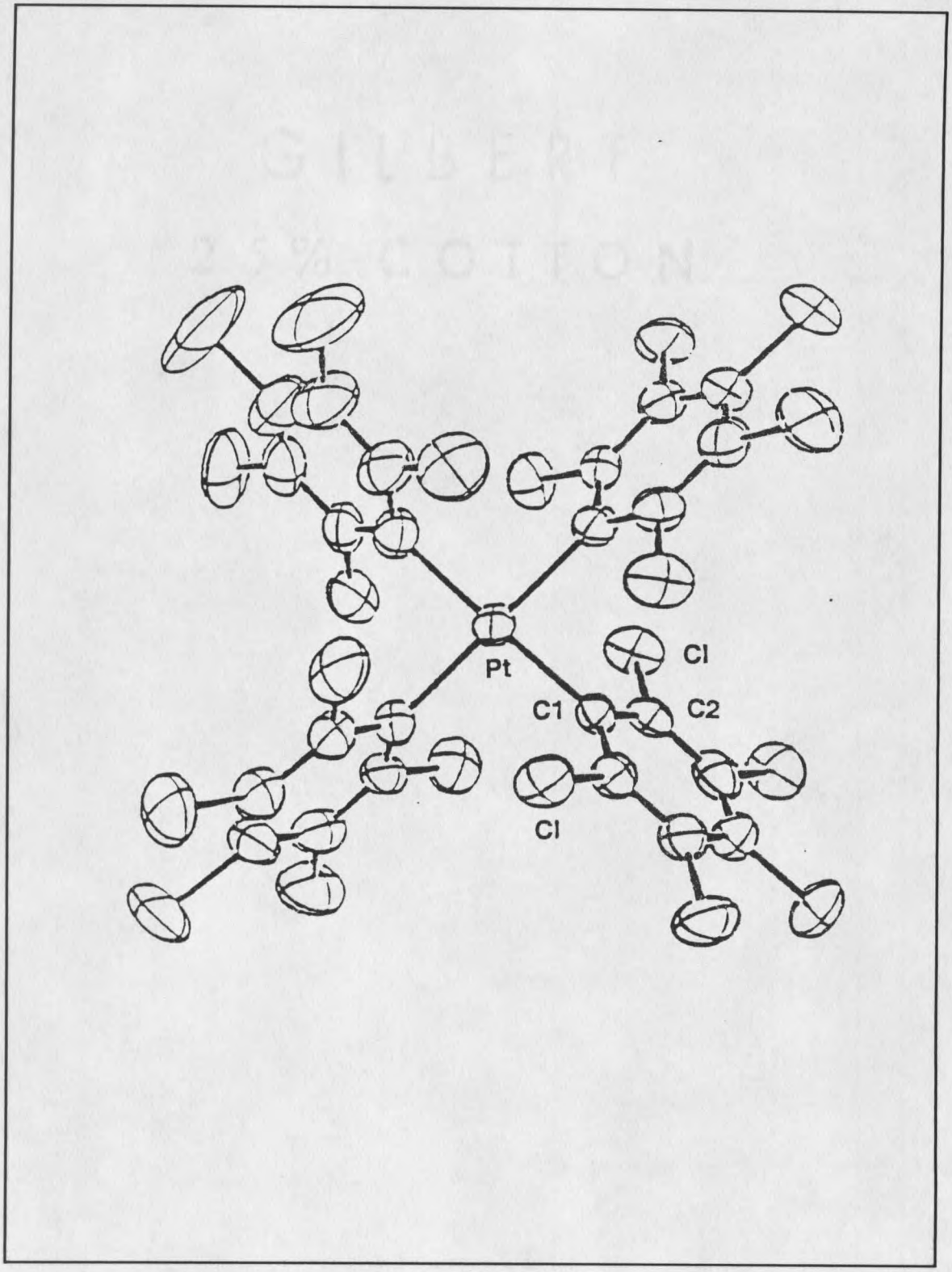

Figure 5. Crystal structure of $[Pt^{III}(C_6Cl_5)_4]^-$ (6).

Dimeric Platinum(III) Complexes

Bridged Complexes

Platinum(III) Sulfates

The tetra-μ-sulfato complex, $K_2[Pt_2(\mu\text{-}SO_4)_4(H_2O)_2]$, was the first diplatinum(III) complex to be characterized using X-ray crystallography (9). Figure 6 show the structure of this complex. This compound is prepared by reacting $K_2[Pt(NO_2)_4]$ with sulfuric acid. Potentiometric titrations have shown that the platinum metal centers are in an oxidation state (+3). X-ray crystallographic studies have shown that this compound contains two Pt(III) centers metal-metal bonded with a bond distance of 2.466 Å. The Pt centers are bridged by four sulfates in a "lantern" structure. Work by Appleton et. al. has shown that the axial Pt-OH_2 bonds in this complex are labile to ligand substitution due to the high *trans* effect of the metal-metal bond (10). Raman spectra show a ν(Pt-Pt) between 150-236 cm^{-1} (11, 12, 13). The electronic spectra of the diaqua, dibromo, dichloro derivatives contain an intense band at 220nm which has been assigned to the metal-metal $\sigma \rightarrow \sigma^*$ transition (12, 13). The complex is diamagnetic since the individual platinum atoms, which are d^7, have formed a metal-metal bond resulting in an orbital scheme of $\sigma^2\pi^4\delta^2\delta^{*2}\pi^{*4}$. NMR data were obtained by Appleton *et al.* (10) on $[Pt_2(\mu\text{-}SO_4)_4XY]^{n-}$ where the axial ligands, X and Y, included H_2O, CN^-, NH_3,

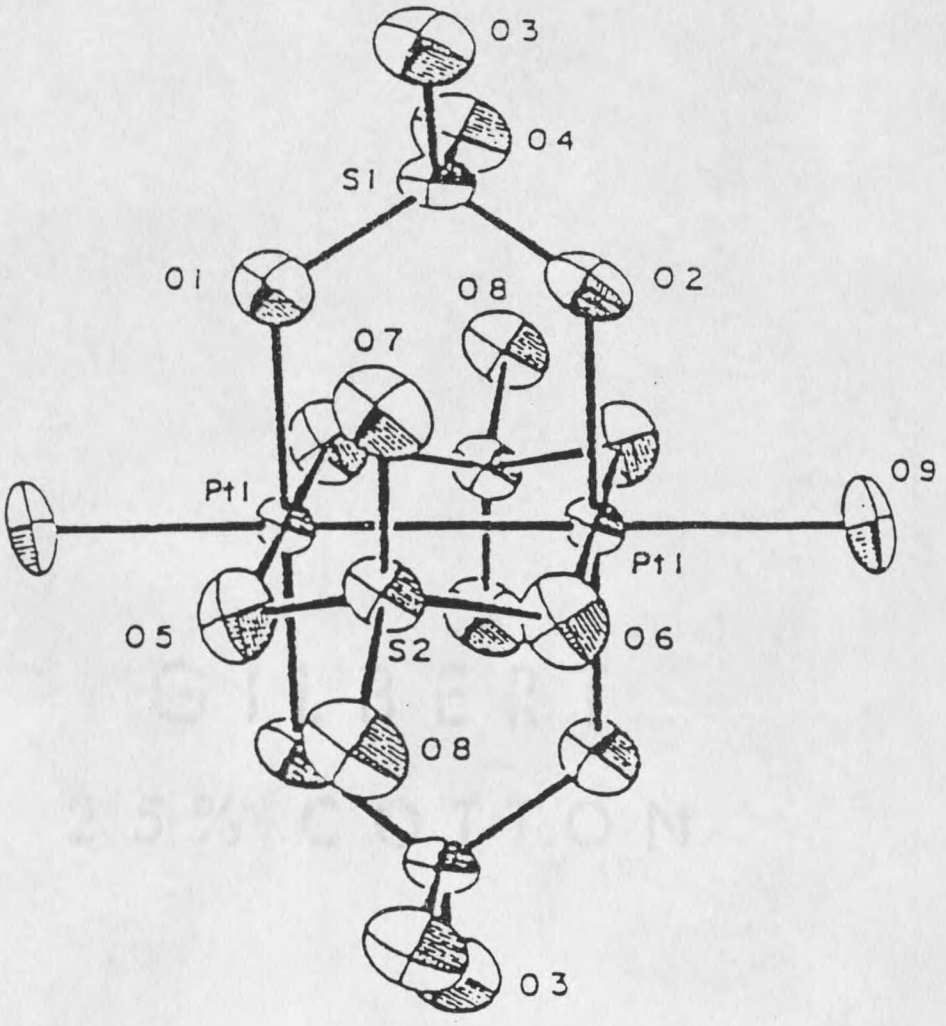

Figure 6. Crystal structure of $[Pt_2(\mu\text{-}SO_4)_4(H_2O)_2]$ (9).

Cl^-, Br^-, I^-, SCN^-, and NO_2. Platinum chemical shifts for these complexes range from 1142 ppm to 2262 ppm. The symmetrical complexes, $[Pt_2(\mu\text{-}SO_4)_4X_2]^{n-}$, give a singlet in the ^{195}Pt NMR spectrum. The unsymmetrical complexes, $[Pt_2(\mu\text{-}SO_4)_4XY]^{n-}$, give two singlets and an AB pattern.

Platinum(III) Phosphates

The phosphate analogue to the Pt(III) sulfate complex was first reported by Muraveiskaya *et al.* (14). The structure of $[Pt_2(\mu\text{-}HPO_4)_4(H_2O)_2]^{2-}$, the phosphate complex, is shown in Figure 7. As with the Pt(III) sulfate dimer, the Pt(III) phosphate dimer also has a "lantern" structure with the four phosphate ligands bridging the Pt-Pt center. The potassium salt of this dimer is prepared by reacting $K_2[Pt(NO_2)_4]$ with 85% H_3PO_4 (11). The Pt-Pt bond distance for this complex is 2.486(2) Å. Many derivatives of this complex have been reported. Electronic absorption studies have been conducted for the complexes $[Pt_2(\mu\text{-}HPO_4)_4L_2]^{n-}$ where L = H_2O, n = 2 and L = Cl^-, Br^-, n = 4 (15). A high energy intense band at 200-350nm is assigned to the intermetallic $\sigma \rightarrow \sigma^*$ transition. These complexes, like the sulfate analogues, are diamagnetic with the same orbital scheme of $\sigma^2\pi^4\delta^2\delta^{*2}\pi^{*4}$. Appleton *et al.* (10) have determined the ^{195}Pt NMR resonance for these complexes to be in the range 1496 ppm to 2017 ppm. The signals, instead of being single lines, are quintets due to coupling to the four equivalent phosphorus nuclei.

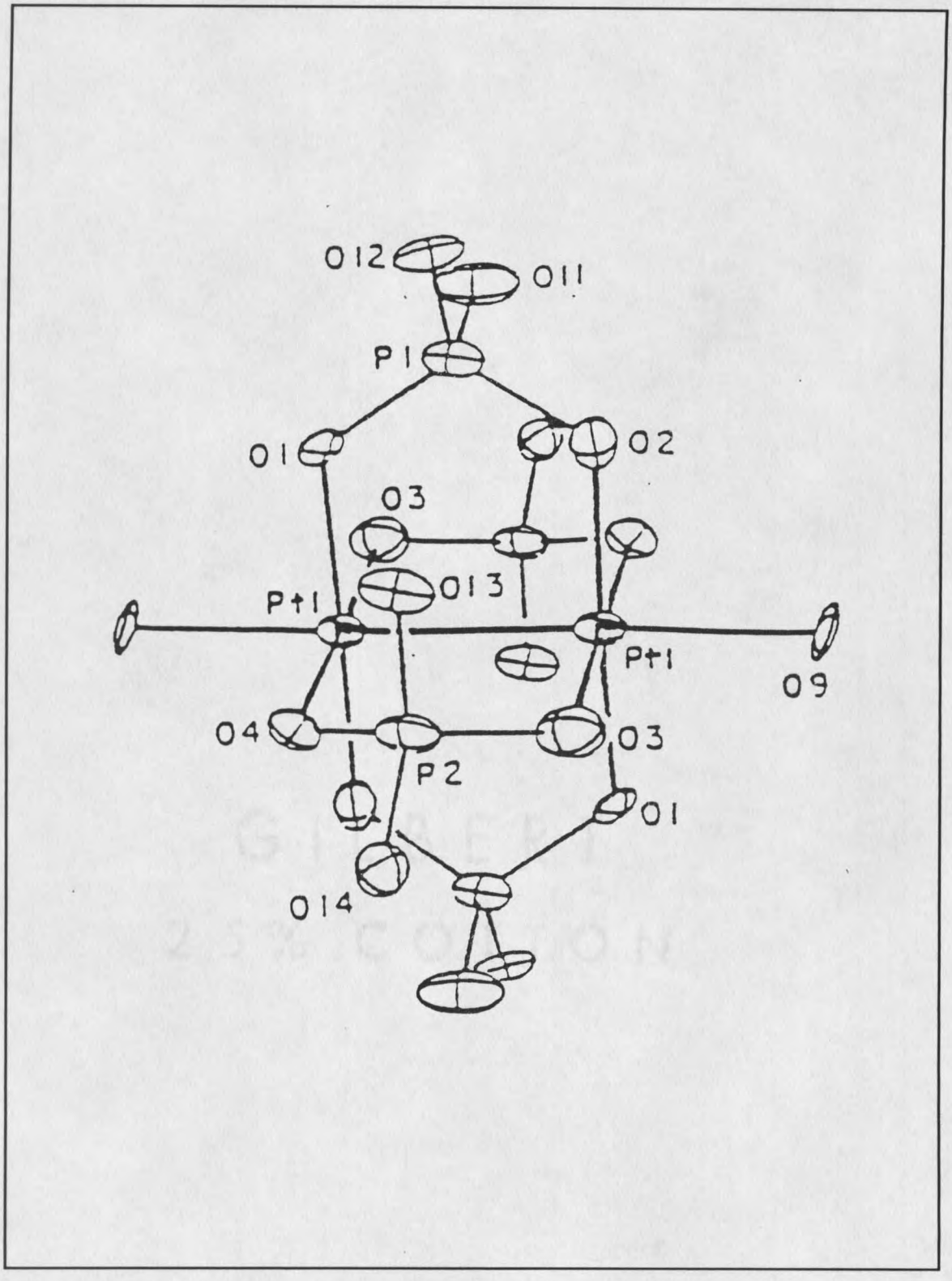

Figure 7. Crystal structure of $[Pt_2(\mu\text{-}HPO_4)_4(H_2O)_2]^{2-}$ (14).

Platinum(III) Pyrophosphites

The most widely studied of all Pt(III) complexes are the diplatinum(III) complexes, $[Pt_2(pop)_4XY]^{n-}$ (pop = μ-$P_2O_5H_2P,P'^{2-}$), which contain bridging pyrophosphito ligands in a lantern arrangement (Figure 8a) (16). These dimeric platinum(III) complexes are formed by oxidation of the Pt(II) dimer $[Pt_2(pop)_4]^{4-}$ (Figure 8b) (17, 18, 19). The Pt-Pt distances of the Pt(III) dimers vary from 2.695 Å to 2.925 Å depending upon the axial ligands that are present. Axial ligands for the complexes have included H_2O, Cl^-, Br^-, I^-, NO_2^-, SCN^-, CH_3^-, and CH_3CN. The diamagnetic Pt(III) complexes, $[Pt_2(pop)_4X_2]^{4-}$ (X = Cl^-, Br^-, I^-), are formed through oxidative addition of the halogens (20, 21). Linear chain complexes of the $[Pt_2(pop)_4]^{n-}$ bridged by either chloride or bromide (Figure 9) have been reported (22, 23). The oxidation state of the metal centers in these complexes is +2.5. The Pt-Pt bond distances in these linear chain complexes are intermediate between those found for $[Pt^{II}_2(pop)_4]^{4-}$ and $[Pt^{III}_2(pop)_4XY]^{4-}$ which is consistent with the observed oxidation states of the platinum. Electronic spectra of the Pt(III) pyrophosphite complexes have been consistent with the sulfato and phosphato Pt(III) complexes exhibiting an intense high energy $\sigma \rightarrow \sigma^*$ at 280 to 345 nm (24). ^{195}Pt NMR data obtained for the complexes $[Pt_2(pop)_4X_2]^{4-}$ (X = Cl^-, Br^-, I^-, NO_2^-) and $[Pt_2(pop)_4XY]^{4-}$ (X = CH_3, Y = I^-) report a δ_{Pt} range of -4236 ppm to -5103 ppm (25, 26).

a)

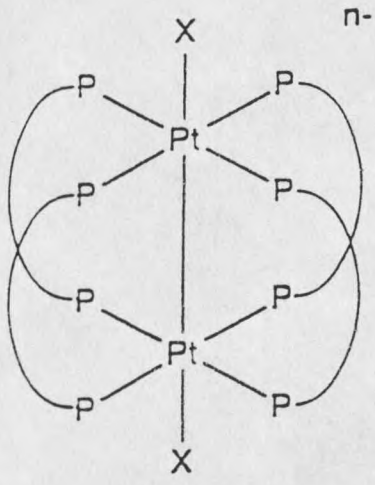

P⌒P = $P_2O_5H_2^{2-}$

b)

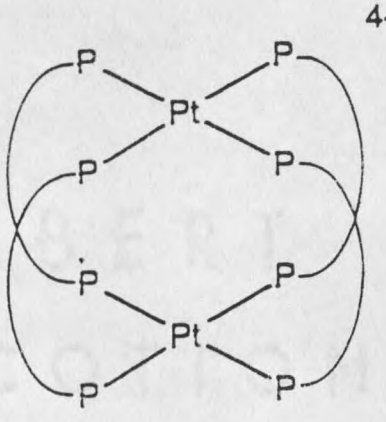

P⌒P = $P_2O_5H_2^{2-}$

Figure 8. Structure of a) $[Pt_2(pop)_4XY]^{n-}$ and b) $[Pt_2(pop)_4]^{4-}$ (16).

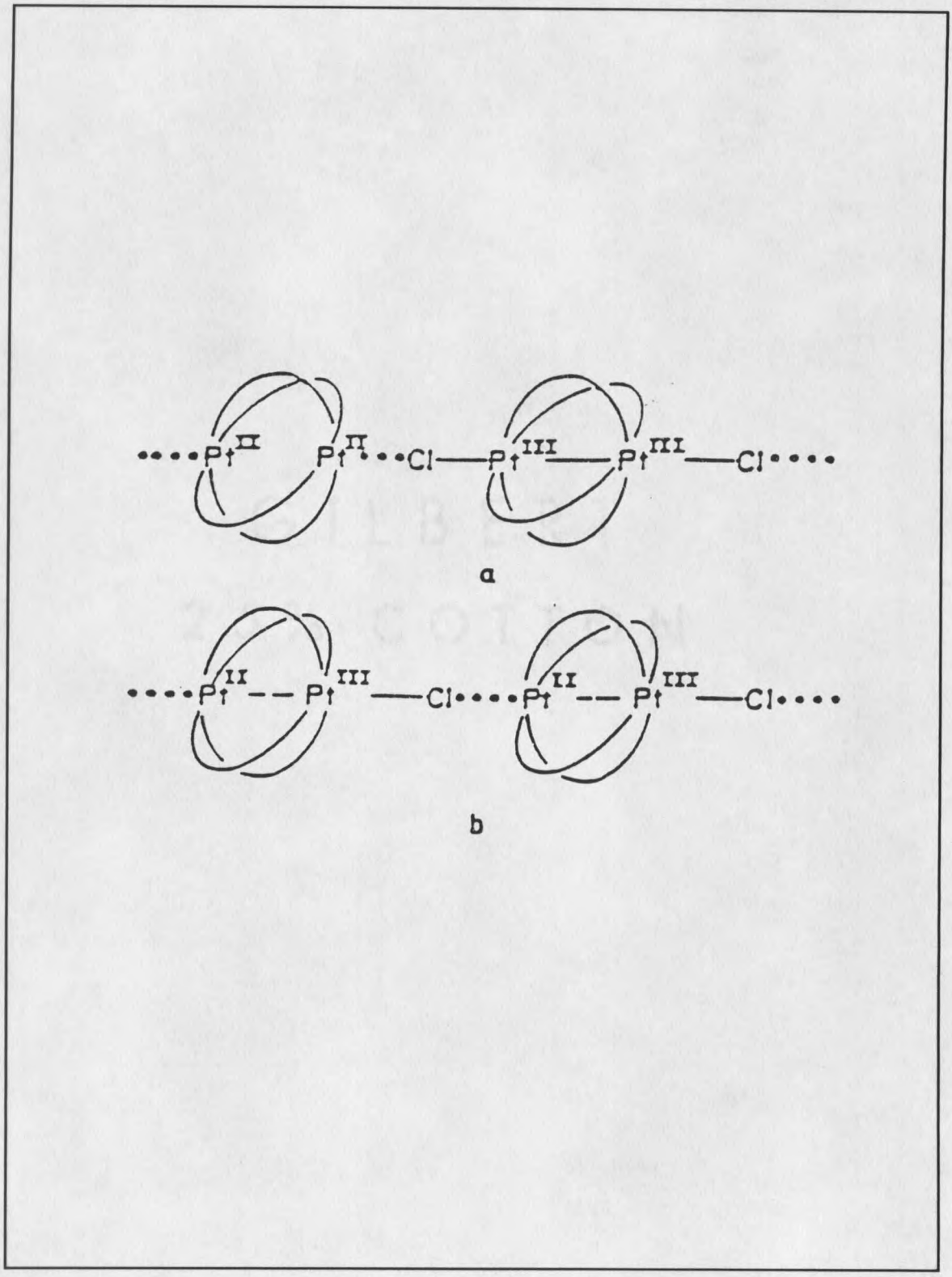

Figure 9. Structure of linear chain complexes of $[Pt_2(pop)_4]^{n-}$ (22).

Platinum(III) Carboxylates

The first reported Pt(III) carboxylato dimers have the general structure shown in Figure 10a where R = $-CH_2CH_3$, $-(CH_2)_2CH_3$, $-CH(CH_3)_2$ and R' = $-CF_3$, $-CH_3$, $-CH(CH_3)_2$ (27) These platinum(III) complexes are prepared by oxidizing the platinum dimer $[Pt(CH_3)_2(SR_2)]_2$ (Figure 10b) with AgO_2CR' or $Hg(O_2CR')_2$ (27). Axial substitution of pyridine, 4-methylpyridine, aniline and chloride have been carried out (28). Appleton *et al.* have recently reported the preparation and structure of a Pt(III) dimeric cation, $[Pt_2(\mu\text{-}CH_3CO_2\text{-}O,O')_4(H_2O)_2](ClO_4)_2$ (Figure 11) (29). They have further reported a ^{195}Pt resonance for this complex at 1520 ppm. The Pt-Pt bond length for the cation is 2.3905 Å.

Non-Bridged Complexes

1-Imino-1hydroxy-2,2-dimethylpropane Complexes

Originally it was thought that bridging ligands were necessary to stabilize Pt(III)-Pt(III) metal-metal bonded units. Reports in 1991 of complexes of Pt(III)-Pt(III) containing non-bridging ligands has shown that these early ideas are not necessarily correct. The first of these non-bridging Pt(III)-Pt(III) complexes to be reported was $[Pt_2Cl_6(NH{=}C(OH)C(CH_3)_3)_4]$ (30) (Figure 12). It is synthesized by chlorine oxidation of the monomeric Pt(II) complex *cis*-$[PtCl_2(NH{=}C(OH)C(CH_3)_3)_2]$

a)

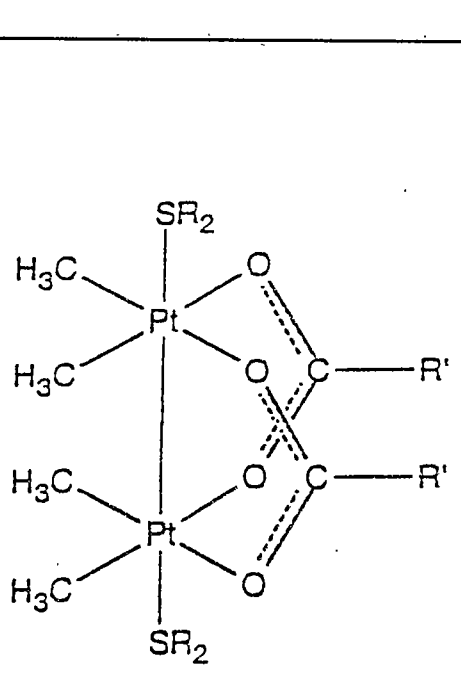

b)

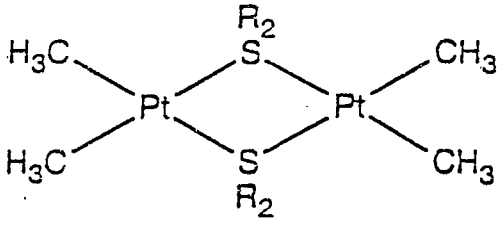

Figure 10. Structure of a) Pt(III) carboxylato dimer and b) $[Pt^{II}(CH_3)_2(SR_2)]_2$ (27).

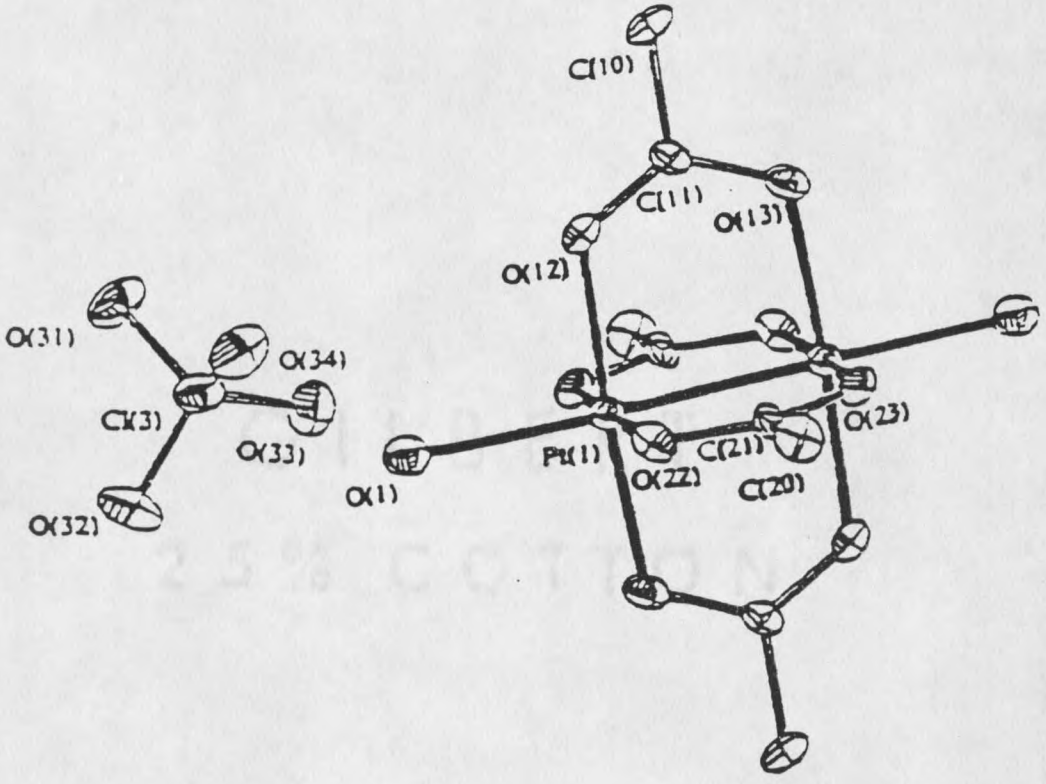

Figure 11. Structure of $[Pt_2(\mu\text{-}CH_3CO_2\text{-}O,O')_4(H_2O)_2](ClO_4)_2$ (29).

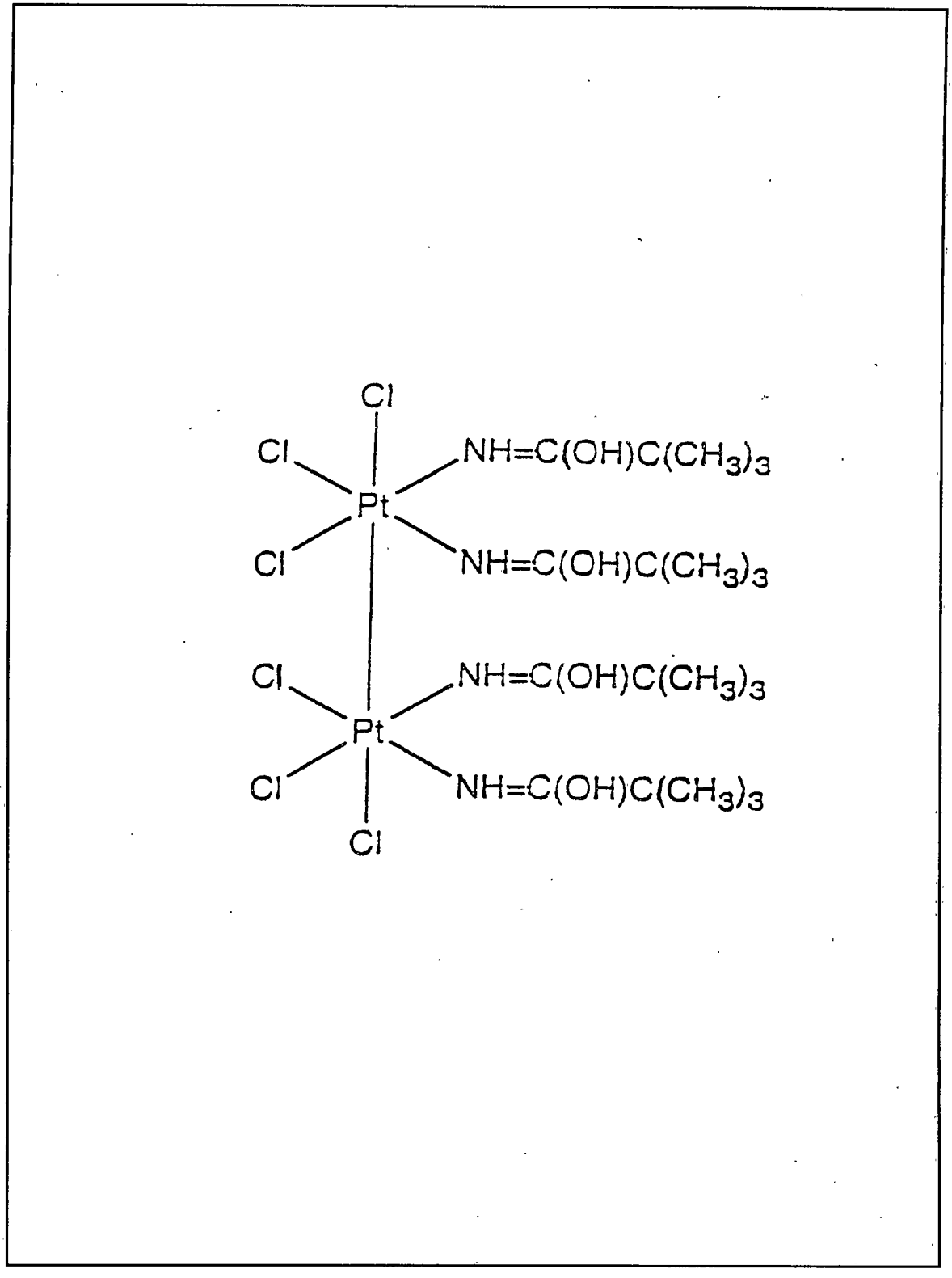

Figure 12. Structure of $[Pt_2Cl_6(NH{=}C(OH)C(CH_3)_3)_4]$ (30).

in dichloromethane solution. This complex is stable in solutions containing Cl_2 for a few days, but in the absence of chlorine it readily disproportionates to the Pt(II) complex mentioned above and the Pt(IV) complex *cis*-$[PtCl_4(NH{=}C(OH)C(CH_3)_3)_2]$. X-ray crystallography has determined the Pt-Pt bond distance to be 2.6964(5)Å (30).

C_8- carbocyclic α-dioximato Complex

In 1992 Baxter *et al.* (31) reported the isolation of the non-bridging Pt(III)-Pt(III) species, $[Pt_2Cl_2(C_8doH)_4]$ (C_8doH = C_8 carbocyclic α-dioximato ligand shown in Figure 13), whose structure is shown in Figure 13. This compound is prepared by controlled chlorination of $[Pt(C_8doH)_2]$ by $PhICl_2$ (Ph = phenyl) or para-ClC_6H_4I Cl_2 in dichloromethane. This complex is much more stable than the previously mentioned non-bridging Pt(III)-Pt(III) species, $[Pt_2Cl_6(NH{=}C(OH)C(CH_3)_3)_4]$. Disproportionation into it respective Pt(II) and Pt(IV) complexes, $[Pt(C_8doH)_2]$ and $[Pt(C_8doH)_2Cl_2]$, occurs after seven weeks in $CHCl_3$. The Pt(III)-Pt(III) bond length for this species has been determined by x-ray crystallography to be 2.694(1) (31).

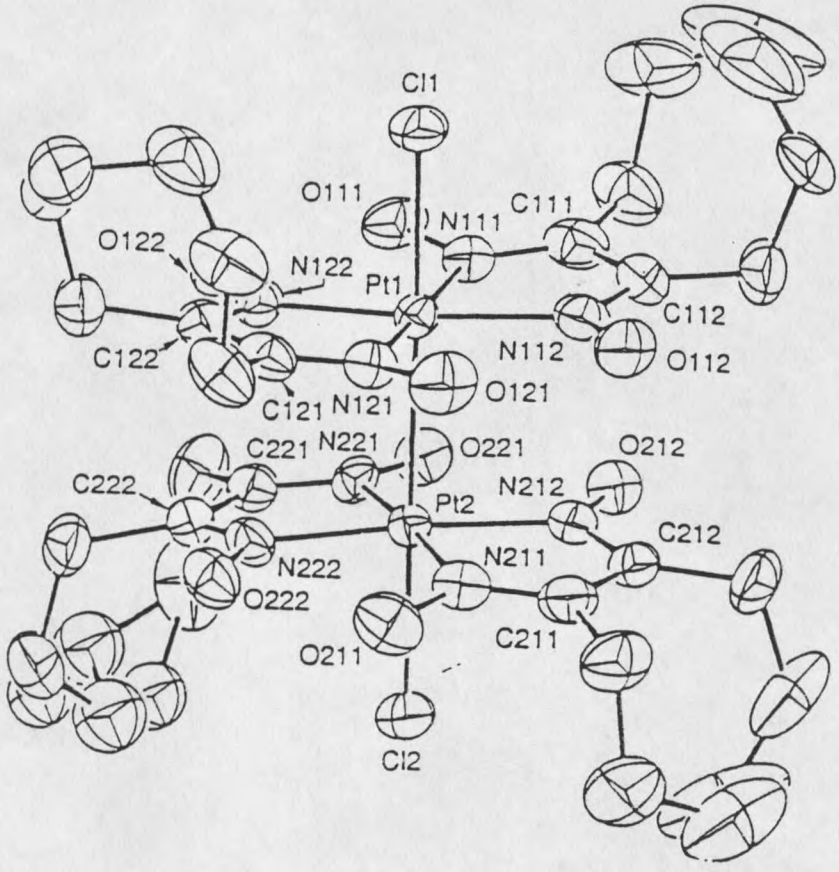

Figure 13. Structure of $[Pt_2Cl_2(C_8doH)_4]$ (31).

Platinum Blues

The platinum blues comprise a general class of polynuclear metal-metal bonded platinum compounds. There are many types of complexes that have been classified as platinum blues. Due to their anti-tumor activity, the platinum blues prepared from the reaction of *cis*-$[Pt(NH_3)_2(H_2O)_2]^{2+}$ and pyrimidines (32, 33, 34) have been the most widely studied. The first complex fully characterized was tetrameric α-pyridone blue (Figure 14). X-ray crystallography has shown the structure to be a dimer of binuclear $[(NH_3)_2Pt(pyr)_2Pt(NH_3)_2]$ units with an average platinum oxidation state of +2.25. The crystal structure is consistent with the delocalization of the electrons over the four Pt atoms in the chain indicating that oxidation state of all Pt atoms is the same. The visible spectrum is characterized by a broad transition around 680 nm (33). Oxidation of this complex with Ce^{+4} reaches an endpoint when 0.77 electron equivalents of Ce^{+4} per platinum have been consumed (36). The product of this oxidation was assumed to be a Pt(III) species. The Pt-Pt bond lengths in this complex are 2.774 and 2.877 Å.

The platinum blue compounds based upon the pyrimidine, α-pyrrolidone, are closely related to the α-pyridone blues. The tan colored $[Pt_4(NH_3)_8(pyrl)_4](NO_3)_6{\cdot}2H_2O$ (pyrl = C_5H_6NO) was isolated by Matsumoto *et al.* (37, 38). The average platinum oxidation state in this complex is +2.5. The Pt-Pt distances in this complex are 2.702 and 2.709 Å. The green complex, α-pyrrolidone green, was also reported by Matsumoto (39). The chemical formula

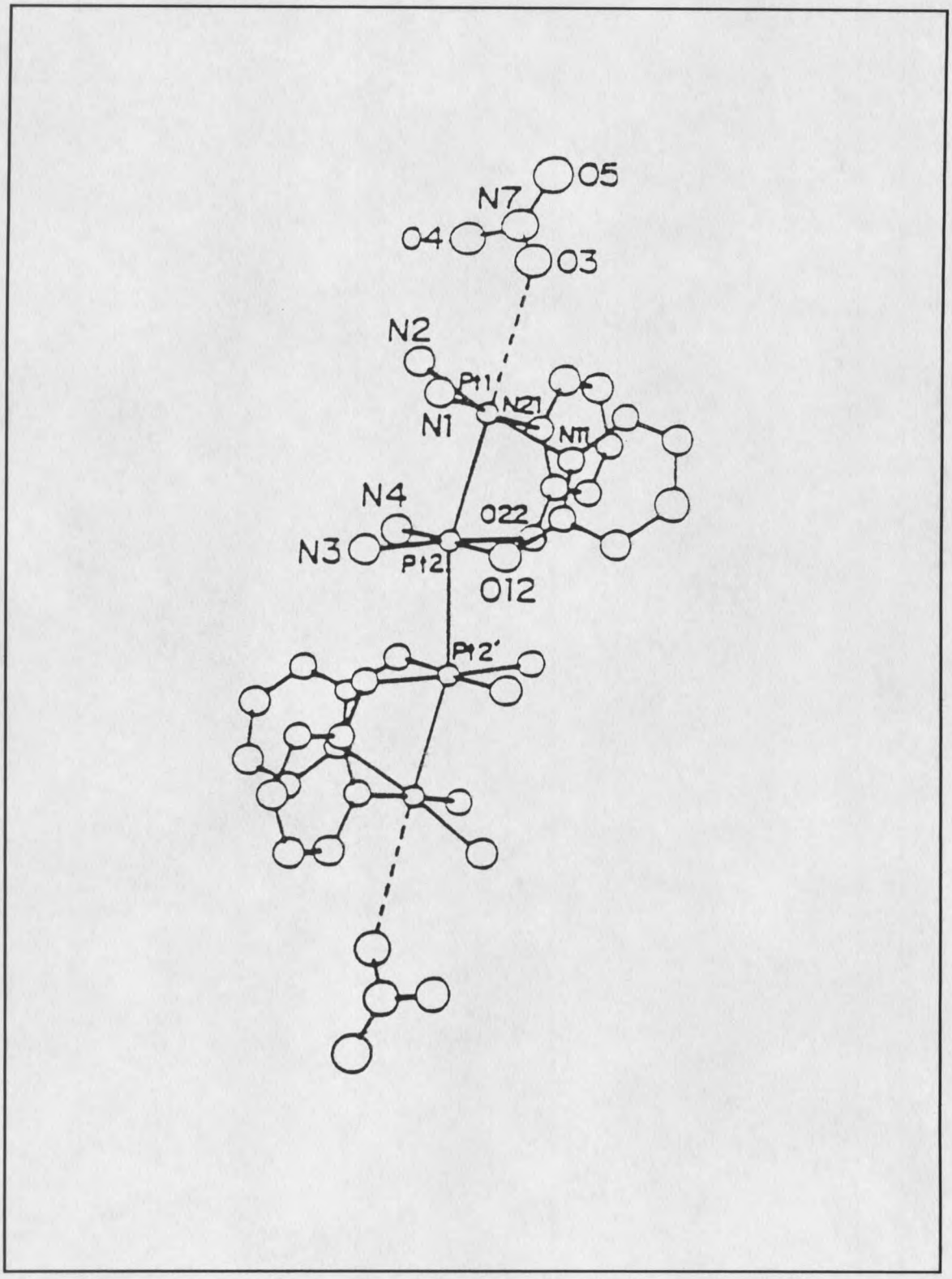

Figure 14. Structure of the tetrameric α-pyridone blue (35).

for this complex is $[Pt_4(NH_3)_8(pyrl)_4](NO_3)_{5.48}]\cdot 3H_2O$. The average oxidation state of the platinum in this compound is +2.37. Oxidation of this complex forms the tan colored α-pyrrolidone complex previously mentioned. Further oxidation of the α-pyrrolidone tan complex results in the formation of a Pt(III) dimeric complex, $[Pt_2(NH_3)_4(pyrl)_2](NO_3)_2$ (40).

Blues have also been prepared with other ligands including phthalimide, phosphate, tryptophan, glutamine, succinic acid, 1-methyl-hydantoin, 1-methyl-nicotinamide, oxamic acid, asparagine, and trimethylacetamide (36). The common theme to these platinum blue complexes is the presence of platinum in various oxidation states reportedly ranging from 2.1 to 3.75 (36). Visible spectra usually exhibit strong absorbances in the 600-700 nm region, and Mitewa *et al.* have demonstrated the formation of monomeric Pt(III) species in most instances as the first step in platinum blues formation (41). The tetrameric platinum blues have been the blues most frequently crystallized, although octameric platinum blues have also been isolated (42, 43).

Partially Oxidized Pt Complexes

Partially Oxidized Tetracyanoplatinate Complexes

The partially oxidized tetracyanoplatinate complexes are synthesized from the oxidation of the tetracyanoplatinate(II) dianion, $[Pt(CN)_4]^{2-}$, shown in Figure 15

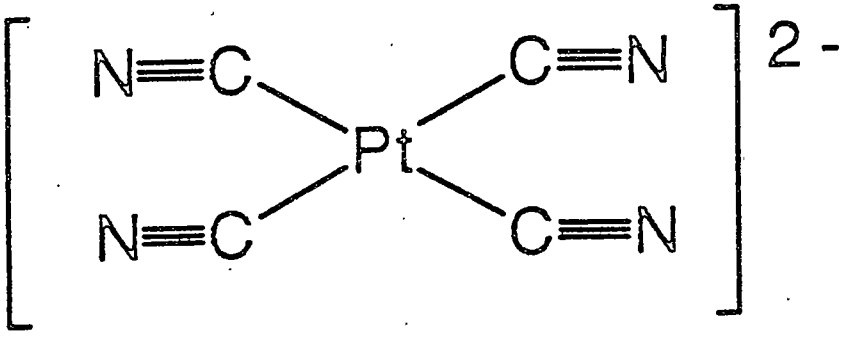

Figure 15. Structure of the tetracyanoplatinate(II) dianion, $[Pt(CN)_4]^{2-}$ (1).

(1). Upon oxidation the $[Pt(CN)_4]^{2-}$ monomers stack one above the other. The platinum atoms are metal-metal bonded to one another through the overlapping d_{z2} orbitals. Figure 16 depicts the structure of the partially oxidized tetracyanoplatinate salts (1). The distinguishing feature of the partially oxidized tetracyanoplatinate salt is the nonintegral oxidation state of the platinum atoms. The degree of partial oxidation (DPO) of the platinum varies depending upon the counterion that is present. The range of the DPO is not large. It varies from 0.19 to 0.40. That is, the platinum oxidation state can vary from Pt(+2.19) to Pt(+2.4). Correlating with this, the distance between the platinum atoms, $d_{Pt\text{-}Pt}$, varies from 3.09Å to over 3.7Å (1). The methods of oxidation that have been used to form these complexes include 1) mixing solutions of the appropriate Pt^{+2} and Pt^{+4} salt, 2) wet chemical oxidation using H_2O_2 or Ce^{+4}, 3) electrolysis using a dc voltage source and a potential of 0.75 to 1.5 Volts (44, 45, 46). These salts exhibit brilliant metallic lusters ranging from copper to bronze to gold in color. Table 1 is a list of the partially oxidized tetracyanoplatinate salts. Since the complexes conduct electricity along the platinum chain but not perpendicular to the platinum chain, they have been called one-dimensional conductors. Electrical conductivity arises from electron delocalization along the overlapped Pt $5d_{z2}$ orbitals. Electrical conductivity parallel to the Pt atom chain, $\sigma_{\parallel}$, is in the range 1 - 2000 $\Omega^{-1}cm^{-1}$. The electrical conductivity perpendicular to the Pt atom chain is on the order of $10^{-3}\Omega^{-1}cm^{-1}$ (1).

Two types of partially oxidized tetracyanoplatinate complexes have been

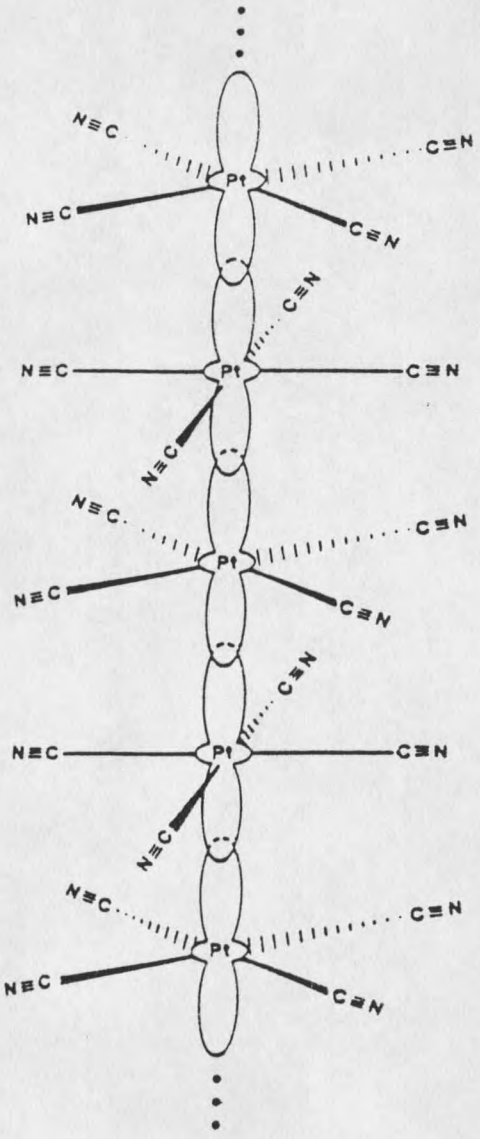

Figure 16. General structure of the partially oxidized tetracyanoplatinate salts (1).

Table 1. Types of partially oxidized tetracyano platinate salts (1).

Complex	Abbreviation	Space group[a]	Intrachain separation d_{Pt-Pt} (Å) (T = 298 K)	Conductivity (Ω^{-1} cm^{-1})[b]	Color
Pt metal			2.775[66]	9.4×10^4	Metallic
$K_2[Pt(CN)_4]Br_{0.30} \cdot 3H_2O$	KCP(Br)	$P4mm$[a,c]	2.89	4–1050	Bronze[86]
$K_2[Pt(CN)_4]Cl_{0.30} \cdot 3H_2O$	KCP(Cl)	$P4mm$[68]	2.87	~ 200	Bronze[86]
$K_2[Pt(CN)_4]Br_{0.15}Cl_{0.15} \cdot 3H_2O$	KCP(Br, Cl)	$P4mm$[69]		—	
$Rb_2[Pt(CN)_4]Cl_{0.3} \cdot 3H_2O$	RbCP(Cl)	$P4mm$[70,71]	2.877(8) and 2.924(8) at T = 298 K[70]; 2.885(6) and 2.862(6) at T = 110 K[71]	10^{90}	Bronze
$Cs_2[Pt(CN)_4]Cl_{0.3}$	CsCP(Cl)	$I4/mcm$[72]	2.859(2)	~ 200[93]	Bronze
$(NH_4)_2(H_3O)_{0.17}[Pt(CN)_4]Cl_{0.42} \cdot 2.83H_2O$	ACP(Cl)	$P4mm$[73]	2.910(5) and 2.930(5)	0.4[92]	Bronze
$Cs_2[Pt(CN)_4](N_3)_{0.25} \cdot 0.5H_2O$	CsCP(N_3)	$P\bar{4}b2$[74]	2.877(1)	—[d]	Reddish-copper
$Rb_3(H_3O)_x[Pt(CN)_4](O_3SO \cdot H \cdot OSO_3)_{0.49} \cdot (1-x)H_2O$	RbCP(DSH)	$P\bar{1}$[75]	2.826(1)	—[d]	Copper
$K_{1.75}[Pt(CN)_4] \cdot 1.5H_2O$	K(def)TCP	$P\bar{1}$[76]	2.965(1) and 2.961(1)	115–125[95,96,105]	Bronze
$Rb_{1.75}[Pt(CN)_4] \cdot xH_2O$	Rb(def)TCP	—[e,77]	2.94[100]	1[105]	Bronze
$Cs_{1.75}[Pt(CN)_4] \cdot xH_2O$	Cs(def)TCP	—[e,78]	2.88	~ 25[141]	Bronze
$K_2[Pt(CN)_4](FHF)_{0.30} \cdot 3H_2O$	KCP$(FHF)_{0.3}$	$P4mm$[79]	2.918(1) and 2.928(1)	—[d]	Reddish-bronze[85]
$Rb_2[Pt(CN)_4](FHF)_{0.40}$	RbCP$(FHF)_{0.4}$	$I4/mcm$[64]	2.798(1)	1600[1]; 2300[94]	Gold
$Rb_2[Pt(CN)_4](FHF)_{0.26} \cdot 1.7H_2O$	RbCP$(FHF)_{0.26}$	$C2/c$[80]	2.89	—[d]	Greenish-bronze[85]
$Cs_2[Pt(CN)_4](FHF)_{0.39}$	CsCP$(FHF)_{0.4}$	$I4/mcm$[65]	2.833(1)	2000[1]; 1600[94]	Reddish-gold[85]
$Cs_2[Pt(CN)_4](FHF)_{0.23}$	CsCP$(FHF)_{0.23}$	$I4/mcm$[81]	2.872(2)	250–350[95]	Reddish-bronze[85]
$Cs_2[Pt(CN)_4]F_{0.19}$	CsCP(F)	$Immm$[82]	2.886(1)	—[d]	Reddish-gold[85]
$[C(NH_2)_3]_2[Pt(CN)_4](FHF)_{0.26} \cdot xH_2O$	GCP$(FHF)_{0.26}$	—[d]	2.90[84]	—[d]	Bronze
$[C(NH_2)_3]_2[Pt(CN)_4]Br_{0.25} \cdot H_2O$[83]	GCP(Br)	$I4cm$[f]	2.908(2)	11[83]	Bronze

[a] In space group $P4mm$ the Pt–Pt intrachain distances are not required to be equal, but often appear so. When they have been determined to be different both distances are given.
[b] The range of literature values reported for room temperature four-probe dc conductivities is given.
[c] For a discussion of the crystal structure as determined by various diffraction methods, see Reference 67.
[d] Under study.
[e] The crystal class is monoclinic but the space group is unknown. The lattice constants for the Cs salt[78] are a = 18.35(1) Å, b = 5.760(3) Å, c = 19.92(1) Å, β = 109.03(4)°; for the Rb salt[77] the lattice constants are a = 10.56(1) Å, b = 33.2(1) Å, c = 11.74(1) Å, β = 114.23(3)°.
[f] Although the space group was not determined unambiguously, $I4cm$ was used. See Reference 83.

characterized to date, the cation-deficient salts and the anion-deficient salts (1). The cation-deficient salts are of the general formula $M_{1.75}[Pt(CN)_4]\cdot xH_2O$ where M = Li^+, K^+, Rb^+, and Cs^+. The anion-deficient salts are of the general formula $M_2[Pt(CN)_4]X_{0.3}$ where M = K^+, Rb^+, and Cs^+ and X = Cl^-, Br^-, and $[FHF]^-$. In the solid state of the partially oxidized tetracyanoplatinate salts, the platinum atoms are all in the same oxidation state. Platinum polymers of the "mixed valence" type do exist where discrete Pt^{+2} and Pt^{+4} ions are present, but these partially oxidized complexes are not like this in that the oxidation state of the platinum atoms is the same in the partially oxidized complexes. All platinum atoms are equivalent in these polymers. The solution chemistry of the polymerization reaction to form the partially oxidized tetracyanoplatinate complexes has not been widely explored. Work by Schindler et. al. has shown that in the spectroscopic and photochemical studies of the K^+ and the Ba^+ salts of the tetracyanoplatinate salts in solution there is definite evidence for the formation of $[Pt(CN)_4]_n^{2n-}$ oligomers which exhibit linear chain pseudo-one-dimensional behavior (1). It seems that much work is needed to characterize the solution chemistry for this polymerization reaction.

Partially Oxidized Bis(oxalato)platinate Complexes

Interest in the partially oxidized bis(oxalato)platinate salts can be attributed to work carried out by Krogmann et. al. in the 1960's (47, 48). As in the case of the partially oxidized tetracyanoplatinate salts, the partially oxidized

bis(oxalato)platinate salts are prepared by subjecting the monomeric Pt^{+2} species, $[Pt(ox)_2]^{2-}$, to oxidation. The structure of $K_2[Pt(ox)_2]\cdot H_2O$ is shown in Figure 17. Platinum is bonded in a square planar fashion to two bidentate oxalato ligands. The structure of the partially oxidized bis(oxalato)platinate complex is similar to that of the partially oxidized tetracyanoplatinate complex. Monomeric units of bis(oxalato)platinate(II) are stacked one above the other and the platinum atoms are metal-metal bonded. Figure 18 shows a typical structure for a partially oxidized bis(oxalato)platinate complex. Preparation of the partially oxidized bis(oxalato)platinate is relatively simple. Bis(oxalato)platinate(II) is subjected to oxidation under acidic conditions. The amount of oxidant used is less than what is required to carry the oxidation of the Pt(II) to Pt(IV). The oxidizing agents that have been used include $[PtCl_6]^{2-}$, Cl_2, Br_2, $[Cr_2O_7]^{2-}$, H_2O_2, air(O_2), and an electrolytic oxidation using a Pt anode (49).

The solubilities of these partially oxidized bis(oxalato)platinate complexes are low, and this has made it difficult to grow high-quality crystals. However, many different crystal types have been grown and characterized. Table 2 is a list of these crystal types (49). The degree of oxidation of the platinum in these complexes ranges from +2.19 to +2.4. Three methods have typically been used to determine the degree of oxidation (DPO) (50). Those are a) from the mole-ratio of the cations to platinum obtained by elemental analysis, b) from the mole-ratio of Pt(IV) to Pt(II) obtained by titration, c) from diffuse x-ray scattering using the relationship,

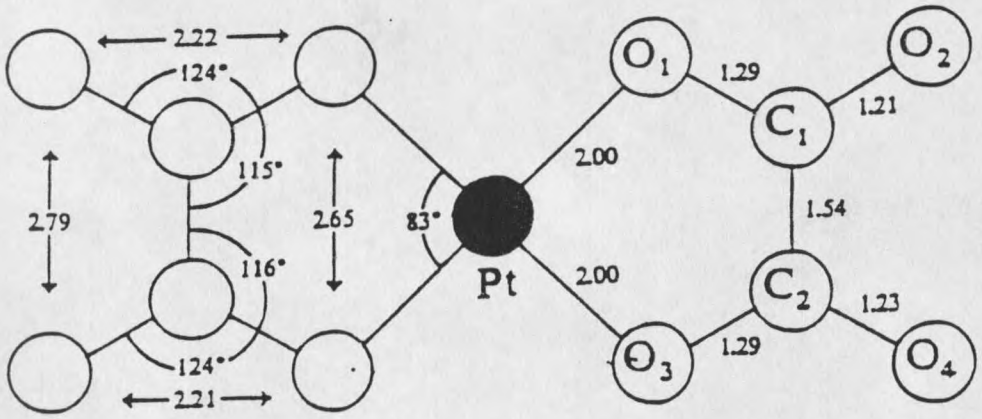

Figure 17. The structure of $[Pt(ox)_2]^{2-}$ dianion (49).

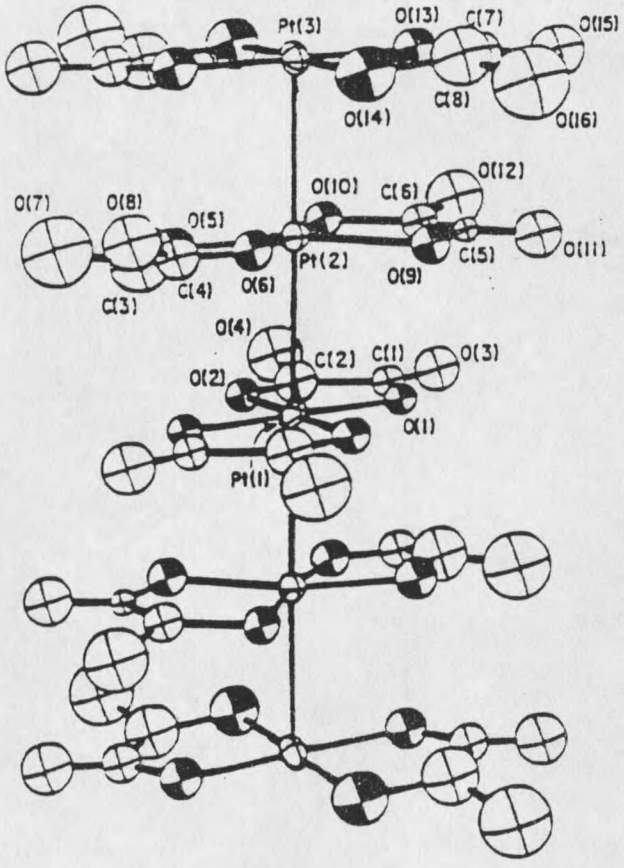

Figure 18. Typical structure of the partially oxidized bis(oxalato)platinate salts (49).

Table 2. Types of partially oxidized bis(oxalato)platinate salts (49).

Compound	Crystal system	a (Å)	b (Å)	c (Å)	α°	β°	γ°	Space group	Intra chain Pt–Pt separation, d_{Pt-Pt} (Å)	Refs.
				Platinum (II) salts						
$K_2[Pt(C_2O_4)_2]\cdot 2H_2O$	Monoclinic	7.086	14.085	6.630	90	127	90	$P2_1/n$	>8 Å	37
$[Cu(en)_2][Pt(C_2O_4)_2]$ (en = $H_2NCH_2CH_2NH_2$)	Triclinic	6.978[a]	9.418	12.351	73.14	100.59	111.73	$P\bar{1}$	3.554	15
$Ca[(Pt(C_2O_4)_2]\cdot 3.5H_2O$	Triclinic	9.33	10.72	6.36[a]	93.7	99.3	115.1		3.855 3.18	38
				Partially oxidized salts						
$K_{1.62}[Pt(C_2O_4)_2]\cdot 2H_2O$ α-K-OP	Monoclinic	21.178	11.283[a]	17.502	90	92.19	90	Pa	2.82	21
	Monoclinic	17.48	11.28[a]	21.12	90	92.27	90	$P2/c$	2.82	42
$K_{1.6}[Pt(C_2O_4)_2]\cdot xH_2O$ β-K-OP	Monoclinic	17.58	11.24[a]	21.08	90	92.30	90	$P2_1/c$	2.81	67
	Monoclinic	17.637	20.704	8.525[a]	90	90	90		2.84	21
$K_{1.61}[Pt(C_2O_4)_2]\cdot 2H_2O$ γ-K-OP	Triclinic	9.749	11.403[a]	10.694	99.54	115.81	102.32	$P\bar{1}$	2.837 2.868	21, 33 39, 43
	Triclinic	9.744	10.700	11.377[a]	80 23	77.97	115.87	$P\bar{1}$	2.833	29, 40
$K_{1.6}[Pt(C_2O_4)_2]\cdot yH_2O$ δ-K-OP	Triclinic	10.47	2.83[a]	9.67	101.4	85.4			2.857	30, 41 21, 39
									2 83	43
ε-K-OP	Monoclinic	19.998	17.132[a]	19.547	90	117.355	90	$C2/c$	2 855	42
$Rb_{1.67}[Pt(C_2O_4)_2]\cdot 1.5H_2O$ α-Rb-OP	Triclinic	12 690	17 108[a]	11 357	102.04	115.17	43 58	$P\bar{1}$	(Average) 2.717, 2 830 and 3 015	26, 27
$Rb_{1.51}(H_3O)_{0.17}[Pt(C_2O_4)_2]\cdot 1.3H_2O$ β-Rb-OP	Triclinic	8.998	11.030	17.104[a]	95.73	104.23	110.26	$P1$ or $P\bar{1}$	2.85(av.)	28
$Rb_{1.5}[Pt(C_2O_4)_2]\cdot H_2O$ γ-Rb-OP	Orthorhombic	11.159	16 596	11.329[a]	90.013	90.023	90 005	$P2_12_12$	2 829(av)	31
Cs-OP	Monoclinic		18.153	17 065	90		90	$P2_1$		31
$Mg_{0.62}[Pt(C_2O_4)_2]\cdot 5.3H_2O$ Mg-OP	Orthorhombic	16 56	14 27	5.70[a]	90	90	90	$Cccm$	2 85	3
		16.58	14 29	5.72[a]	90	90	90	$Ccc2$	2 86	44
$Mg_{0.62}[Pt(C_2O_4)_2]\cdot 5.3H_2O$[b] Mg-OP	Monoclinic	16 56	14 27	5.72[a]	89.05	90	90	C_s or $C2/c$	2 86	44
$Mg_{0.62}[Pt(C_2O_4)_2]\cdot 4H_2O$	Triclinic	11.46	9.75	2.84[a]	89.9	93.3	107.0		2 84	3
$Mg_{0.62}[Pt(C_2O_4)_2]\cdot 3\,75H_2O$	Orthorhombic	9.71	16 80	2.84[a]	90	90	90		2.84	3
$Co_{0.83}[Pt(C_2O_4)_2]\cdot 6H_2O$ Co-OP	Orthorhombic	14 379	16.501	5.682[a]	90	90	90	$Cccm$	2 841	23
	Orthorhombic	16 54	14.43	5 70[a]	90	90	90	$Pc2m$	2 85	45, 46
$Mn_{0.81}[Pt(C_2O_4)_2]\cdot 6H_2O$ Mn-OP	Orthorhombic	16.79	14.28	5.67[a]	90	90	90	$Cccm$	2.835	24
$Ni_{0.84}[Pt(C_2O_4)_2]\cdot 6H_2O$ Ni-OP	Orthorhombic	16.40	14 35	5.65[a]	90	90	90	$Cccm$	2.825	24
$Zn_{0.81}[Pt(C_2O_4)_2]\cdot 6H_2O$ Zn-OP	Orthorhombic	16.52	14 36	5.665[a]	90	90	90	$Cccm$	2 838	17
$Cu_{0.84}[Pt(C_2O_4)_2]\cdot 7H_2O$ Cu-OP	Triclinic	5.75[a]	9.95	11.67	107.48	93 50	105.02		2.876	16

[a] Denotes Pt atom chain direction.
[b] Exists only below 283 K.

$$DPO = 2(1 - k_F d_{Pt\text{-}Pt}/\pi) \quad (49)$$

where k_F is the Fermi wave vector and $d_{Pt\text{-}Pt}$ is the average intrachain platinum-platinum separation. The range of $d_{Pt\text{-}Pt}$ for the partially oxidized bis(oxalato)platinate salts is 2.81 to 2.88Å. Generally speaking, the DPO is somewhat dependent upon the countercation since it is the cation that determines how closely the Pt atoms lie next to each other in the crystal. The crystals of the partially oxidized bis(oxalato)platinate salts exhibit several crystalline phases each with similar stoichiometry and the same countercation. For instance, the potassium salts of the partially oxidized bis(oxalato)platinate complex exhibit at least five crystalline phases. Four of these phases (α-,β-,δ-, and ε-K-OP) have the stoichiometry $K_{1.6}[Pt(ox)_2]\cdot xH_2O$, and one phase (γ-K-OP) has the stoichiometry $K_{1.8}[Pt(ox)_2]\cdot 2H_2O$ (49).

Solid state electrical conductivity has been widely studied. For the partially oxidized bis(oxalato)platinate salts, the conductivity at room temperature parallel to the Pt atom chain direction, $\sigma_{\parallel}$ lies in the range of 1 - 100 $\Omega^{-1}cm^{-1}$. The conductivity at room temperature perpendicular to the Pt atom chain is on the order of 10^{-3} $\Omega^{-1}cm^{-1}$ (49). The conductivities at room temperature of these partially oxidized complexes are considerably less than the partially oxidized tetracyanoplatinate salts.

Solution chemistry of the polymerization reaction to form the partially oxidized bis(oxalato)platinate complexes has received little attention. Most of the studies that have been done were done by Krogmann et. al. in the late 1960's

(48). Krogmann carried out osmotic pressure and solution conductivity measurements and from the measurements was able to show that solutions containing increasing concentrations of $(H_3O)_{1.6}[Pt(ox)_2]\cdot xH_2O$ contain increasingly polymerized anions in solution. He interpreted the data to mean that 0.4M blue solutions contain chains whose average length is 46 monomer units and that 0.01M orange solutions contain only monomeric species. Table 3 lists the concentrations, chain lengths, and colors that Krogmann reported. Krogmann further demonstrated that the polymerization reaction is pH dependent, concentration dependent, and temperature dependent. He proposed the following reaction scheme:

Scheme: $$[Pt(ox)_2]_n^{1.6n-} + 0.4nH_2O \rightleftharpoons 0.8n[Pt^{II}(ox)_2]^{2-} + 0.2n[Pt^{IV}(ox)_2(H_2O)_2]$$

$$[Pt^{IV}(ox)_2(H_2O)_2] \rightleftharpoons [Pt^{IV}(ox)_2(H_2O)(OH)]^- + H^+$$

Table 3. Concentrations, chain length, and color of species in bis(oxalato)platinate polymerization reaction reported by Krogmann (48).

Concentration (molar)	n*	Solution Color
0.4	46.0	blue
0.2	8.7	blue
0.095	3.1	blue
0.0475	1.9	violet
0.04	1.6	brown
0.02	1.1	brown
0.01	1.0	orange

* n is the degree of polymerization (# of Pt atoms in chain)

Addition of acid favors the formation of $[Pt^{IV}(ox)_2(H_2O)_2]$ which has water molecules in axial positions. The water molecules may then be displaced by the Pt(II) species to give a polymer chain in solution. Concentrating the solution removes water molecules and therefore favors polymerization, and heating causes depolymerization of the chains.

Comparison of the Partially Oxidized Tetracyano and Bis(oxalato)platinate Salts

Initially it was thought that the partially oxidized tetracyanoplatinate salts and the partially oxidized bis(oxalato)platinate salts would be very much alike with respect to their chemical, structural, and solid state properties. Studies have shown that this is not necessarily the case. The two types are similar in certain aspects and very different in other aspects. Table 4 lists the general comparisons of the partially oxidized tetracyanoplatinate salts and the partially oxidized bis(oxalato)platinate salts. The partially oxidized tetracyanoplatinate salts occur as both cation-deficient and anion-deficient salts while the partially oxidized bis(oxalato)platinate salts occur only in the cation-deficient form. The partially oxidized bis(oxalato)platinate polymers have been found to form with both monovalent and divalent countercations. The partially oxidized tetracyanoplatinate polymers that have been isolated to date contain only the monovalent countercations. The partially oxidized tetracyanoplatinate species occur in both hydrated and anhydrous forms, but the partially oxidized bis(oxalato)platinate

compounds occur only in hydrated forms. Finally, significant to this work, solutions of the partially oxidized bis(oxalato)platinate salts appear to contain polymerized anions, and the solutions of the partially oxidized tetracyanoplatinate salts appear to contain no polymerized anions. In addition, the formation of the partially oxidized bis(oxalato)platinate polymers is acid dependent whereas the partially oxidized tetracyanoplatinate salts are formed in neutral solution.

Table 4. General comparisons of the partially oxidized tetracyano and bis(oxalato)platinate salts (49).

	Bis(oxalato)platinate salts	Tetracyanoplatinate salts
Cation-deficient	Yes	Yes
monovalent cations	Yes	Yes
divalent cations	Yes	No
Anion-deficient	No	Yes
Hydrated	Yes	Yes
Anhydrous	No	Yes
Range of d_{Pt-Pt} (Å)	2.81 - 2.876	2.798 - 2.963
Range of DPO	0.19 - 0.36	0.19 - 0.4
Range of σ (Ω^{-1} cm^{-1})	10^{2} - 10^{-2}	(2 x 10^{3}) - 1

EXPERIMENTAL METHODS

Preparation of Compounds

Starting Materials

$H_2C_2O_4$ (oxalic acid), $H_2C_3H_2O_4$ (malonic acid), KCl, 98% CF_3SO_3H (trifluoromethanesulfonic acid), 98% CF_3SO_3D (deuterated trifluoromethanesulfonic acid), $(NH_4)_2Ce(NO_3)_6$ (diammonium cerium(IV) hexanitrate), $K_2C_2O_4$ (potassium oxalate), 30% H_2O_2, all reagent grade, were purchased from Aldrich Chemicals and used as supplied. $K_2[PtCl_4]$ (**1**) (99.9%) was obtained from Johnson Matthey and used as supplied. $K_2[PtCl_6]$ (**2**) was prepared as previously described (51).

Synthesis of Complexes

Potassium Bis(oxalato)platinate(II) Dihydrate, $K_2[Pt(ox)_2]\cdot 2H_2O$ (**3**) The complex was prepared by the method of Krogmann and Dodel from $K_2[PtCl_4]$ (**1**) and $K_2C_2O_4$ (47, 48, 52).

Potassium Bis(malonato)platinate(II) Dihydrate, $K_2[Pt(mal)_2]\cdot 2H_2O$ (**4**)

The complex was prepared by the method of Dunham and Abbott from $K_2[PtCl_4]$ (**1**) and malonic acid (53).

Partially Oxidized Bis(oxalato)platinate salt, $K_{1.6}[Pt(ox)_2]\cdot 2H_2O$ (**5**) The complex was prepared by the method of Krogmann and Dodel from $K_2[Pt(ox)_2]\cdot 2H_2O$ (**3**) (47). Oxidants that were used included $(NH_4)_2Ce(NO_3)_6$, $K_2[Pt(ox)_2(OH)_2]\cdot 6H_2O$ (**6**), $K_2[PtCl_6]$ (**2**), and H_2O_2.

Potassium *trans*-dihyroxobis(oxalato)platinate(IV) Hexahydrate (**6**) The preparation is essentially the same as first reported by Werner and more recently modified by Preetz and Dunham (53, 54, 55, 56). One equivalent of $K_2[Pt(ox)_2]\cdot 2H_2O$ (**3**) is oxidized to the Pt(IV) complex with two electron equivalents of H_2O_2. The excess peroxide is removed by evaporation.

Instrumentation and Techniques

Nuclear Magnetic Resonance (NMR)

All NMR spectra were obtained on either Bruker WM250, AC300, or AM500 spectrometers. ^{195}Pt NMR spectra were recorded in 5 mm or 10 mm dual frequency probes operating at 53.52, 64.48 or 107.47 MHz. ^{195}Pt NMR were typically run at 50,000 Hz spectral width for WM250, 60,000 Hz spectral width for AC300, and 125,000 Hz spectral width for the AM500, with 4000-64000 scans, 16K data points, and 0.04 second delay between 30 μs pulses, 50° tilt (WM250); 5 μs pulses, 60° tilt (AC300); 10 μs pulses, 60° tilt (AM500). Signal to noise enhancement was achieved by the application of an exponential weighting of the

data before fourier transformation. The typical exponential weighting was 25 to 75 Hz. Gaussian lineshapes were obtained for high resolution spectra by the application of a gaussian weighting factor before fourier transformation. The typical gaussian weighting factor was -10 to -20 Hz with gaussian broadening of 0.2 to 0.6. High resolution ^{195}Pt NMR spectra were obtained with a 0.5 sec delay between scans. Chemical shifts were measured relative to an external reference of 0.1M $Na_2[PtCl_6]$ (0 ppm) at 25 °C..

Ultraviolet and Visible Spectroscopy

Ultraviolet-Visible (UV-Vis) spectra were collected on a Hewlett Packard HP 8452A Diode Array spectrophotometer at 25 °C. The spectral data were accumulated on an IBM personal computer equipped with Hewlett Packard software. The sample cell and blank cell were quartz cells 1 mm in thickness. The typical concentration of the Pt(II) complex, $K_2[Pt(ox)_2]\cdot 2H_2O$ or $K_2[Pt(mal)_2]\cdot 2H_2O$, was $1x10^{-3}M$ to $5x10^{-3}M$. The diluent employed was various concentraions of CF_3SO_3H and H_2O. Three oxidants were employed; $(NH_4)_2Ce(NO_3)_6$ dissolved in various concentrations of CF_3SO_3H and in H_2O, $K_2[PtCl_6]$ dissolved in various concentrations of CF_3SO_3H and in H_2O, and *trans*-$[Pt(ox)_2(H_2O)_2]$ dissolved in various concentrations of CF_3SO_3H. To monitor the reaction the oxidant was added to the Pt(II) in a reaction vessel and allowed to equilibrate for 20 minutes at 25°C. Samples were then removed from the vessel and measured on the spectrometer.

Fourier Transformed-Infrared (FT-IR) Spectroscopy

FT-IR spectra were recorded on a Bruker 25 FT-IR spectrometer. The collected data were stored and analyzed by a Bruker software package, OPUS 25, on an IBM type personal computer. The solvent for the solution reactions was various concentration of CF_3SO_3D where the acid diluent was D_2O. The concentration of the Pt(II) species, $K_2[Pt(ox)_2]\cdot 2H_2O$, was typically $1x10^{-3}$ M to $5x10^{-3}$ M. The oxidant, dissolved in various concentrations of CF_3SO_3D, was added to the Pt(II) in a reaction vessel at 25°C and allowed to equilibrate for 20 minutes. Samples were removed from the vessel and measured in a BaF_2 cell with a pathlength of 0.2 mm.

pH Measurements

pH measurements were made on a Radiometer Copenhagen multimeter equipped with a standard pH electrode. Two point calibrations were carried out, using pH Standards provided by Aldrich, prior to sample pH base titration measurements and pH oxidative titration measurements. The measurements were made at 25°C with constant stirring. The concentrations of $K_2[Pt(ox)_2]\cdot 2H_2O$ (**3**) used in the oxidative titration was typically $1x10^{-3}$ M to $5x10^{-3}$ M. pH measurements were made at 20 minutes after the samples had equilibrated. The concentration of $K_{1.6}[Pt(ox)_2]\cdot 2H_2O$ (**5**) used in the base titration was $1x10^{-4}$ M (diluent was H_2O). pH measurements were made at 20 minutes after the sample had equilibrated.

RESULTS AND DISCUSSION

Solution Studies of the Oxidation Reaction of $K_2[Pt(ox)_2]\cdot 2H_2O$

This section of the thesis describes the solution chemistry of the oxidation reaction of $K_2[Pt(ox)_2]\cdot 2H_2O$ under acidic conditions to produce the one-dimensional partially oxidized bis(oxalato)platinate polymer, $K_{1.6}[Pt(ox)_2]\cdot 2H_2O$. An understanding of the solution chemistry that occurs in the formation of this one-dimensional polymer is a prerequisite to controlling the polymerization reaction. It is hoped that the eventual control of this reaction will lead to new types of electrical circuitry. In addition, it seems possible that other Pt(II) species such as $[Pt(mal)_2]^{2-}$ may be used in similar polymerization reactions either as a control measure or to form new types of one dimensional platinum polymers. The overall intent of this study, then, is to examine the solution chemistry that is observed in the polymerization reaction to produce the one-dimensional partially oxidized bis(oxalato)platinate polymer, $K_{1.6}[Pt(ox)_2]\cdot 2H_20$, and to investigate the possibility of using another Pt(II) starting material, $K_2[Pt(mal)_2]\cdot 2H_2O$, to form new partially oxidized platinate polymers.

Relatively little has been done to study the polymerization reaction. Solution chemistry studies carried out by Krogmann *et al.* (47, 48) in the late 1960's is essentially the last experimental data available on the solution chemistry of this polymerization. Important information obtained from his work included identifying

solution species of different chain length, proposing a polymerization reaction scheme, and suggesting reasons for the acid dependency of the polymerization reaction. New techniques are now available to reinvestigate this polymerization reaction. Specifically, ^{195}Pt NMR spectroscopy, FT-IR spectroscopy, and UV-Vis spectroscopy (using diode array detectors) have all helped to enhance the experiments which may now be performed on solution reactions.

^{195}Pt NMR is a well established noninvasive method for structure elucidation and determination of reaction mechanisms of platinum complexes (57). In this study it is used to investigate the nature of the specific platinum species formed in solution during the oxidation reaction to produce the polymer. Two principles were used to assign the observed NMR resonances:

1. For monodentate complexes, ^{195}Pt shifts depend in a additive way on the nature of the donor atom (57).

2. When five and six membered bidentate chelate rings are formed between given donor atoms, large upfield shifts are observed (57).

FT-IR spectroscopy is also established as a good noninvasive method for studying the nature of the organic ligands bound to the platinum atoms. The advent of fourier-transformation has increased the capabilities of the old infrared spectrometers tremendously. In this study FTIR is used to study the vibrational frequencies of specific bonds in the organic oxalate ligand bound to the various platinum species formed in solution during the polymerization reaction.

Finally, with the advent of photodiode array detectors, UV-Vis spectroscopy

has become a very valuable tool in studying reactions that occur on a very short time scale, since essentially all visible light wavelengths may be observed at the same time (58). The polymerization reaction to form the partially oxidized platinum chains is quite rapid at ~$10^4 sec^{-1}$ (59). It is therefore reasonable to assume that the new diode array detectors will increase the resolution of the UV-Vis results obtained by Krogmann. This study utilizes UV-Vis spectroscopy to observe solution species formed during oxidation to produce the partially oxidized polymer.

The Results and Discussion section of this thesis is separated into several parts. The first section, "Identification of Solution Species", describes experimental results obtained from the oxidation of $K_2[Pt(ox)_2]\cdot 2H_2O$ under acidic conditions. Four solution species are identified and a polymerization reaction scheme is proposed. The second section of this thesis, "Investigation of the Proposed Reaction Scheme and Solution Species", describes experimental investigation of the four solution species and describes results to support the proposed reaction scheme. The third section, "Examination of the $K_{1.6}[Pt(ox)_2]\cdot 2H_2O$ Polymer", describes experimental results, obtained upon depolymerization of the polymer, that further substantiates the presence of the four solution species and the proposed polymerization reaction scheme. The fourth section, "Role of the Acid in the Polymerization Reaction", describes experimental results that provide insight into the role of the acid in the polymerization reaction to produce the $K_{1.6}[Pt(ox)_2]\cdot 2H_2O$ polymer. Finally, the last section, "Solution Studies of the Oxidation of $K_2[Pt(mal)_2]\cdot 2H_2O$", describes attempts to oxidize $K_2[Pt(mal)_2]\cdot 2H_2O$

in order to form a partially oxidized bis(malonato)platinate polymer.

Identification of Solution Species

UV-Vis Studies

Determination of Solution Species When oxidative titrations of $K_2[Pt(ox)_2]\cdot 2H_2O$ were carried out in 2.2M CF_3SO_3H utilizing Ce^{+4} (supplied as $(NH_4)_2Ce(NO_3)_6$) as an oxidant, four distinct absorbance bands were observed in the UV-Vis spectra. These four absorbance bands occurred at λ_{max} = 426 nm, 510 nm, 600 nm, and 680 nm. In addition, these absorbances appeared as the color of the oxidation reaction proceeded from yellow to orange to brown to blue. The intensity of each of these four absorbances varied as the amount of oxidant added varied. Depending upon the amount of oxidant added, a brownish precipitate of $K_{1.6}[Pt(ox)_2]\cdot 2H_2O$ appeared, after a reaction time of several hours from the blue colored solutions. Also, if the concentration of $[Pt(ox)_2]^{2-}$ in the reaction vessel was increased to a concentration greater than $5x10^{-3}$M the brown $K_{1.6}[Pt(ox)_2]$ precipitate immediately formed. Because of this immediate precipitation reaction, the experiments were all run with the concentration of $[Pt(ox)_2]^{2-}$ at or less than $5x10^{-3}$M. Initial experiments were carried out to determine when the reaction reached steady-state. Figure 19 and Figure 20 are graphs that plot the intensity of each of the four absorbances over time. In Figure 19 Ce^{+4} is the oxidant and

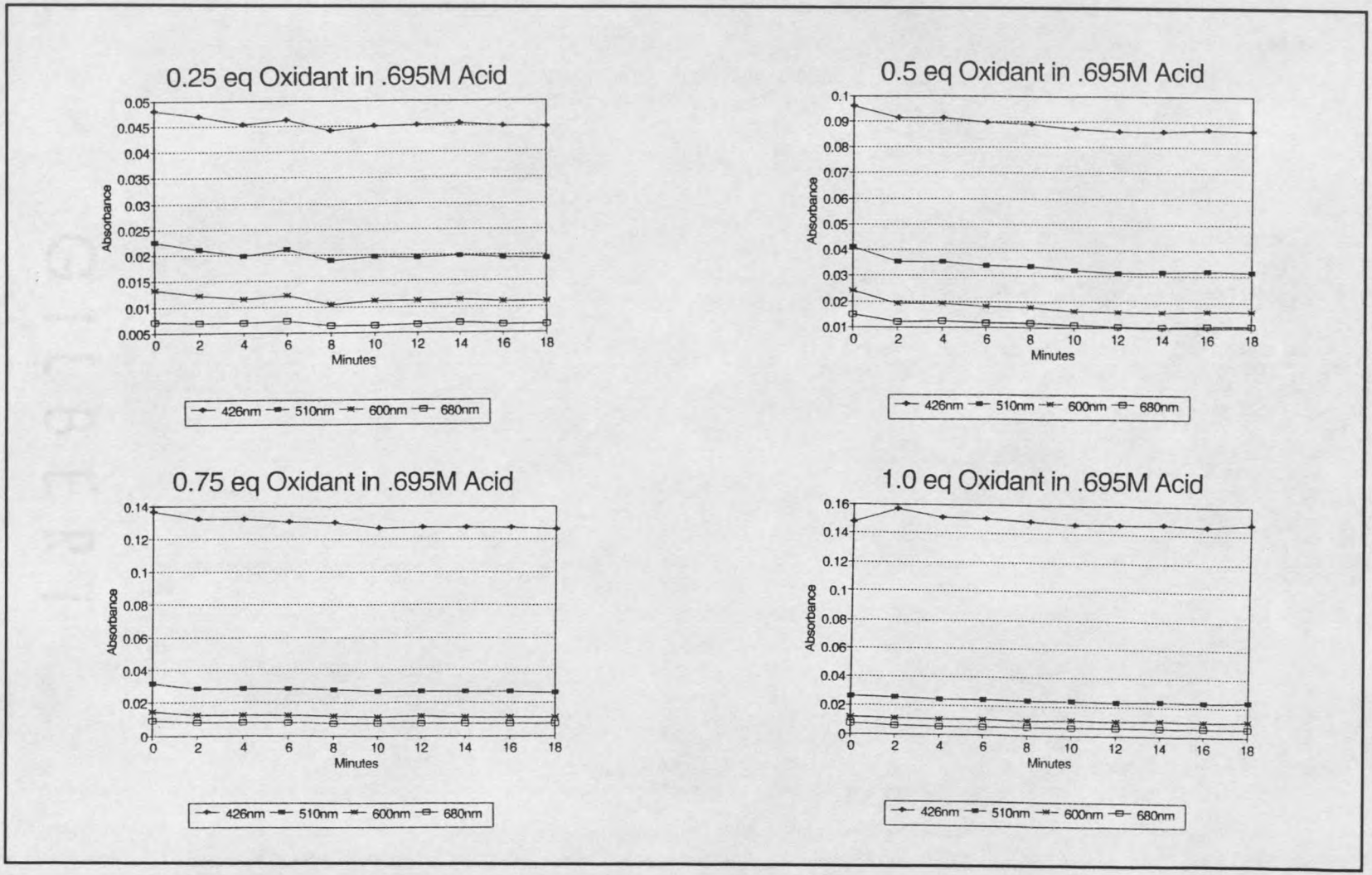

Figure 19. Absorbance values at 426 nm, 510 nm, 600 nm and 680 nm are plotted versus time after the addition of varying electron equivalents of Ce^{4+} to $[Pt(ox)_2]^{2-}$ in .695M CF_3SO_3H.

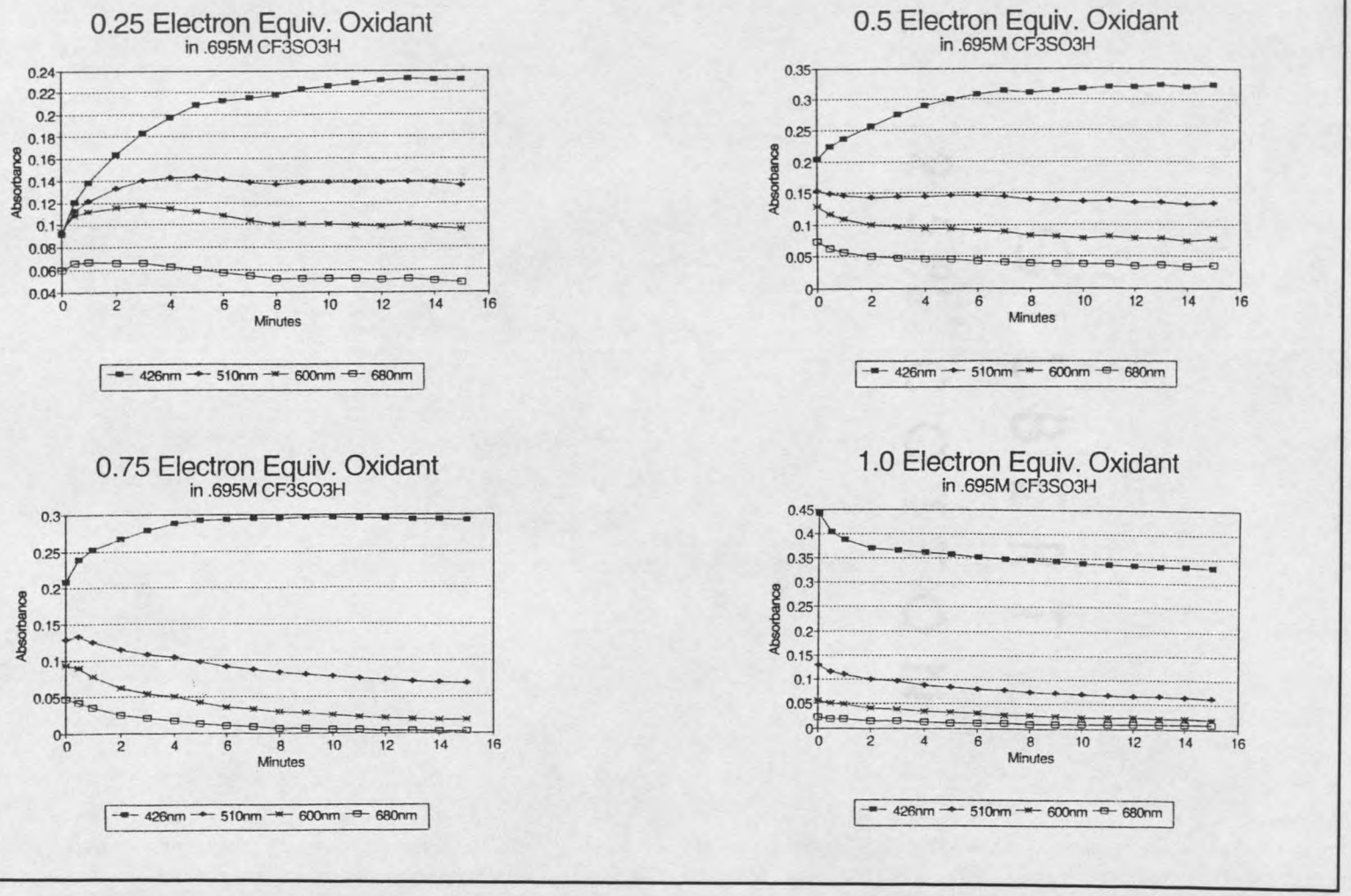

Figure 20. Absorbance values at 426 nm, 510 nm, 600 nm and 680 nm are plotted versus time after the addition of varying electron equivalents of $[PtCl_6]^{2-}$ to $[Pt(ox)_2]^{2-}$ in .695M CF_3SO_3H.

in Figure 20 $[PtCl_6]^{2-}$ is the oxidant. It can be seen that in both cases all four absorbances reach steady-state at 15 to 20 minutes. Because of these results, the oxidative titration measurements were taken at 20 minutes into the reaction. Figure 21 is a graph that plots the results of the oxidative titration experiments. In this experiment Ce^{4+} was utilized as the oxidant. From the plot one observation about the four absorbances can be made. Each of the four absorbances reached maximum intensities at different additions of electron equivalents of oxidant. This means that the four absorbances must correspond to four independent solution species. pH experiments that were conducted (and will be discussed later in this thesis) also confirmed the independent nature of the four solution species. Since each of the four species absorbances reached maxima at different electron equivalents of oxidant, the oxidation state of the platinum in each of the four distinct species may be determined. Referring again to Figure 21, the species at λ_{max} = 426 nm reached its maximum absorbance when 1.0 electron equivalents of oxidant had been added. The color of the reaction solution was orange. A maximum at 1.0 electron equivalents of oxidant would indicate that the average oxidation state of the platinum in the species absorbing at λ_{max} = 426nm is +3.0. The minimum amount of platinum atoms that could be present in a complex with an average Pt oxidation state of +3.0 is one. The chemical formula for such a complex would be $[Pt(ox)_2]_n^{1.0n-}$,**8,** where ≥ 1. Such complexes have precedent and mononuclear Pt(+3) species have been previously isolated (6). Complexes of binuclear platinum compounds containing sulfate, phosphate, and pyrophosphite

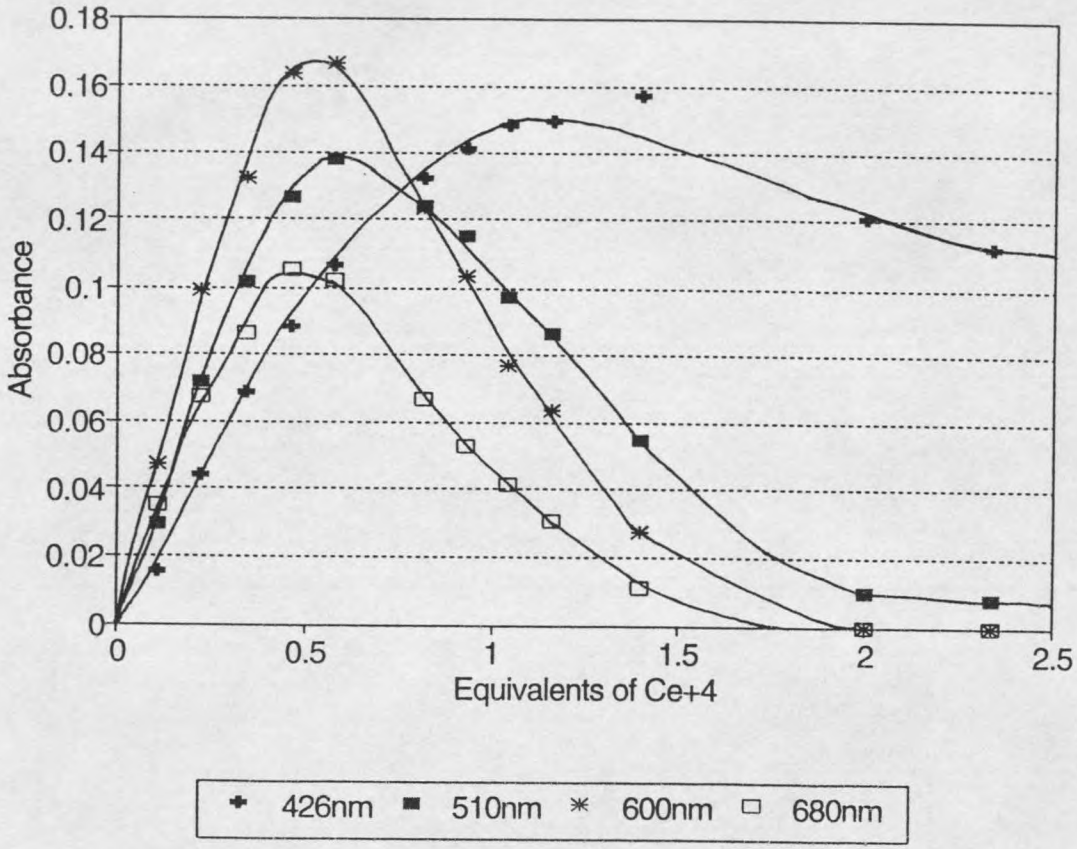

Figure 21. UV-Vis data collected from the oxidative titration of $[Pt(ox)_2]^{2-}$ in 2M CF_3SO_3H. Four absorbance peaks at 426 nm, 510 nm, 600 nm and 680 nm are observed. Ce^{4+} is the oxidant.

bridging ligands were mentioned previously (9, 14, 16). Krogmann's osmotic pressure and conductivity measurements showed the average platinum chain length for this species to be in the range of 1.0 - 1.6 bis(oxalato)platinate units. A maximum chain length of two would be all that could be expected for this species based on Krogmann's values. This would suggest a dimeric Pt(+3) species. The absorption of this Pt(+3) species at λ_{max} = 426 nm is also consistent with the absorption spectra of dinuclear sulfato and phosphato Pt(+3) complexes (12). Reported UV-Vis spectra of the $[Pt_2(pop)_4X_2]^{4-}$ complexes, where X = Cl, Br, and I, reveal absorbance maximums for these complexes at 345 nm, 340 nm, and 435 nm respectively (36).

The species absorbing at λ_{max} = 510 nm reached a maximum at 0.67 electron equivalents of oxidant. The color of the solution was brown. Reaching a maximum at 0.67 electron equivalents of oxidant would be consistent with a complex whose average platinum oxidation state is +2.67. The minimum atoms of platinum that would be required to produce this oxidation state is three. Two Pt(+3) ions, or one dimeric Pt(+3) molecule, could combine with one Pt(+2) ion to give an overall platinum average oxidation state of +2.67. Formally, the chemical formula for such a species would be $[Pt(ox)_2]_n^{1.33n-}$ (9) where $n \geq 3$. The extent of polymerization is unknown, but Krogmann's work suggested a range for the platinum chain length of 1.6 - 1.9 bis(oxalato)platinate monomeric units. If Krogmann's results are accurate a chain length of three would be the maximum degree of polymerization since $n \geq 3$ for this complex.

The species absorbing at λ_{max} = 600 nm reached its maximum at 0.5 electron equivalents of oxidant. The color of the reaction solution was violet. The addition of 0.5 electron equivalents of oxidant would correspond to a species whose average platinum oxidation state is +2.5. This oxidation state could be obtained if one Pt(+3) ion combined with one Pt(+2) ion, or if two Pt(+3) ions (or one dimeric Pt(+3) complex) combined with two Pt(+2) ions. The minimum number of Pt atoms in this species would be two. Formally, the chemical formula for such a complex would be $[Pt(ox)_2]_n^{1.5n-}$ (**10**) where $n \geq 2$. The range of platinum chain length for this species determined by Krogmann was 1.9 - 3.1. The degrees of polymerization determined by Krogmann were based upon comparison of conductivity measurements, f_λ, and freezing point depression measurements, f_{osm}. Because the correlation of f_λ and f_{osm} is not very accurate and there is large error associated with measuring f_{osm}, Krogmann's work is subject to some error. Since Krogmann's work is subject to some error, a maximum degree of polymerization could be at most n = 4. A similar type of polymeric platinum compounds, platinum blues, have been previously studied. These compounds were first reported in 1908 by Hofmann and Bugge from the reaction of $[Pt(CH_3CN)_2Cl_2]$ with $K_2[PtCl_4]$ (60). The major interest in platinum blues came with the discovery of the powerful anti-tumor activities of the platinum blues prepared by the reaction of [*cis*-$Pt(NH_3)_2(H_2O)_2]^{2+}$ with pyrimidines (32, 33, 34). These complexes are blue in color and are composed of chains of platinum atoms. Work by Barton et al. has shown that the α-pyridone blue is formed by the reaction of one Pt(+3) ion with three

Pt(+2) ions to give the four Pt(+2.25) ions found in the α-pyridone blue complex (35, 61, 62, 63, 64). The occurrence of Pt(+3) in the oxidation reaction of $[Pt(ox)_2]^{2-}$ to form the partially oxidized chain compound, $[Pt(ox)_2]_n^{1.6n-}$, and the reaction of this Pt(+3) ion with Pt(+2) ions to produce platinum complexes with platinum in nonintegral oxidation states between Pt(+2) and Pt(+3) seems reasonable. Another typical platinum blue, the tan colored pyridone compound, $[Pt_4(NH_3)_8(C_4H_6NO)_4]^{6+}$, is a tetrameric platinum compound in which the average platinum oxidation state is +2.5 (37, 38). It is interesting to note that the visible spectra of most platinum blues feature a strong absorbance in the 600 nm to 700 nm range (36).

Finally, the species absorbing at λ_{max} = 680 nm reached its maximum at 0.4 electron equivalents of oxidant. This indicates that the average oxidation state of the platinum in this species is +2.4. An average platinum oxidation state of +2.4 could be obtained if three Pt(+2) monomers combined with two Pt(+3) monomers or if three Pt(+2) monomers combined with one Pt(+3) dimer. The minimum amount of platinum atoms in such a species would be five atoms. Formally the chemical formula for this complex would be $[Pt(ox)_2]_n^{1.6n-}$ (**11**) where $n \geq 5$. It should be noted that the platinum oxidation state in the partially oxidized bis(oxalato)platinate salt, $K_{1.6}[Pt(ox)_2]\cdot 2H_2O$, is +2.4, the same as that observed for the species absorbing at λ_{max} = 680 nm. This species was observed by both Krogmann and Pappavasilou, and each assigned the absorbance to an oligomeric bis(oxalato)platinate species (48, 69). The degree of polymerization for this

species is unknown but Krogmann's osmotic pressure/conductivity experiments indicated that the range of the polymerization is 3.1 - 8.7 platinum atoms (48). This is consistent with the minimum n = 5 atoms that has been proposed in this thesis.

Table 5 is a list of the proposed chemical formulae and the corresponding λ_{max} for each of the four species. When $[PtCl_6]^{2-}$ or $[Pt(ox)_2(OH)_2]^{2-}$ were used as oxidants instead of Ce^{+4} the same four absorbances were observed to reach maximums at exactly the same electron equivalents of oxidant as was observed when Ce^{+4} was used as the oxidant. Based on the proposed chemical structures, the idea that the Pt(+3) species is dimeric (evidence for which will be provided later in this paper) and what makes sense chemically, reaction Scheme 1 is proposed for the polymerization reaction of bis(oxalato)platinate(II) to form the partially oxidized bis(oxalato)platinate salt, $[Pt(ox)_2]_n^{1.6n-}$. The initial step is the formation of a Pt(+3) dimeric species, $[Pt^{3+}(ox)_2]_2^{2-}$, upon oxidation of two Pt(+2) monomers, $[Pt(ox)_2]^{2-}$. The simple addition, in each subsequent step, of one $[Pt(ox)_2]^{2-}$ monomer increases the chain length of the resulting species and also changes the average platinum oxidation state. In this manner the trimeric Pt(+2.67) complex, $[Pt^{2.67+}(ox)_2]_3^{4-}$, is formed in the second step. The tetrameric Pt(+2.5) complex, $[Pt^{2.5+}(ox)_2]_4^{6-}$, is formed in the third step. Finally the pentameric Pt(+2.4) complex, $[Pt^{2.4+}(ox)_2]_5^{8-}$, is formed in the fourth step. This scheme is consistent with what is observed experimentally in these experiments and also by Krogmann. The simplicity of the addition reactions also makes sense chemically.

Table 5. The chemical formulae and corresponding λ_{max} for the four species observed in the oxidation reaction of $[Pt(ox)_2]^{2-}$.

COMPLEX	Absorbance Maximum (λ_{max})
$[Pt(ox)_2]_n^{1.0n-}$ (**8**) $n \geq 1$	426 nm
$[Pt(ox)_2]_n^{1.33n-}$ (**9**) $n \geq 3$	510 nm
$[Pt(ox)_2]_n^{1.5n-}$ (**10**) $n \geq 4$	600 nm
$[Pt(ox)_2]_n^{1.6n-}$ (**11**) $n \geq 5$	680 nm

A similar type of cationic monomeric Pt(+2) addition to a cationic dimeric Pt(+3)compound has been reported by Wienkoter et al. for the addition of monomeric *trans*-$[(NH_3)Pt(1\text{-}MeC\text{-}N3)(H_2O)_2]^{2+}$ to dimeric $[Pt_2(NH_3)_2(1\text{-}MeC^{-}\text{-}N3,N4)_2(H_2O)_2]^{2+}$ (1-MeC = 1-methylcytosine) (69).

Scheme 1:

$$2[Pt^{2+}(ox)_2]^{2-} + \text{oxidant} \rightarrow [Pt^{3+}(ox)_2]_2^{2-} \quad [426nm]$$

$$[Pt^{3+}(ox)_2]_2^{2-} + [Pt^{2+}(ox)_2]^{2-} \rightleftharpoons [Pt^{2.67+}(ox)_2]_3^{4-} \quad [510nm]$$

$$[Pt^{2.67+}(ox)_2]_3^{4-} + [Pt^{2+}(ox)_2]^{2-} \rightleftharpoons [Pt^{2.5+}(ox)_2]_4^{6-} \quad [600nm]$$

$$[Pt^{2.5+}(ox)_2]_4^{6-} + [Pt^{2+}(ox)_2]^{2-} \rightleftharpoons [Pt^{2.4+}(ox)_2]_5^{8-} \quad [680nm]$$

This reaction scheme suggests that the addition of $[Pt^{2+}(ox)_2]^{2-}$ to **8** should

shift the equilibrium to form the complexes containing longer chains of platinum atoms, **9**, **10**, **11**. The species absorbing at longer wavelengths in the UV-Visible spectrum would then be favored. When increasing amounts of $[Pt^{2+}(ox)_2]^{2-}$ were added to a reaction mixture of $[Pt^{3+}(ox)_2]_2^{2-}$ in 2.2M CF_3SO_3H the UV-Vis spectra did indeed show the shift in absorbances from the lower wavelength at 426 nm to the longer wavelengths at 600 nm and 680 nm (Figure 22). Initially only the dimeric $[Pt^{3+}(ox)_2]_2^{2-}$, was present and absorbing at 426 nm. As $[Pt(ox)_2]^{2-}$ was added to the $[Pt^{3+}(ox)_2]_2^{2-}$ dimer, the absorbance at 426 nm decreased and the absorbance at 510 nm increased. As more $[Pt(ox)_2]^{2-}$ was added the dominant species absorbing in the UV-Vis region was at 600 nm and then at 680 nm. These results were consistent with the proposed reaction scheme.

^{195}Pt NMR Studies

Determination of Solution Species When increasing amounts of Ce^{+4} were added to $[Pt(ox)_2]^{2-}$ in 2.2M CF_3SO_3H the ^{195}Pt resonance of $[Pt(ox)_2]^{2-}$, initially a sharp peak at -525 ppm, broadened until finally no peak for $[Pt(ox)_2]^{2-}$ the species was observed at all. Corresponding with this, the color of the reaction mixture changed from yellow to blue (λ_{max}= 680 nm and 600 nm). When 1.0 electron equivalent of Ce^{+4} had been added the reaction mixture was an orange color (λ_{max} = 426 nm), and one ^{195}Pt resonance was observed at 1150 ppm (Figure 23). The resonance at 1150 ppm is consistent with that of a Pt(+3) dimeric species in which the platinum atoms are equivalent since only one peak is observed. This same

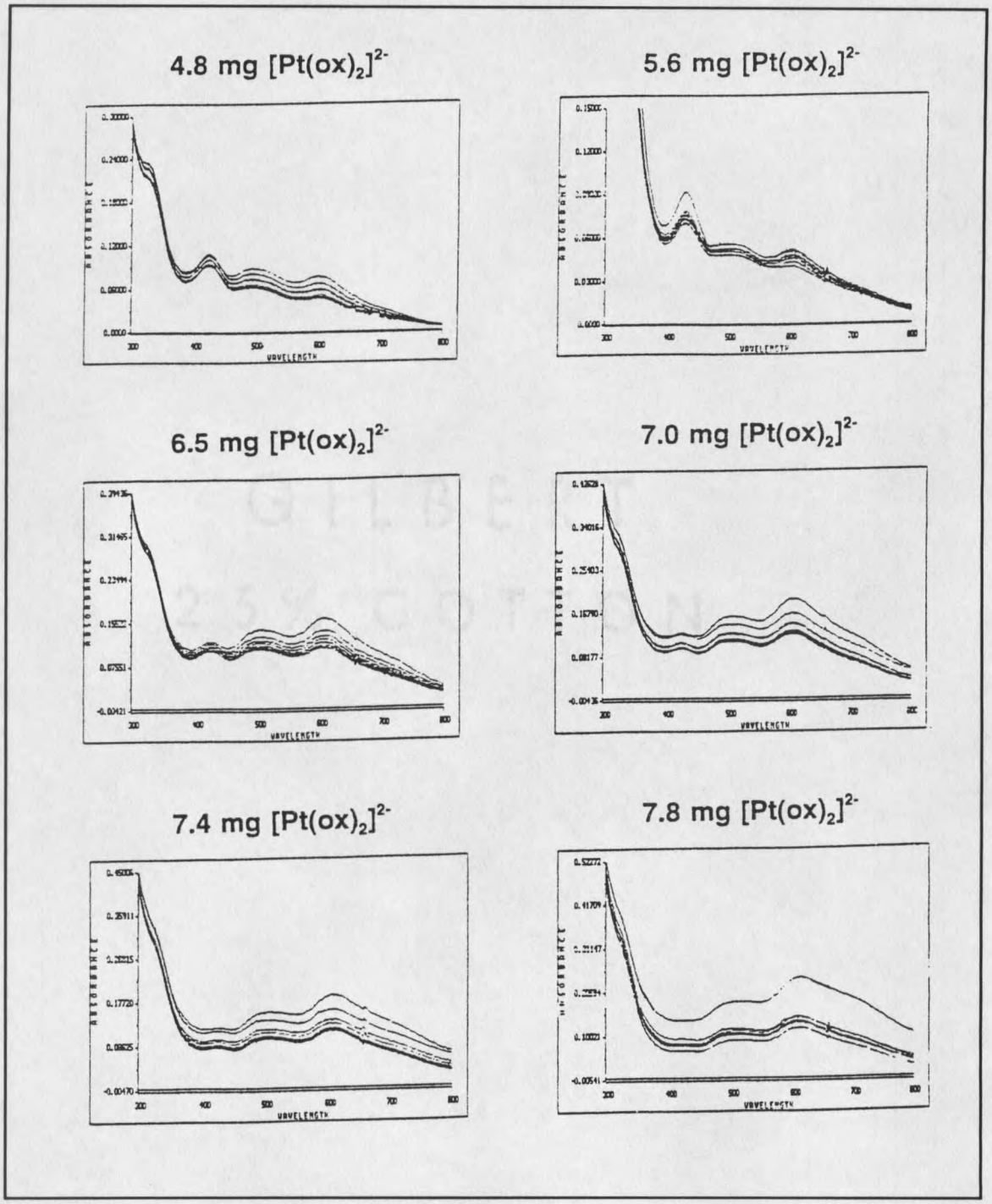

Figure 22. Increasing amounts of $[Pt(ox)_2]^{2-}$ are added to a fixed concentration of $[Pt^{3+}(ox)_2]_2^{2-}$. Each of these spectra represent the addition of a different amount of $[Pt(ox)_2]^{2-}$ (in mg) to the dimer, $[Pt^{3+}(ox)_2]_2^{2-}$. In each case the overlayed spectra represent absorbance measurements made at two minute intervals for 20 minutes.

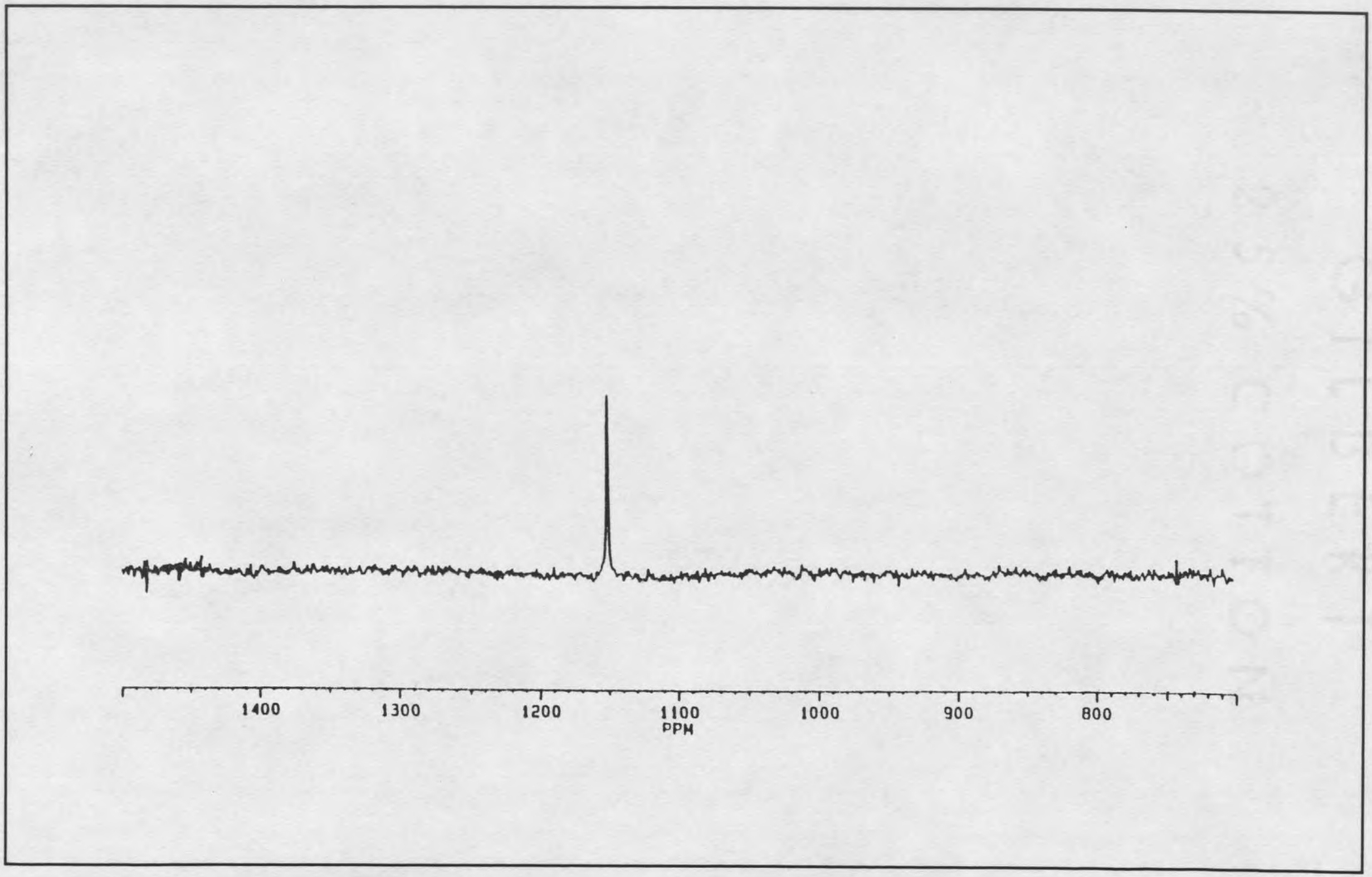

Figure 23. ^{195}Pt NMR spectra obtained after 1.0 electron equivalents of Ce^{4+} has been added to $[Pt(ox)_2]^{2-}$ in 2M CF_3SO_3H.

species had been previously observed by Dunham *et al.* (59). Mononuclear Pt(+3) would be paramagnetic (d^7), and would not be observed in the ^{195}Pt NMR spectrum. The chemical shift, 1150 ppm, is 600 ppm upfield from known binuclear Pt(+3) complexes with oxygen donating ligands. The $[Pt_2(\mu\text{-}SO_4)_4(H_2O)_2]^{2-}$ complex has a ^{195}Pt resonance occurring at 1756 ppm (10), and the $[Pt_2(\mu\text{-}HPO_4)_4(H_2O)_2]^{2-}$ complex has a ^{195}Pt resonance at 1796 ppm (10). Two possible structures for the dimeric Pt(+3) species are shown in Figure 24. The oxalato ligands may be bound in one of two ways. The first would be the formation of a bridge between the two platinum metal centers. This bridging is consistent with the sulfato and phosphato dimers previously mentioned. The second type of binding for the oxalato ligand is bidentate nonbridging. Although it was once thought that bridging ligands were necessary to stabilize the Pt(III)-Pt(III) complex, recent reports have shown this not to be the case. The first report of a dinuclear Pt(III) complex having no ligands bridging the two metal centers was presented in 1991 (30). The isolated complex, $[Pt_2Cl_6(NH{=}C(OH)C(CH_3)_3)_4]$, is shown in Figure 25a. It is synthesized by chlorine oxidation of the monomeric platinum(II) complex *cis*-$[PtCl_2(NH{=}C(OH)C(CH_3)_3)_2]$ (Figure 25b). The complex is stable in solution containing Cl_2 for a few days, but disproportionates into the corresponding Pt (II) and Pt(IV) species, *cis*-$[PtCl_2(NH{=}C(OH)C(CH_3)_3)_2]$ and *cis*-$[PtCl_4(NH{=}C(OH)C(CH_3)_3)_2$ respectively (Figures 25b and 25c) when Cl_2 is not present. Interestingly, $[Pt^{3+}(ox)_2]_2^{2-}$ (**8**) is not stable for periods longer than a few days, as will be described later in this thesis. In addition, $[Pt^{3+}(ox)_2]_2^{2-}$ (**8**) is more

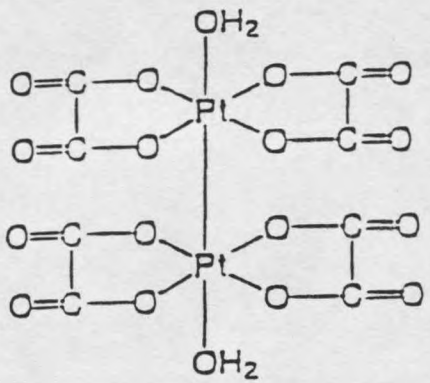

I

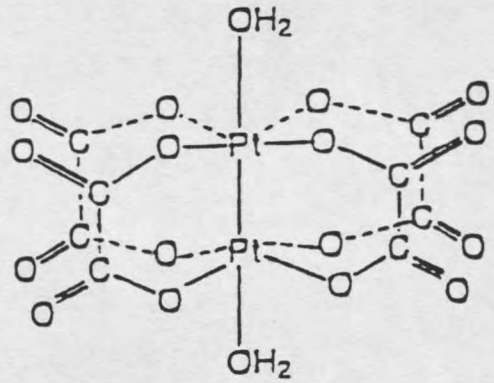

II

Figure 24. Possible structures for the dimeric Pt^{3+} complex, $[Pt^{3+}(ox)_2(OH_2)]_2^{2-}$.

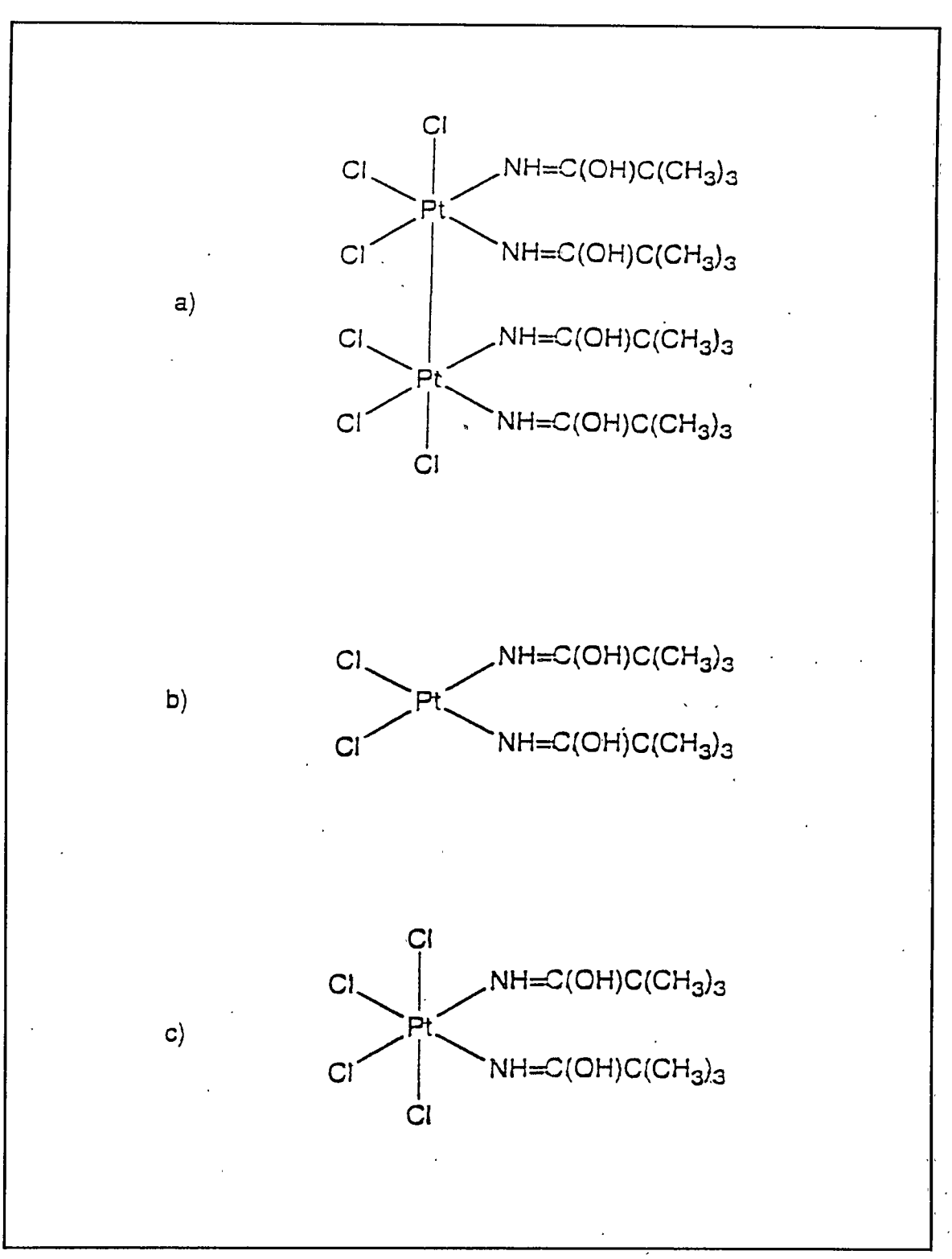

Figure 25. Structures of a) $[Pt_2Cl_6(NH{=}C(OH)C(CH_3)_3)_4]$ b) *cis*-$[PtCl_2(NH{=}C(OH)C(CH_3)_3)_2]$ c) *cis*-$[PtCl_4(NH{=}C(OH)C(CH_3)_3)_2]$.

stable in the presence of the oxidant, O_2, than it is in the absence of O_2. The 600 ppm upfield shift relative to the sulfato and phosphato dimeric Pt(III) would also be consistent with bidentate oxalate ligands. Table 6 lists the ^{195}Pt NMR resonances that were observed in this study along with known resonances of other relevant Pt complexes.

Table 6. ^{195}Pt NMR resonances for Pt complexes observed in this study and other pertinent Pt complexes.

COMPLEX	^{195}Pt Resonance
$[Pt(ox)_2]^{2-}$ (**3**)	- 525 ppm
[*trans*-$Pt(ox)_2(OH)_2]^{2-}$ (**6**)	2873 ppm
$[Pt(ox)_2]_2^{2-}$ (**8**)	1150 ppm
$[Pt_2(\mu\text{-}SO_4)_4(H_2O)_2]^{2-}$	1756 ppm
$[Pt_2(\mu\text{-}HPO_4)_4(H_2O)_2]^{2-}$	1796 ppm

Investigation of the Proposed Reaction Scheme and Solution Species

This section of the thesis describes the investigation of the specific solution species and the polymerization reaction scheme proposed in the previous section. Each of the four solution species were investigated. Due to its ease of isolation, the Pt^{3+} complex, $[Pt(ox)_2]_3^{4-}$, was the first species to be examined. Experiments were carried out to determine whether this complex is a diamagnetic or paramagnetic species, and thereby give evidence for or against the proposed

dimeric structure. The determination of an extinction coefficient enabled subsequent experiments to be performed to determine the concentration of Pt^{3+} in the polymeric $K_{1.6}[Pt(ox)_2]\cdot 2H_2O$. Finally, reactions of this Pt^{3+} complex with $[Pt(mal)_2]^{2-}$ and KCl were examined to provide information supporting the proposed chemical formula.

The second complex to be examined in this section is the $Pt^{2.67+}$ complex, $[Pt(ox)_2]_3^{4-}$. The ability to isolate this complex is somewhat limited, but it can be accomplished through control of concentration and pH. As will be discussed later, each of the four solution complexes have unique pH requirements. Because of this pH distinction between the species, conditions were found whereby the Pt^{3+} complex, $[Pt(ox)_2]_2^{2-}$, and the $Pt^{2.67+}$ complex, $[Pt(ox)_2]_3^{4-}$, could be isolated from the $Pt^{2.5+}$ complex, $[Pt(ox)_2]_4^{6-}$, and the $Pt^{2.4+}$ complex, $[Pt(ox)_2]_5^{8-}$. In addition, dilution of the reaction mixture reverses the polymerization reaction, so by choosing appropriately dilute solution conditions the Pt^{3+} complex, $[Pt(ox)_2]_2^{2-}$, and the $Pt^{2.67+}$ complex, $[Pt(ox)_2]_3^{4-}$, could be isolated from the $Pt^{2.5+}$ complex, $[Pt(ox)_2]_4^{6-}$, and the $Pt^{2.4+}$ complex, $[Pt(ox)_2]_5^{8-}$. An extinction coefficient was determined for this species which allowed for subsequent determination of a conditional formation constant. Examination of the conditional formation constant under conditions of varying oxidation can utilized to confirm or refute the proposed reaction scheme to produce the $Pt^{2.67+}$ complex.

Finally, a limited examination of the $Pt^{2.5+}$ and $Pt^{2.4+}$ complexes was attempted. Reaction conditions were not found where the two complexes could

be separated from one another to any significant extent. Although the pH requirements of these two species is different, conditions were not found whereby the two complexes could be separated.

Investigation of the Pt^{3+} Species, $[Pt(ox)_2]_2^{2-}$

UV-Vis Studies

Determination of an Extinction Coefficient for $[Pt^{3+}(ox)_2]_2^{2-}$ When oxidative titrations were carried out in H_2O only the $[Pt^{3+}(ox)_2]_2^{2-}$ species absorbing at 426 nm was observed. Figure 26 shows the results of the oxidative titration of $[Pt(ox)_2]^{2-}$ in H_2O using $[PtCl_6]^{2-}$ as the oxidant. As before, the absorbance at λ_{max} = 426 nm reached a maximum at 1.0 electron equivalent of oxidant. In acidic solution all four species were observed in various amounts relative to the equilibrium relationships they have with each other. Because there is overlap of the four absorbances extinction coefficients were not able to be determined. Since only the Pt (+3) dimeric species, $[Pt^{3+}(ox)_2]_2^{2-}$, (absorbing at λ_{max} = 426) was present when the oxidation was carried out in H_2O an extinction coefficient for this species could be determined. The extinction coefficient for the Pt(+3) dimer at 426 nm is 1220 cm^{-1} M^{-1}.

Reacting $[Pt(mal)_2]^{2-}$ with $[Pt^{3+}(ox)_2]_2^{2-}$ Quite by accident it was discovered that if $[Pt(mal)_2]^{2-}$ (**4**) was added to the dimeric $[Pt^{3+}(ox)_2]_2^{2-}$ species in H_2O or acid,

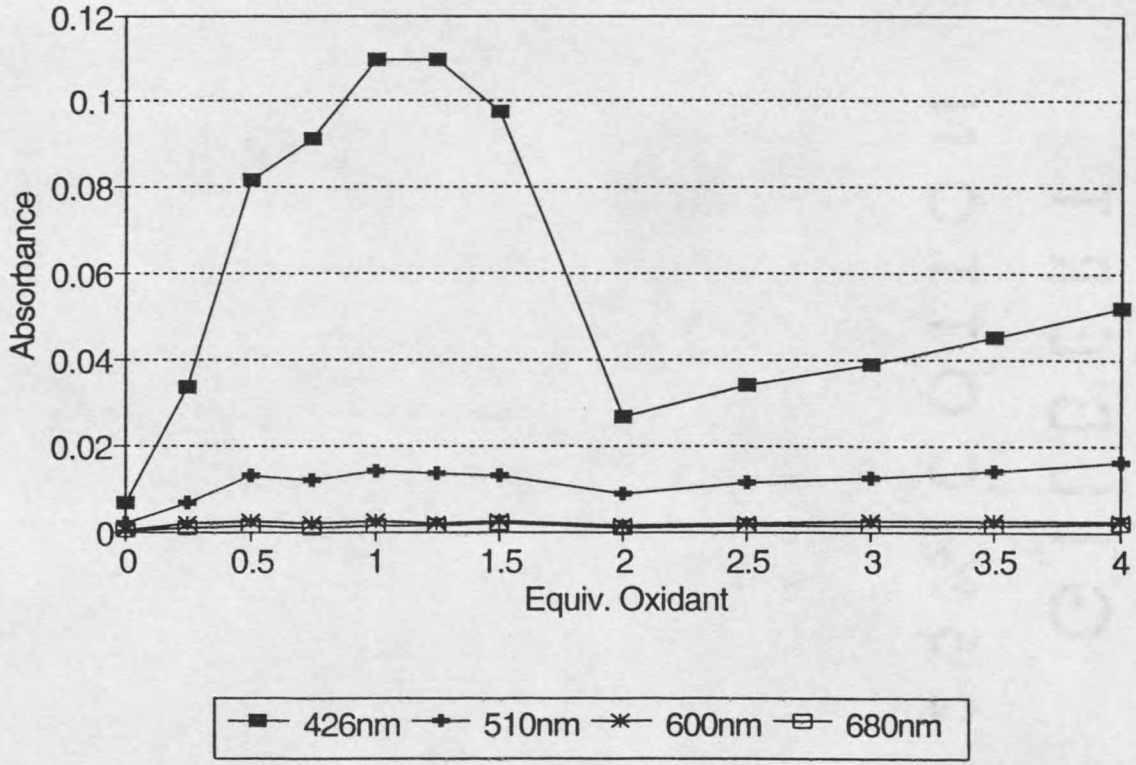

Figure 26. UV-Vis data collected of the oxidative titration of $[Pt(ox)_2]^{2-}$ in H_2O. Four absorbance peaks are monitored at 426 nm, 510 nm, 600 nm and 680 nm. The oxidant is $[PtCl_6]^{2-}$.

the absorbance at λ_{max} = 426 nm could be made to disappear. Specifically, when the ratio of $[Pt(mal)_2]^{2-}$ /$[Pt(ox)_2]^{2-}$ reached 1:4 the absorbance at 426 nm is gone (Figure 27). It is not known what specifically has happened to the $[Pt(ox)_2]_2^{2-}$ dimer, **8**, but ^{195}Pt NMR (discussed below) correlates the disappearance of the 1150 ppm resonance and the appearance of two new Pt(+3) species at 1438 ppm and 1440 ppm. These same results were observed if only malonic acid was added to the dimeric $[Pt^{3+}(ox)_2]_2^{2-}$ complex. However, the reaction time was significantly increased. The $[Pt(mal)_2]^{2-}$ reacted within minutes while the malonic acid reacted over 24 hours. The resonances at 1438 ppm and 1440 ppm were only present when both oxalate and malonate were present with the $[Pt^{3+}(ox)_2]_2^{2-}$ complex. This same result was observed by Dunham *et al.* (59). The disappearance of the absorbance at 426 nm and the corresponding disappearance of the ^{195}Pt resonance at 1150 ppm further substantiate that the same solution species (i.e. $[Pt^{3+}(ox)_2]_2^{2-}$)is responsible for both the electronic absorption at 426 nm and the ^{195}Pt resonance at 1150 ppm.

Determination of the Stability of $[Pt^{3+}(ox)_2]_2^{2-}$ Experiments were carried out to determine the stability of the Pt species. Essentially, the $[Pt^{3+}(ox)_2]_2^{2-}$ dimeric complex was made under both oxidative (aerobic) conditions and nonoxidative (anaerobic) conditions and the absorbance at λ_{max}= 426 nm was observed over time (Figures 28 and 29). It is apparent that the dimer is more stable under aerobic conditions where O_2 is present. This result is similar to that observed by

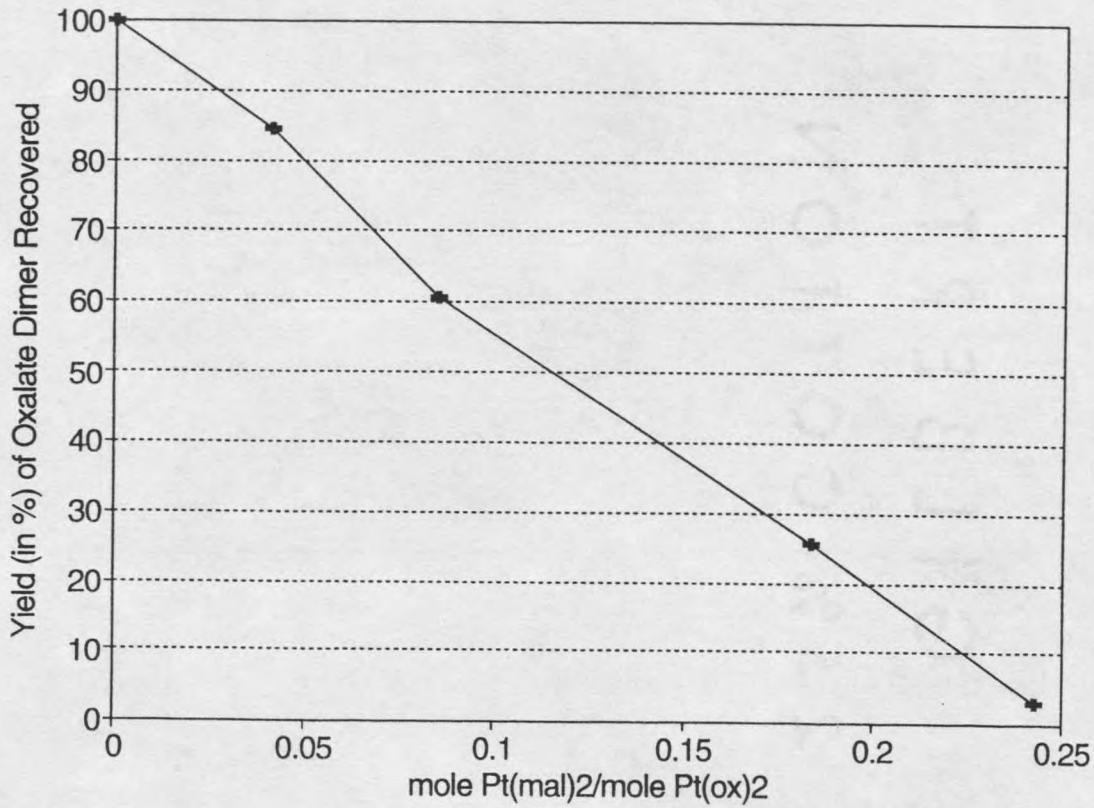

Figure 27. The observed yield of $[Pt^{3+}(ox)_2]_2^{2-}$ is plotted versus the ratio of $[Pt(mal)_2]^{2-}$ to $[Pt(oxl)_2]^{2-}$ present in the oxidation reaction of $[Pt(ox)_2]^{2-}$ with Ce^{4+} (oxidant) under acidic conditions. The addition of $[Pt(mal)_2]^{2-}$ inhibits the formation of the $[Pt^{3+}(ox)_2]_2^{2-}$.

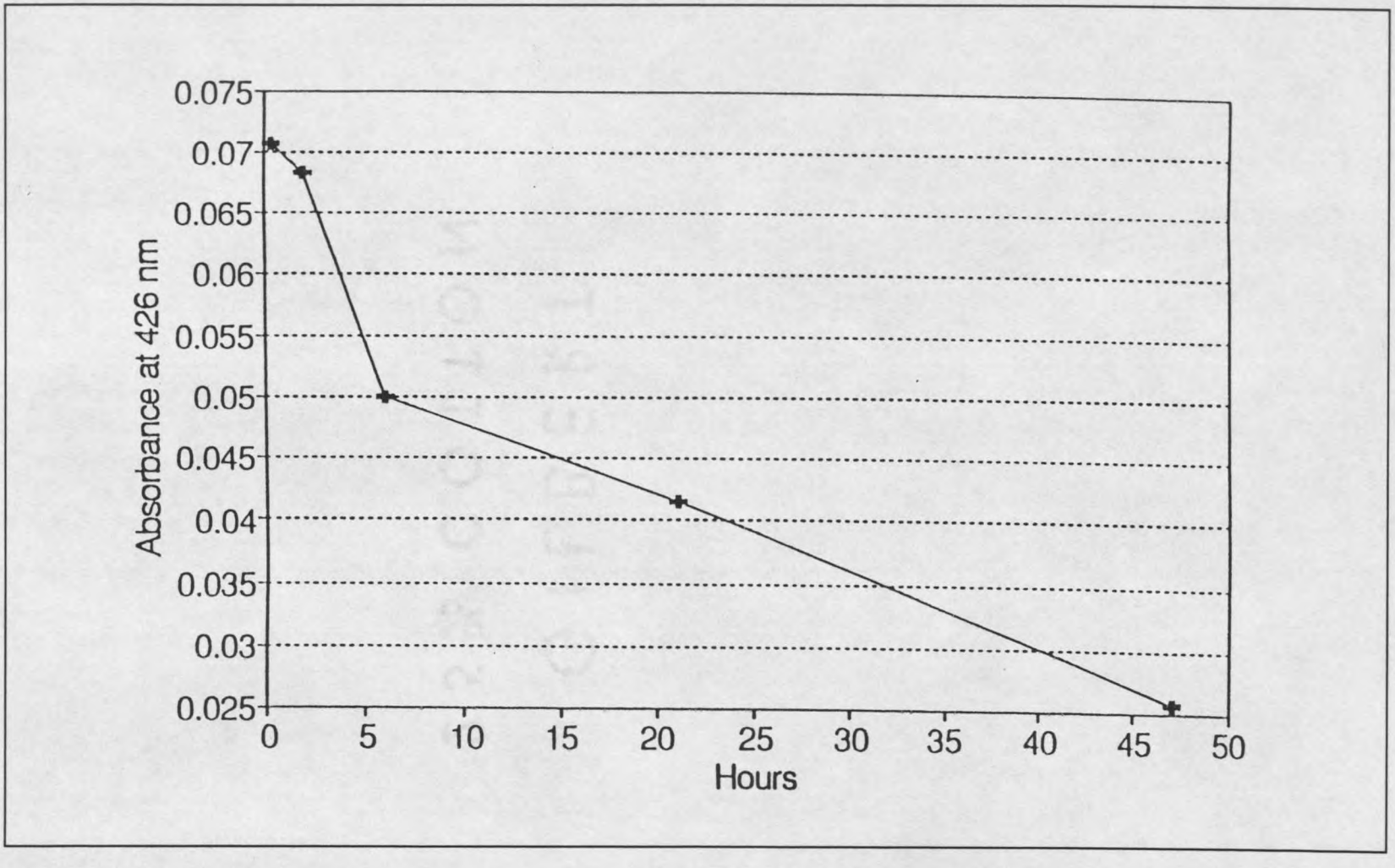

Figure 28. UV-Vis is utilized to observe the disappearance of $[Pt^{3+}(ox)_2]_2^{2-}$ through the disappearance of the 426 nm absorbance band over time. Here the absorbance at 426 nm is plotted against time (hours). The reaction conditions are acidic and aerobic (O_2 is present).

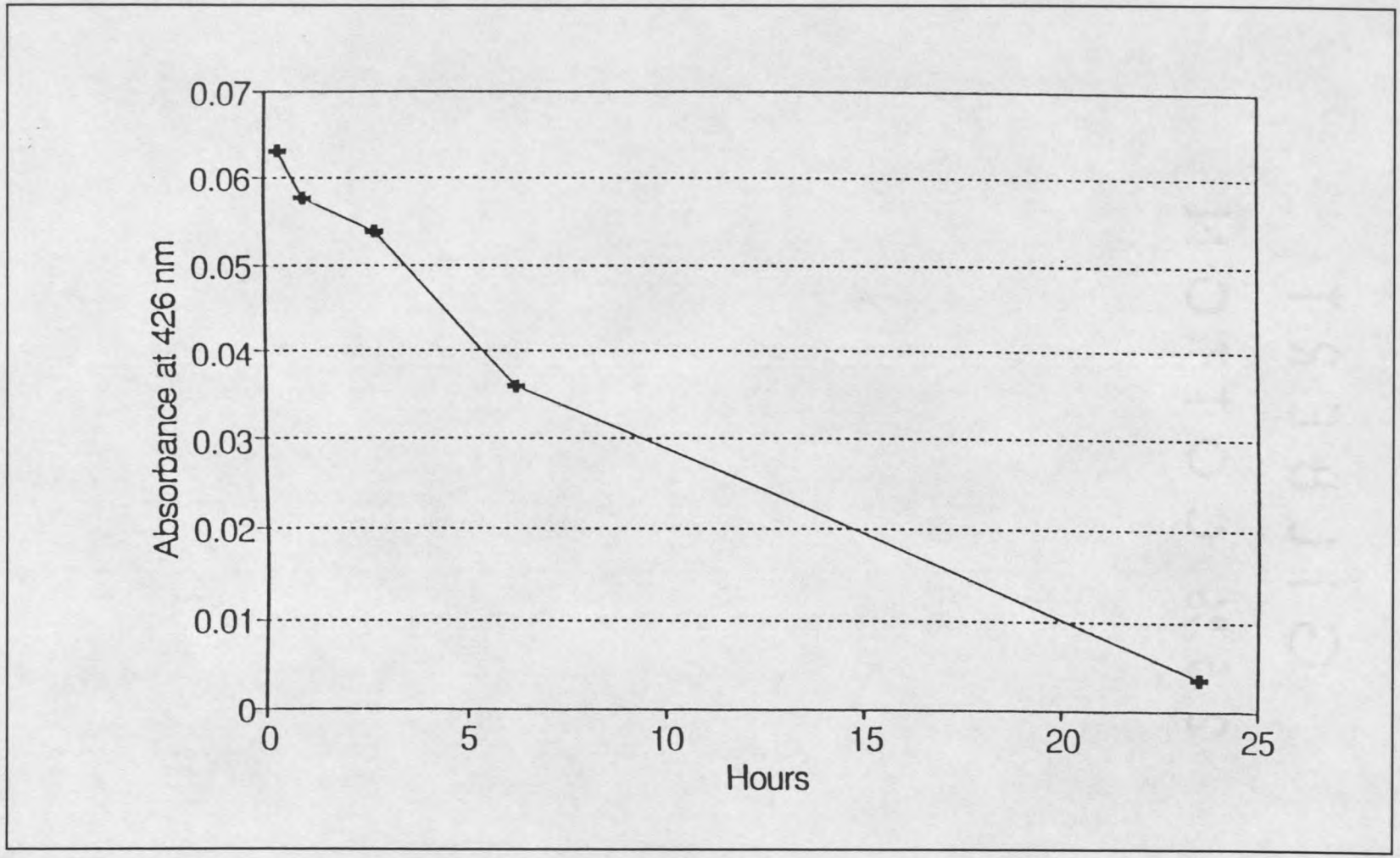

Figure 29. UV-Vis is utilized to observe the disappearance of $[Pt^{3+}(ox)_2]_2^{2-}$ through the disappearance of the 426 nm absorbance band over time. Here the absorbance at 426 nm is plotted against time (hours). The reaction conditions are acidic and anaerobic (O_2 is not present).

Cini *et al.* (30) for the nonbridging Pt(III) dimer, $[Pt_2Cl_6(NH=C(OH)C(CH_3)_3)_4]$. This dimeric Pt(III) species is stable only for a few days in solution containing the oxidant Cl_2. Under nonoxidative conditions this dimer rapidly disproportionates into the corresponding Pt(II) and Pt(IV) species (Figure 25c). The instability of the $[Pt^{3+}(ox)_2]_2^{2-}$ dimeric complex in this study explains the inability to obtain crystals of the Pt(III) complex, $[Pt^{3+}(ox)_2]_2^{2-}$.

^{195}Pt NMR Studies

Reaction of $[Pt(mal)_2]^{2-}$ with $[Pt^{3+}(ox)_2]_2^{2-}$ When the oxidative titration of $[Pt(ox)_2]^{2-}$ was carried out in water only two ^{195}Pt resonances were observed, the $[Pt(ox)_2]^{2-}$ resonance at -525 ppm and the Pt(III) dimer, $[Pt^{3+}(ox)_2]_2^{2-}$, resonance at 1150 ppm. When $[Pt(mal)_2]^{2-}$ was added to the dimeric $[Pt^{3+}(ox)_2]_2^{2-}$ complex in increasing increments the ^{195}Pt NMR spectrum reflected the results observed in the UV-Vis experiments described above. The 1150 ppm resonance disappeared as the $[Pt(mal)_2]^{2-}$ was added in increasing amounts. In addition a new resonance appeared at 1440 ppm and increased as the $[Pt(mal)_2]^{2-}$ was added. A second ^{195}Pt resonance at 1438 ppm appeared half way through the addition of the malonato complex and increased until both resonances at 1438 ppm and 1440 ppm were equal in intensity. Figure 30 shows the ^{195}Pt NMR spectra observed as the $[Pt(mal)_2]^{2-}$ species was added to the $[Pt^{3+}(ox)_2]_2^{2-}$ dimeric complex . As mentioned above this experiment confirms that the $[Pt^{3+}(ox)_2]_2^{2-}$ species, absorbing

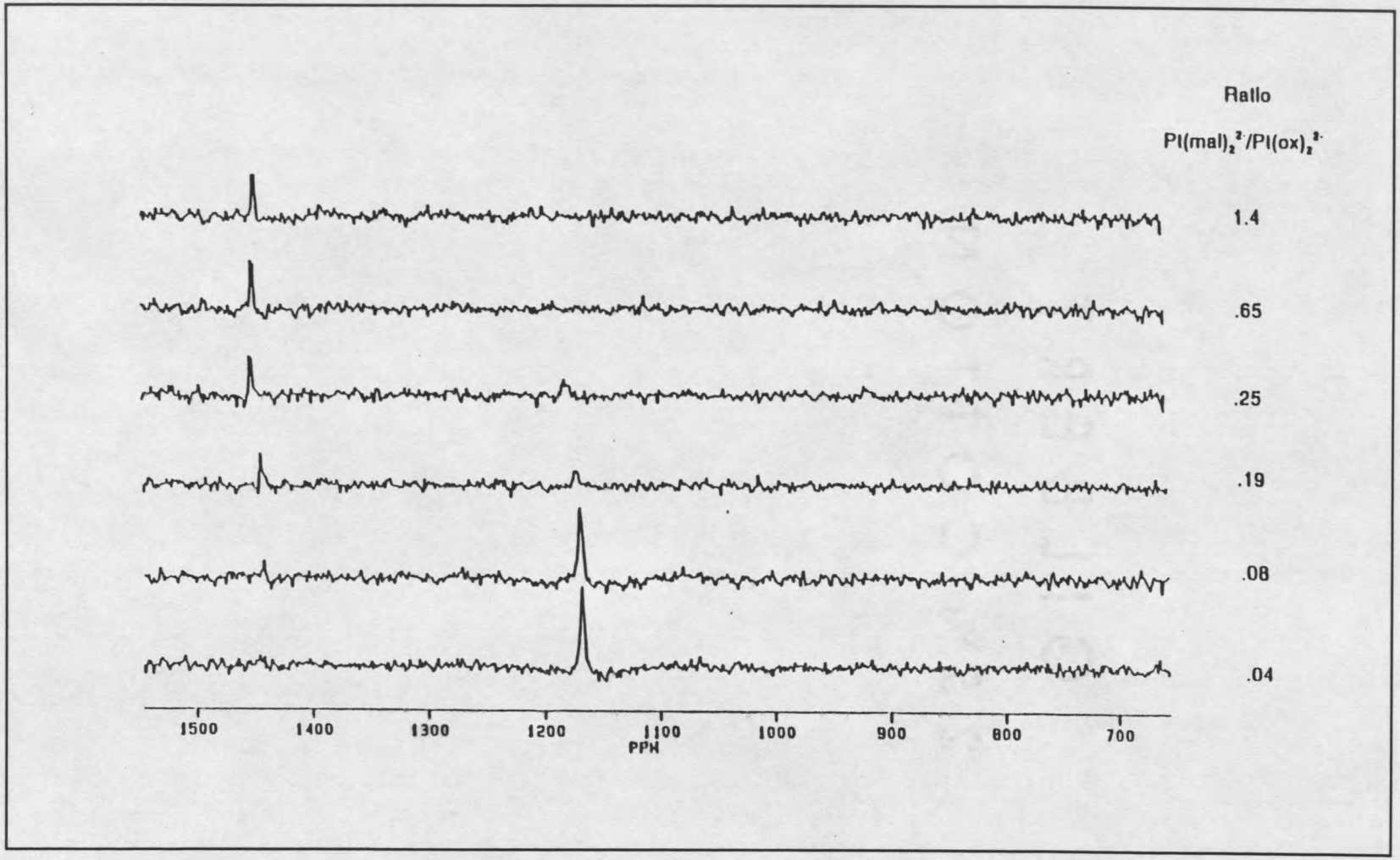

Figure 30. ^{195}Pt NMR spectra of $[Pt^{3+}(ox)_2]_2^{2-}$ is observed as increasing amounts of $[Pt(mal)_2]^{2-}$ is added to the $[Pt(ox)_2]^{2-}$ in the oxidation reaction to produce $[Pt^{3+}(ox)_2]_2^{2-}$. The overlayed spectra represent the $[Pt^{3+}(ox)_2]_2^{2-}$ resonance that is observed when the ration of $[Pt(mal)_2]^{2-}$ to $[Pt(ox)_2]^{2-}$ in the oxidation reaction is changed.

at λ_{max} = 426 nm, is indeed the same species that produces the ^{195}Pt resonance at 1150 ppm. It is not known what platinum complex(es) produced the 1438 ppm and 1440 ppm resonances. It is known that both oxalate and malonate are required. The 1438 ppm and 1440 ppm resonances are consistent with dimeric Pt(III) complexes containing oxygen ligands for the same reasons previously described for the $[Pt^{3+}(ox)_2]_2^{2-}$ dimer.

Addition of KCl to $[Pt^{3+}(ox)_2]_2^{2-}$ When acidic solutions of the $[Pt^{3+}(ox)_2]_2^{2-}$ complex were subjected to the addition of a saturated solution of KCl the solution color changed from orange to yellow. The color change was accompanied by the disappearance of the 426 nm band in the UV-Vis spectrum. ^{195}Pt NMR of the sample revealed the disappearance of the ^{195}Pt resonance at 1150 ppm and the appearance of two ^{195}Pt resonances at -1660 ppm and 2421 ppm (Figure 31). The -1660 ppm resonance correlates to the $[PtCl_4]^{2-}$ complex and the 2421 ppm resonance has been previously assigned to *trans*-$[Pt(OH)Cl(ox)_2]^{2-}$ (45). The ratio of the two species to one another was 0.9. This evidence further supports a dimeric Pt(III) structure where the oxalate ligands are bound in a bidentate fashion rather than in a bridging fashion. It appears from the experimental results that the addition of the KCl to the dimer resulted in a Cl^- ligand replacing a water molecule in one of the trans positions on the Pt(III) dimer. The adding of the Cl^- would then displace the electron density around the metal-metal center such that disproportionation into a Pt(II) complex and a Pt(IV) complex would occur (Figure

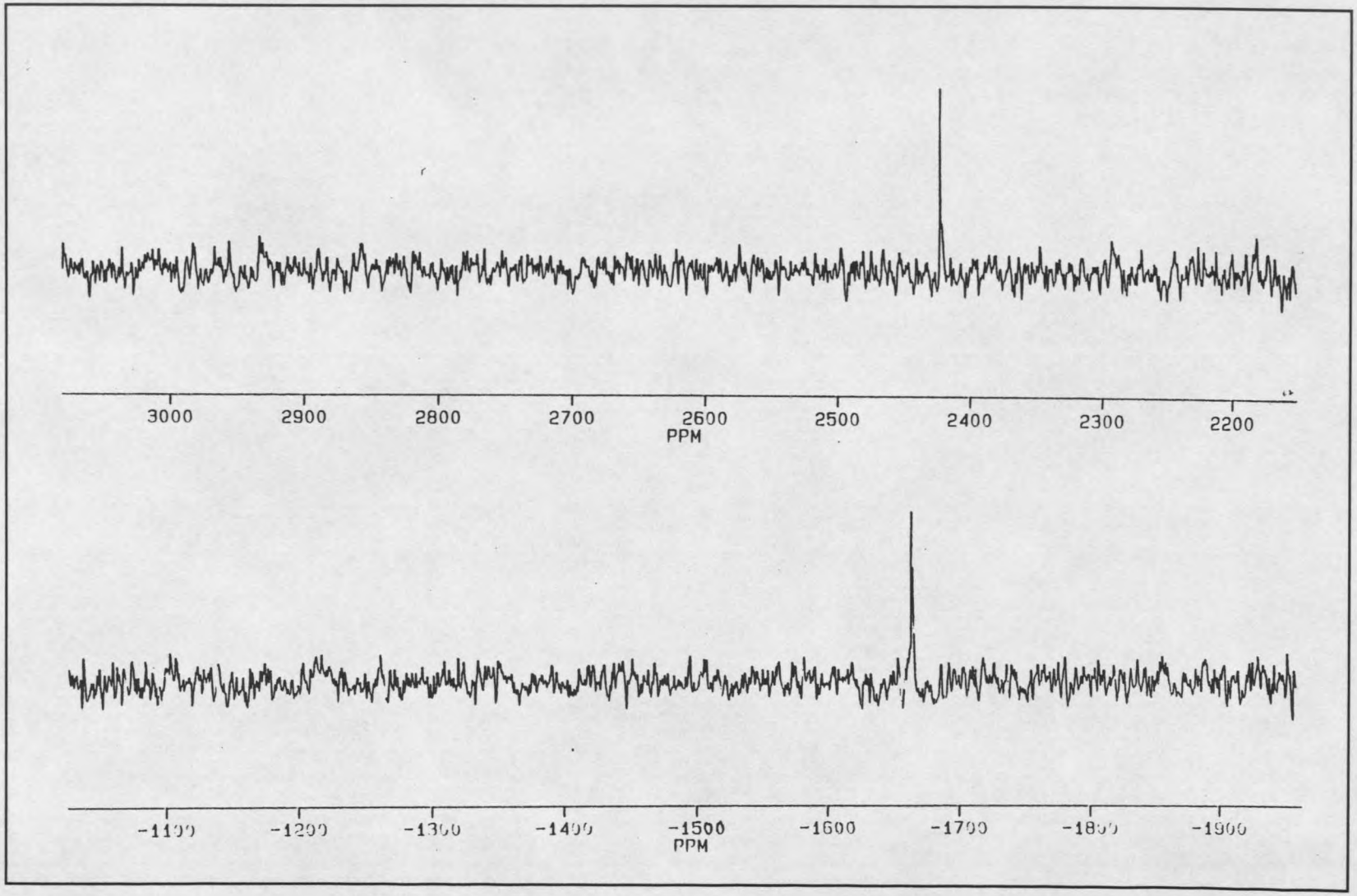

Figure 31. ^{195}Pt NMR spectra observed when KCl is added to a solution containing $[Pt^{3+}(ox)_2]_2^{2-}$.

32). Since Pt(IV) is inert to substitution the oxalate ligands remain bound to the Pt metal and a H_2O molecule is immediately taken up in the second trans position. The Pt(II) species is not inert to substitution, and Cl^- ligands would immediately substitute for the oxalate ligands to produce the $[PtCl_4]^{2-}$ complex.

Investigation of the $Pt^{2.67+}$ Species, $[Pt(ox)_2]_3^{4-}$

UV-Vis Studies

Determination of an Extinction Coefficient for $[Pt(ox)_2]_3^{4-}$ As will be discussed later in this thesis, the four solution species exhibit different dependencies upon H^+ concentration. At lower H^+ concentrations it is possible to create a condition whereby only the species absorbing at λ_{max} = 426 nm and λ_{max} = 510 nm are present. When oxidative titrations of $[Pt(ox)_2]^{2-}$,utilizing Ce^{4+} as the oxidant, were carried out in less acidic (0.25 M CF_3SO_3H) and more dilute conditions (Concentration of $[Pt(ox)_2]^{2-} = 4x10^{-4}$ M; UV-Vis cell pathlength = 2.5 cm) only the $[Pt^{3+}(ox)_2]_2^{2-}$ species absorbing at λ_{max} = 426 nm and the $[Pt^{2.67+}(ox)_2]_3^{4-}$ species absorbing at λ_{max} = 510 nm were observed. Since the amount of oxidant added to the $[Pt(ox)_2]^{2-}$ was known and the extinction coefficient of the $[Pt^{3+}(ox)_2]_2^{2-}$ species absorbing at λ_{max} = 426 nm was known the concentrations of $[Pt^{3+}(ox)_2]_2^{2-}$ and $[Pt^{2.67+}(ox)_2]_3^{4-}$ could be determined. The extinction coefficient of the $[Pt^{2.67+}(ox)_2]_3^{4-}$ species absorbing at λ_{max} = 510 nm was determined to be 600 cm^{-1} M^{-1}.

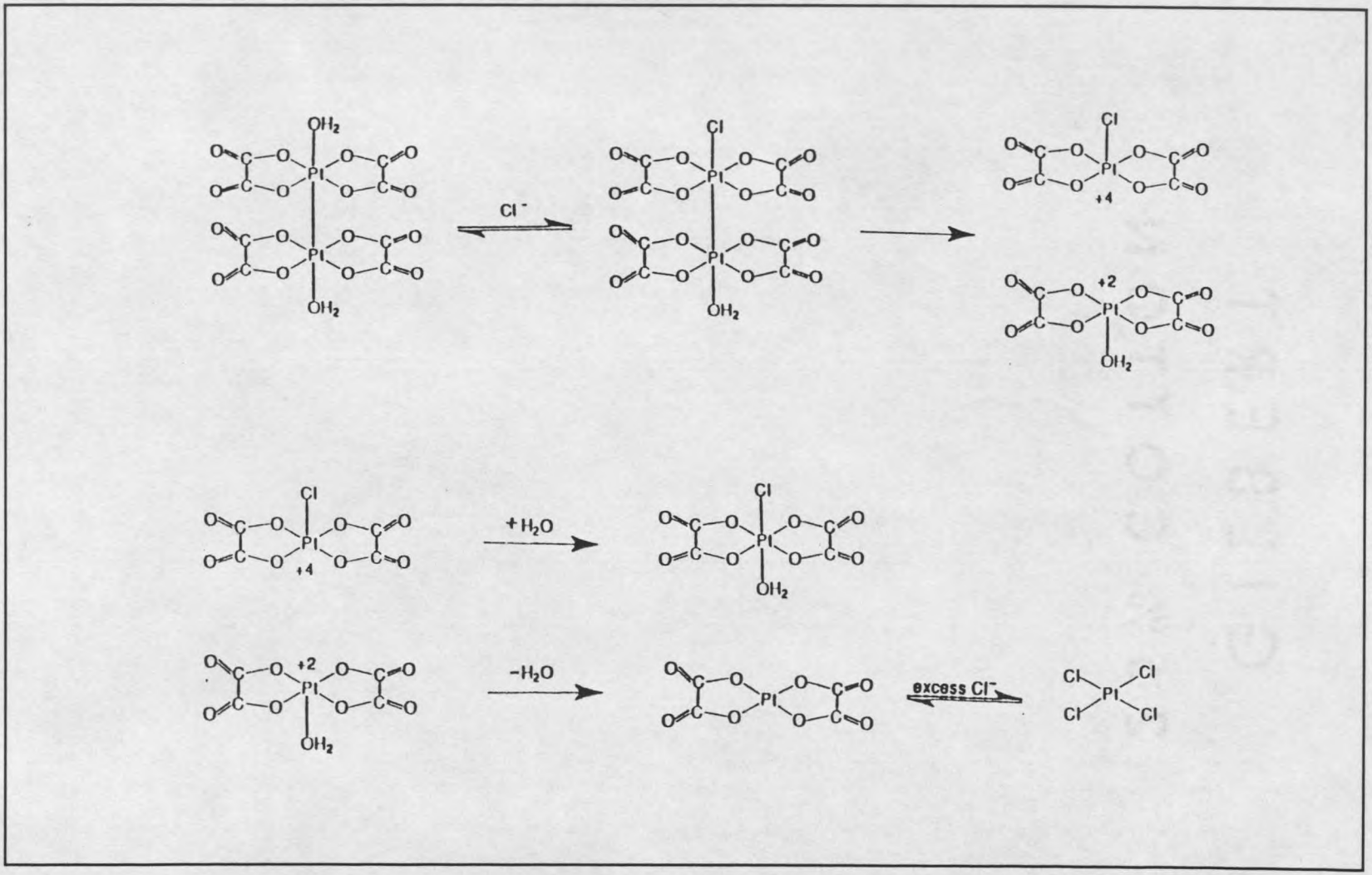

Figure 32. A possible disproportionation reaction of $[Pt^{3+}(ox)_2]_2^{2-}$ upon the addition of KCl to an acidic solution containing $[Pt^{3+}(ox)_2]_2^{2-}$.

Determination of a Conditional Formation Constant As previously discussed, it is possible to control conditions and create an experimental environment where only the two species $[Pt^{3+}(ox)_2]_2^{2-}$ and $[Pt^{2.67+}(ox)_2]_3^{4-}$ are present. A conditional equilibrium constant can then be calculated for the formation $[Pt^{2.67+}(ox)_2]_3^{4-}$ from the reaction of $[Pt^{3+}(ox)_2]_2^{2-}$ with $[Pt(ox)_2]^{2-}$ as expressed in the second step of Scheme 1. When oxidative titrations of $[Pt(ox)_2]^{2-}$,utilizing Ce^{4+} as the oxidant, were carried out in 0.25 M CF_3SO_3H under more dilute conditions (i.e. $4x10^{-4}$ M $[Pt(ox)_2]^{2-}$) only the absorbances of the $[Pt^{3+}(ox)_2]_2^{2-}$ and $[Pt^{2.67+}(ox)_2]_3^{4-}$ species at λ_{max} = 426 nm and λ_{max} = 510 nm, respectively, were observed (UV-Vis cell pathlength = 2.5 cm). Utilizing the extinction coefficients for each of the two complexes, the concentrations of each complex were determined. A conditional formation constant, K_f , for the formation of $[Pt^{2.67+}(ox)_2]_3^{4-}$, was determined based upon the postulated reaction previously presented in step two of Scheme 1. That reaction is:

$$[Pt^{3+}(ox)_2]_2^{2-} + [Pt^{2+}(ox)_2]^{2-} \rightleftharpoons [Pt^{2.67+}(ox)_2]_3^{4-}$$

The conditional formation constant, K_f , for this reaction was determined to be an averaged value of 630. Table 7 is a list of calculated formation constants for $[Pt^{2.67+}(ox)_2]_3^{4-}$ in 0.25M CF_3SO_3H at various electron equivalents of oxidant. The relative agreement of the formation constants at various electron equivalents of oxidant supports the proposed reaction scheme.

Table 7. Formation constants are determined for the formation of $[Pt(ox)_2]_3^{4-}$ under conditions of varying electron equivalents of oxidant in 0.25M CF_3SO_3H . The oxidant is Ce^{4+}. The temperature is 25°C.

Equiv. Oxid.	M $[Pt(ox)_2]_3^{4-}$	M $[Pt(ox)_2]_2^{2-}$	M $[Pt(ox)_2]^{2-}$	K_f
.737	$2.9x10^{-5}$	$1.55x10^{-4}$	$2.23x10^{-4}$	839
.632	$3.2x10^{-5}$	$1.65x10^{-4}$	$2.93x10^{-4}$	662
.553	$3.9x10^{-5}$	$1.82x10^{-4}$	$3.46x10^{-4}$	619
.491	$4.5x10^{-5}$	$2.08x10^{-4}$	$3.82x10^{-4}$	566
.442	$5.6x10^{-5}$	$2.33x10^{-4}$	$4.13x10^{-4}$	582
.402	$5.9x10^{-5}$	$2.21x10^{-4}$	$5.29x10^{-4}$	505

Investigation of the $Pt^{2.5+}$ and $Pt^{2.4+}$ Complexes, $[Pt(ox)_2]_4^{6-}$, and $[Pt(ox)_2]_5^{8-}$

UV-Vis Studies Attempts to separate the $Pt^{2.5+}$ complex, $[Pt(ox)_2]_4^{6-}$, and the $Pt^{2.4+}$ complex, $[Pt(ox)_2]_5^{8-}$, were unsuccessful. Figure 33 depicts a typical spectra obtained while trying to find conditions whereby the two complexes could be separated. As can be seen in Figure 33 there is significant overlap of the absorbance peaks at λ_{max} = 600 nm and λ_{max} = 680 nm. Although attempts to character these species were unsuccessful, it is still reasonable to postulate their formation based upon reaction Scheme 1. Evidence supporting the first step of Scheme 1 to form the dimeric Pt^{3+} complex has been previously presented, and evidence to support the formation of the $Pt^{2.67+}$ complex through the reaction described in the second step of Scheme 1 has also been presented. Since the first two steps of Scheme 1 have been supported experimentally, it seems reasonable that steps three and four are correct as well.

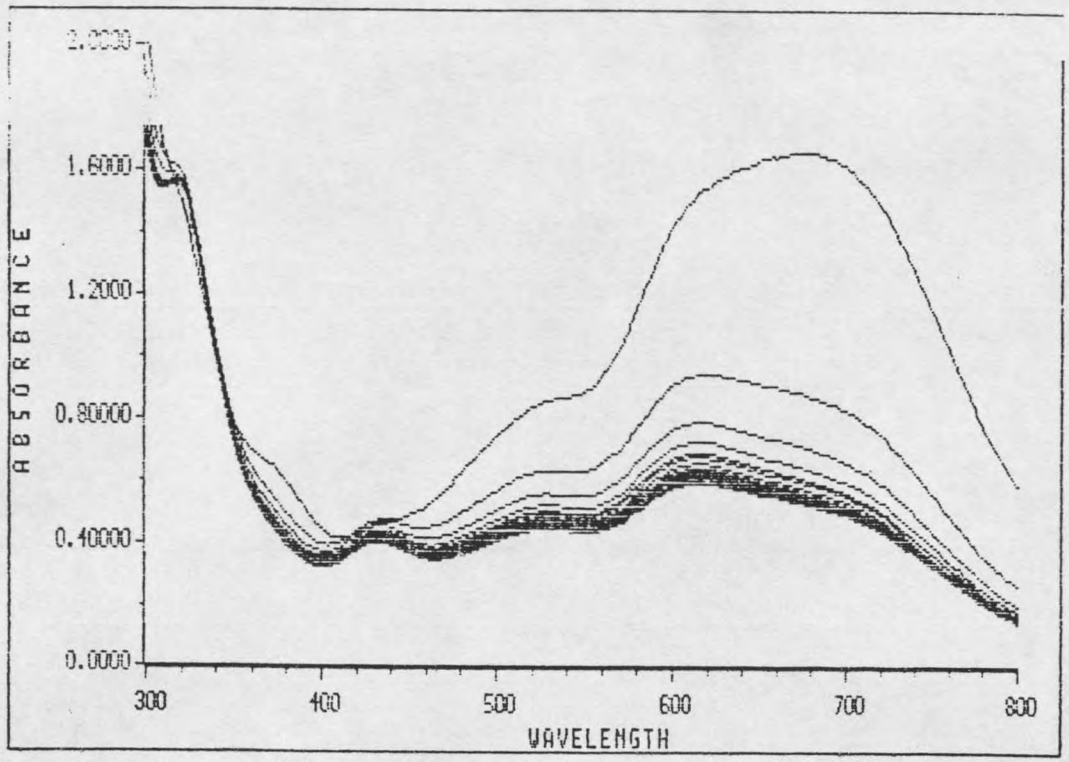

Figure 33. UV-Vis spectra depicting the overlap of the $[Pt^{2.5+}(ox)_2]_4^{6-}$ complex absorbing at 600 nm and the $[Pt^{2.4+}(ox)_2]_5^{8-}$ complex absorbing at 680 nm. The overlayed spectra are of the same reaction taken at two minute intervals for twenty minutes. 0.2 electron equivalents of Ce^{4+} was used as oxidant in 3.5M CF_3SO_3H.

Examination of the $K_{1.6}[Pt(ox)_2]\cdot 2H_2O$ Polymer

This section of the thesis describes results of experiments on the polymer, $K_{1.6}[Pt(ox)_2]\cdot 2H_2O$. It was hoped that the depolymerization reaction could be examined to lend support for the proposed polymerization reactions. Depolymerization of the polymer should lead to the observance of the same four species that were observed in the oxidation of $K_2[Pt(ox)_2]\cdot 2H_2O$ to produce the polymer. In addition, pH experiments were performed to determine pKa values for deprotonation of the H_2O ligands in the Pt^{3+} complex, $[Pt(ox)_2(H_2O)]_2^{2-}$, formed in the depolymerization reaction. Krogmann had proposed that the polymer depolymerizes to form the $[Pt(ox)_2]^{2-}$ and the *trans*-$[Pt(ox)_2(H_2O)_2]$ complexes (47,48). pK_a values for $[Pt(ox)_2(H_2O)_2]$ have been reported (59, 68). Comparing the pK_a values obtained in these experiments to those reported for the *trans*-$[Pt(ox)_2(H_2O)_2]$ complex would determine whether Krogmann was correct or not, and thereby lend support for or against the proposed polymerization reaction scheme, Scheme 1.

UV-Vis Studies

Dissolution of $K_{1.6}[Pt(ox)_2]\cdot 2H_2O$ in H_2O and Acidic Medium When $K_{1.6}[Pt(ox)_2]\cdot 2H_2O$ was dissolved in 2.2 M CF_3SO_3H the copper colored needles

disappeared and the solution forms a dark blue color. This dark blue solution absorbed at λ_{max} = 426 nm, 510 nm, 600 nm, and 680 nm (Figure 34). Very little absorbance at λ_{max} = 426 nm and 510 nm was observed although the absorbance at each wavelength was definitely above background. Most of the absorbance occurred at λ_{max} = 680 nm and then 600nm. When $K_{1.6}[Pt(ox)_2]\cdot 2H_2O$ was dissolved in neutral H_2O the copper needles disappear and a yellow colored solution is observed. Only one peak was observed at λ_{max} = 426 nm in the yellow solution. These results suggest that the species absorbing at λ_{max} = 510 nm, 600 nm and 600 nm all require the presence of acid in order to form. The Pt(III) dimeric species, $[Pt^{3+}(ox)_2]_2^{2-}$, occurred in both acid medium and H_2O, and was observed by its absorption at 426 nm in the UV-Vis spectrum. These results are consistent with those observed in the oxidation reaction of $K_2[Pt(ox)_2]\cdot 2H_2O$ to form the polymer, $K_{1.6}[Pt(ox)_2]\cdot 2H_2O$. When the oxidation was carried out in acidic medium four absorbances at λ_{max} = 426 nm, 510 nm, 600nm and 680 nm were observed prior to the formation of the polymer, $K_{1.6}[Pt(ox)_2]\cdot 2H_2O$. When the oxidation of $K_2[Pt(ox)_2]\cdot 2H_2O$ is carried out in neutral H_2O only the absorbance at λ_{max} = 426 nm was observed and the polymer, $K_{1.6}[Pt(ox)_2]\cdot 2H_2O$, did not form. It appears that the presence of acid is therefore necessary for the formation of the three species absorbing at λ_{max} = 510 nm, 600 nm and 680 nm and the subsequent formation of polymer, $K_{1.6}[Pt(ox)_2]\cdot 2H_2O$. As can be seen in Figure 34, the relative intensities of the absorbances in this acidic dissolution is 680 nm > 600 nm > 510 nm > 426 nm. This is what would be expected. The platinum

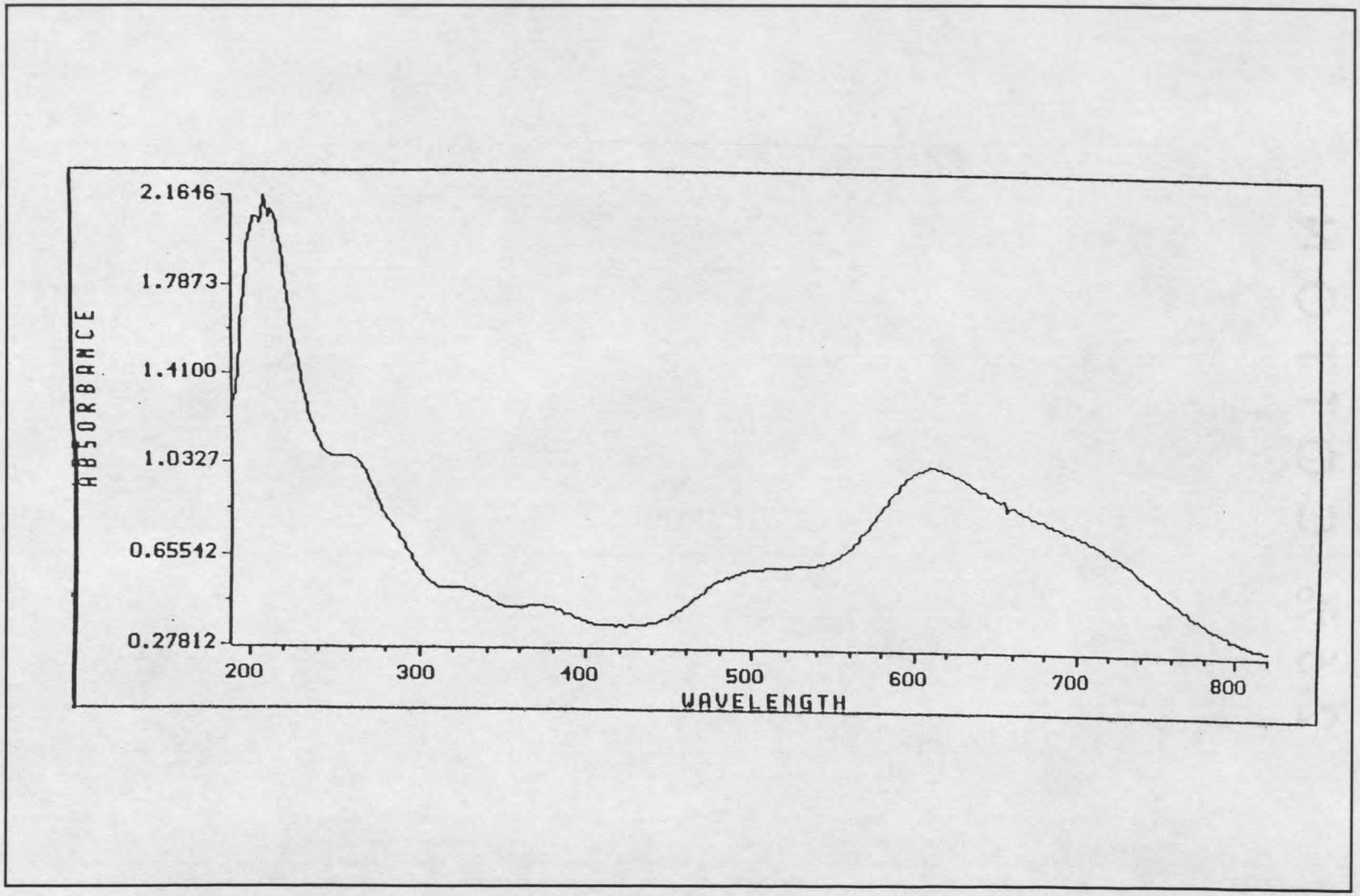

Figure 34. UV-Vis spectra of the $K_{1.6}[Pt(ox)_2]\cdot 2H_2O$ polymer dissolved in 2M CF_3SO_3H.

oxidation state in the polymer is +2.4. This oxidation state is the same as that observed for the solution species that absorbs at λ_{max} = 680 nm. If the proposed polymerization scheme (Scheme 1) is correct then there would be an equilibrated distribution of the Pt(+2.4) solution complex, $[Pt^{2.4+}(ox)_2]_5^{8-}$, into the Pt(+2.5) solution complex, $[Pt^{2.5+}(ox)_2]_4^{6-}$; the Pt(+2.67) solution complex, $[Pt^{2.67+}(ox)_2]_3^{4-}$; and finally the Pt(+3) solution complex, $[Pt^{3+}(ox)_2]_2^{2-}$, with the concentration of each depending upon the respective equilibrium constants. The $[Pt^{2.4+}(ox)_2]_5^{8-}$ solution complex, absorbing at λ_{max}= 680 nm, would be the predominant species since its oxidation state is exactly that of the dissolved polymer. Krogmann noted that the addition of base reversed the polymerization reaction (48), and these experiments demonstrate the requirement of acid for the formation of the solution species absorbing at λ_{max} = 510 nm, 600 nm, and 680 nm. It is of interest that these three species are also the species that must add a $[Pt^{2+}(ox)_2]^{2-}$ monomer in increasing amounts (510 nm< 600 nm< 680 nm). Further discussion of this relationship will occur later in this thesis.

Determination of $[Pt^{3+}(ox)_2]_2^{2-}$ in the Polymer As mentioned, when $K_{1.6}[Pt(ox)_2]\cdot 2H_2O$ is dissolved in H_2O only the dimeric $[Pt^{3+}(ox)_2]_2^{2-}$, absorbing at λ_{max} = 426 nm, was observed. Using the extinction coefficient, 1220 M^{-1} cm^{-1}, (determined in this work for the $[Pt^{3+}(ox)_2]_2^{2-}$ complex absorbing at 426 nm) the concentration of $[Pt^{3+}(ox)_2]_2^{2-}$ in the polymer, $K_{1.6}[Pt(ox)_2]\cdot 2H_2O$, was calculated. The experimentally determined amount of dimeric $[Pt^{3+}(ox)_2]_2^{2-}$ in the polymer was

19.5 % (mole %). If the reactions mentioned before in Scheme 1 are correct, the reverse reaction for the depolymerization (Scheme 2) would simply be the polymerization reaction in reverse.

Scheme 2:

$$5[Pt^{2.4+}(ox)_2]^{1.6-} \rightleftharpoons 1[Pt^{3+}(ox)_2]_2^{2-} + 3[Pt^{2+}(ox)_2]^{2-}$$

From Scheme 2 is it apparent that if 5 moles of polymer is dissolved then one mole of the Pt(III) dimer , $[Pt^{3+}(ox)_2]_2^{2-}$, will be recovered. Theoretically then, 1/5 or 20 % (mole %) of the polymer is composed of the dimeric $[Pt^{3+}(ox)_2]_2^{2-}$ complex. As mentioned, experimentally 19.5 % dimeric $[Pt^{3+}(ox)_2]_2^{2-}$ was observed upon the dissolution of $K_{1.6}[Pt(ox)_2]\cdot 2H_2O$ in H_2O. This is in excellent agreement with what is expected theoretically. This result further confirms that the calculated extinction coefficient for the dimeric $[Pt^{3+}(ox)_2]_2^{2-}$ at 426 nm (1220 $M^{-1}cm^{-1}$) is correct.

^{195}Pt NMR Studies

Dissolution of the Polymer in H_2O and Acidic Medium When $K_{1.6}[Pt(ox)_2]\cdot 2H_2O$ was dissolved 2.2 M CF_3SO_3H a dark blue colored solution resulted. When the blue solution was scanned with ^{195}Pt NMR spectroscopy no resonances were observed. When $K_{1.6}[Pt(ox)_2]\cdot 2H_2O$ was dissolved in H_2O a yellow solution resulted. When ^{195}Pt NMR spectroscopy was performed on the

yellow solution two resonances were observed. One ^{195}Pt resonance was observed at 1150 ppm and another ^{195}Pt resonance was observed at -525 ppm (Table 8). These resonances are consistent with the dimeric Pt(III) complex mentioned previously, $[Pt^{3+}(ox)_2(H_2O)]_2^{2-}$, and the Pt(II) monomer, $[Pt^{2+}(ox)_2]^{2-}$, respectively. The ratio of the dimeric $[Pt^{3+}(ox)_2]_2^{2-}$ to the monomeric $[Pt^{2+}(ox)_2]^{2-}$ was 1/3.5. This would suggest that the polymer was composed of 1 mole of $[Pt^{3+}(ox)_2]_2^{2-}$ and 3.5 moles of $[Pt^{2+}(ox)_2]^{2-}$. From Scheme 2 above, the expected results of the depolymerization would be one mole of $[Pt^{3+}(ox)_2]_2^{2-}$ and 3 moles of $[Pt^{2+}(ox)_2]^{2-}$ or a $[Pt^{3+}(ox)_2]_2^{2-}$ to $[Pt^{2+}(ox)_2]^{2-}$ ratio of 1/3. The observed experimental results are in good agreement with the predicted theoretical values. This is further confirmation of the proposed reaction schemes. No resonances were observed when the polymer was dissolved in acid because this dissolution results in the formation of all four solution species as evidenced by the UV-Vis results mentioned above. If the proposed chemical formulae are correct, all of these solution species, except the dimeric $[Pt^{3+}(ox)_2]_2^{2-}$ complex, are paramagnetic. The paramagnetic compounds would not be observed in the ^{195}Pt NMR spectroscopy.

Table 8. ^{195}Pt NMR results from the dissolution of $K_{1.6}[Pt(ox)_2]\cdot 2H_2O$ in H_2O.

COMPLEX	^{195}Pt RESONANCE
$[Pt^{2+}(ox)_2]^{2-}$	-525 ppm
trans-$[Pt^{4+}(ox)_2(OH)_2]^{2-}$	2873 ppm
$n[Pt^{2.4+}(ox)_2]^{1.6n-}$ dissolved in H_2O	1150 ppm, -525 ppm

In addition, since the dimeric $[Pt^{3+}(ox)_2]_2^{2-}$ species is in equilibrium with each of these paramagnetic complexes, the observation of the ^{195}Pt resonance of the diamagnetic $[Pt^{3+}(ox)_2]_2^{2-}$ species would be inhibited. The gyromagnetic ratio of an unpaired electron is ~657 times greater than that of a proton (66). Consequently, the presence of even trace amounts of paramagnetic species can provide a very efficient pathway for relaxation. Because the relaxation is extremely rapid, it would be impossible to detect the ^{195}Pt resonance of the dimeric $[Pt^{3+}(ox)_2]_2^{2-}$ species in the presence of and in equilibrium with the paramagnetic complexes.

pH Studies

Titration of $K_{1.6}[Pt(ox)_2]\cdot 2H_2O$ Dissolved in H_2O When a known amount of $K_{1.6}[Pt(ox)_2]\cdot 2H_2O$ was dissolved in H_2O and titrated with 0.01 N NaOH two equivalence points were observed (Figure 35). The first equivalence point corresponded to the titration of 0.17 moles of H^+ per mole $K_{1.6}[Pt(ox)_2]\cdot 2H_2O$. Figure 36 is a blowup of that part of the titration curve showing the first equivalence point since it is difficult to see the changes in slope that occur as the dissolved polymer is titrated in Figure 35. The second equivalence point corresponded to the titration of 0.395 moles of H^+ per $K_{1.6}[Pt(ox)_2]\cdot 2H_2O$. These results are consistent with the depolymerization reaction shown in Scheme 2. In reaction Scheme 2, five moles of polymer dissociates into 1 mole of dimeric $[Pt^{3+}(ox)_2]_2^{2-}$ and three moles of $[Pt^{2+}(ox)_2]^{2-}$. Another way to express this

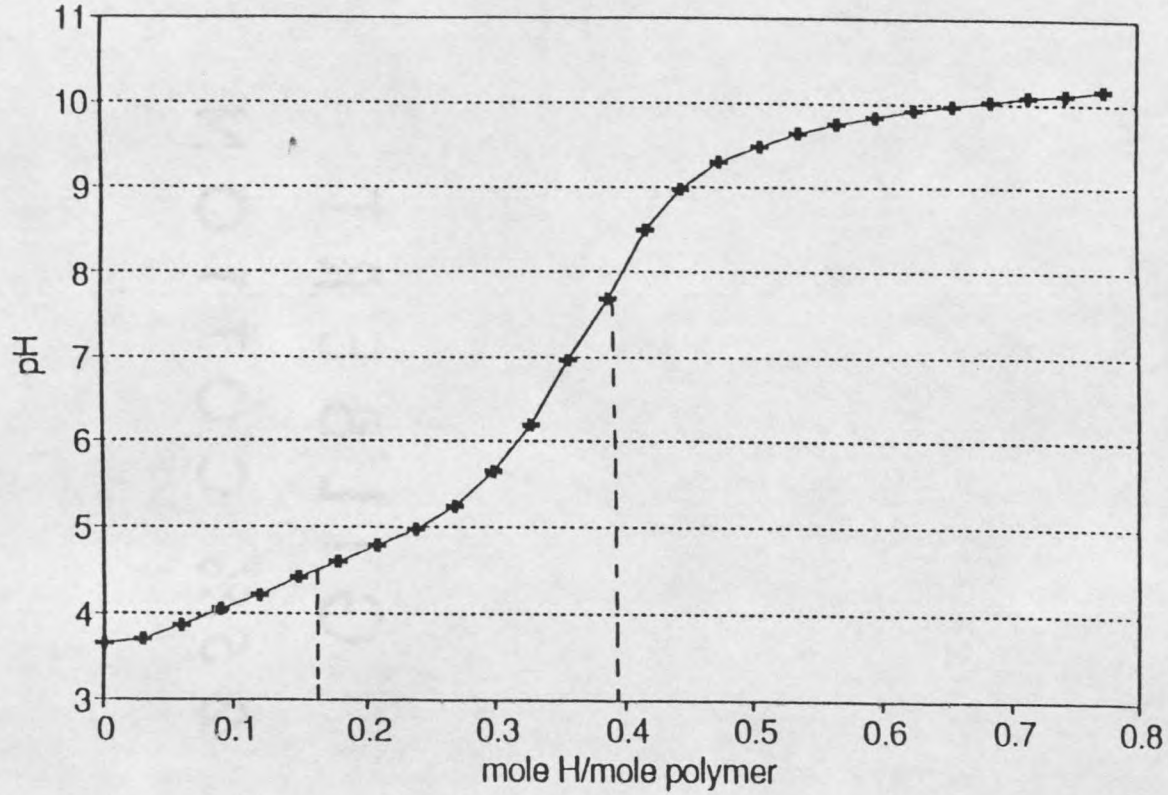

Figure 35. Titration curve obtained when 3.4×10^{-5} moles of $K_{1.6}[Pt(ox)_2] \cdot 2H_2O$ is dissolved in 20 ml H_2O and titrated with 0.01N NaOH.

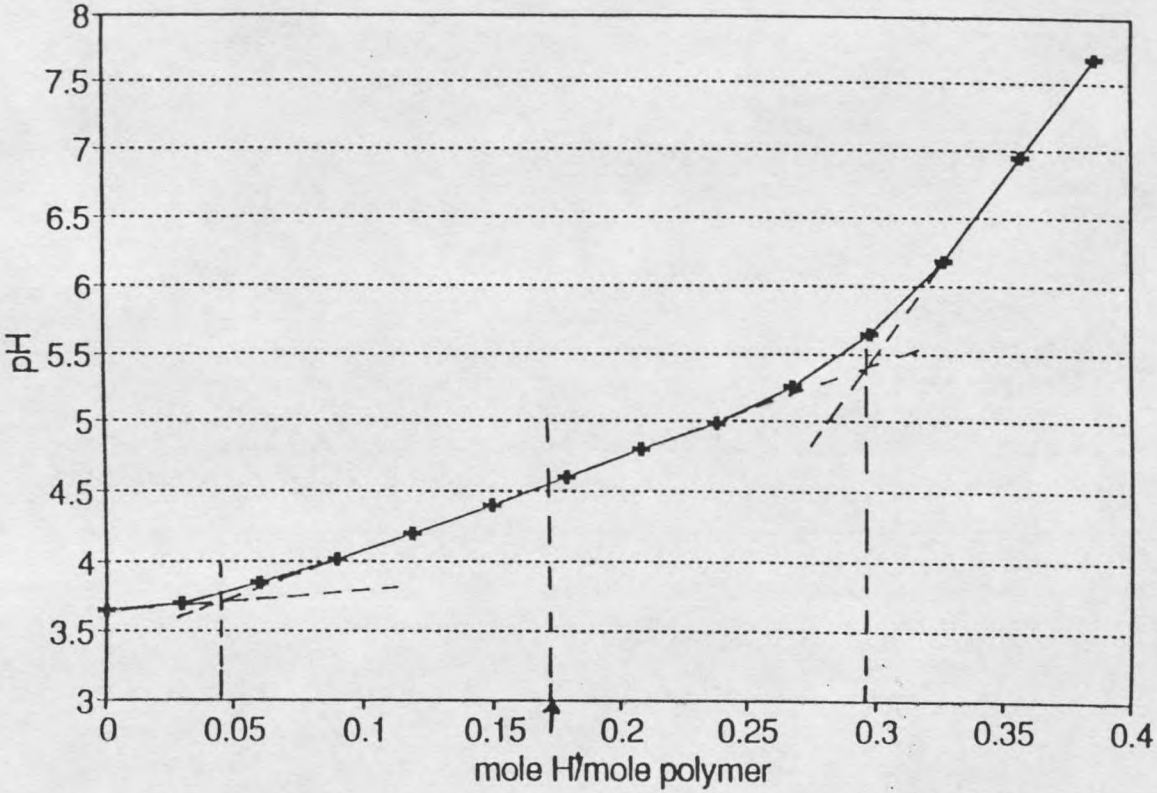

Figure 36. Blowup of the titration curve in Figure 35 showing the region of the first equivalence point.

depolymerization is to say that 1 mole of polymer dissociates into 0.2 moles of dimeric $[Pt^{3+}(ox)_2]_2^{2-}$ and 0.6 moles of $[Pt^{2+}(ox)_2]^{2-}$. The dimeric $[Pt^{3+}(ox)_2]_2^{2-}$ complex would contain H_2O molecules in axial positions since the dissolution was in an aqueous medium. These axial H_2O molecules could further dissociate protons as the base titration is carried out. Scheme 3 depicts this depolymerization reaction and subsequent dissociation of protons from the axial H_2O ligands of the dimeric Pt(III) species.

Scheme 3:

$$1[Pt^{2.4+}(ox)_2]^{1.6-} \rightleftharpoons 0.2[Pt^{3+}{}_2(ox)_4(H_2O)_2]^{2-} + 0.6[Pt^{2+}(ox)_2]^{2-}$$

$$0.2[Pt^{3+}{}_2(ox)_4(H_2O)_2]^{2-} \rightleftharpoons 0.2[Pt^{3+}{}_2(ox)_4(H_2O)(OH)]^{3-} + 0.2H^+$$

$$0.2[Pt^{3+}{}_2(ox)_4(H_2O)(OH)]^{3-} \rightleftharpoons 0.2[Pt^{3+}{}_2(ox)_4(OH)_2]^{4-} + 0.2H^+$$

Figure 37 depicts this reaction scheme in another way that may be easier to visualize. Theoretically, a total of 0.4 moles of H^+ would be titrated when one mole of polymer is dissolved in H_2O and titrated with base. The first equivalence point in the base titration would occur at 0.2 mole H^+ per mole polymer and the second equivalence point would occur at 0.4 mole H^+ per mole polymer. As mentioned this work found that the two equivalence points occurred at 0.17 mole H^+ per mole polymer and at 0.395 mole H^+ per mole polymer. These results are in good

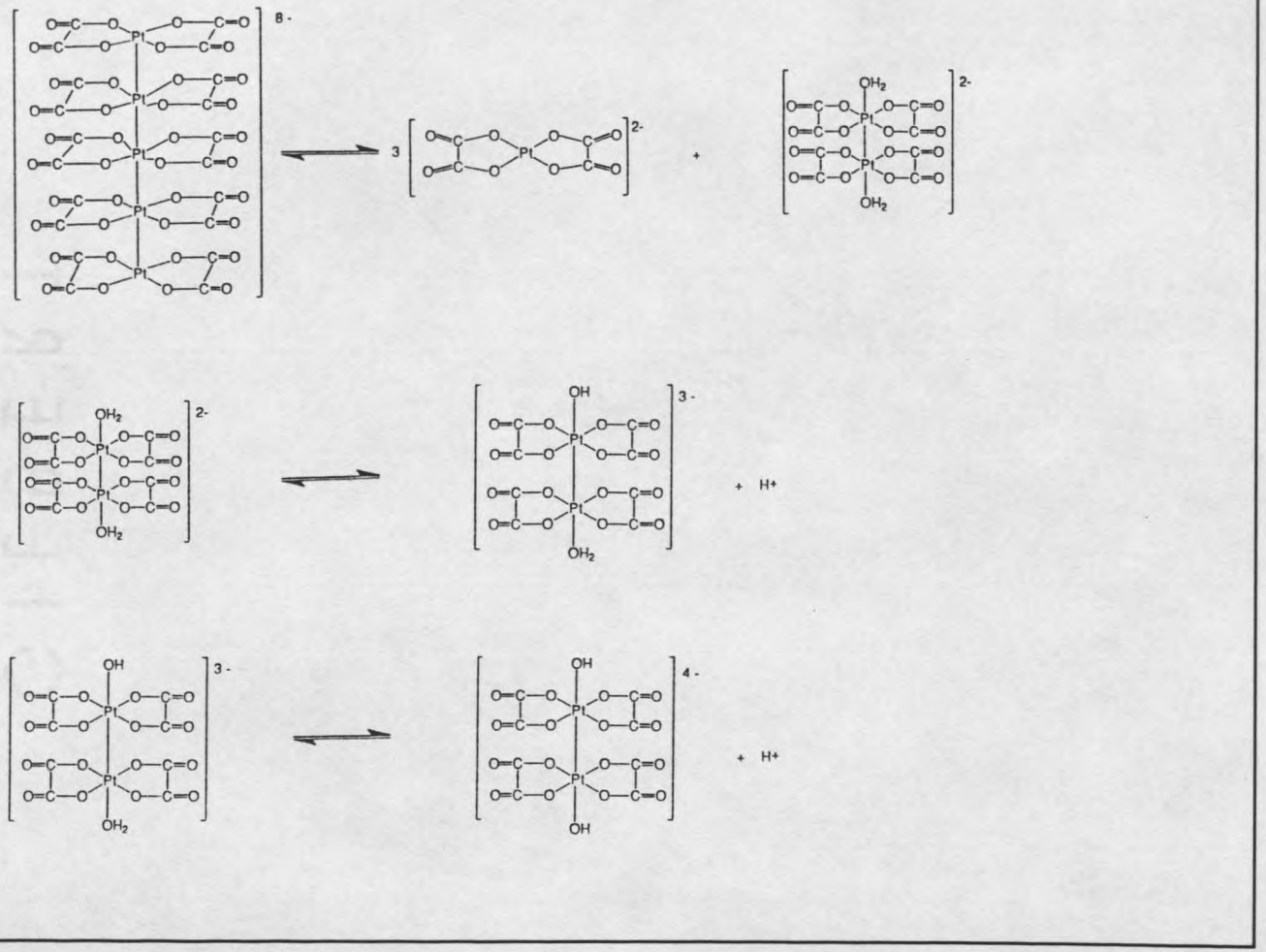

Figure 37. Proposed dissociation reaction of the polymer, $[Pt(ox)_2]_5^{8-}$, into a Pt^{2+} monomeric complex, $[Pt(ox)_2]^{2-}$, and a dimeric Pt^{3+} complex, $[Pt(ox)_2(OH_2)]_2^{2-}$.

agreement with the theoretical values, and thus substantiate the proposed reaction schemes for both polymerization and depolymerization.

Determination of pKa Values for $[Pt^{3+}(ox)_2(H_2O)]_2^{2-}$ pKa measurements were determined for the dissociation of the two protons from the axial water molecules on the dimeric $[Pt^{3+}(ox)_2(H_2O)]_2^{2-}$ complex. Those pKa values were determined to be $pKa_1 = 3.9$ and $pKa_2 = 5.2$. These pKa values are consistent with pKa values observed by Schollhorn *et al.* (67) for the dimeric Pt(III) complex, $[(OH_2)(NH_3)_2Pt_2L_2(NH_3)_2(OH_2)]^{4+}$ (L = 1-methyluracil anion, $C_5H_5N_2O_2$). The pKa values observed by Schollhorn for this dimeric Pt(III) complex were $pKa_1 = 3.5$ and $pKa_2 = 6.7$. In addition, the reported pKa values for the Pt(IV) complex, *trans*-$[Pt(ox)_2(H_2O)_2]^{2-}$ are $pKa_1 = 2.3$ and $pKa_2 = 2.83$ (59, 68). These pKa values are significantly different than those observed in these experiments. This is more evidence confirming that the oxidized species in the formation of the polymeric $K_{1.6}[Pt(ox)_2]\cdot 2H_2O$ compound is indeed a dimeric Pt(III) complex and not the Pt(IV) complex, $[Pt(ox)_2(H_2O)_2]^{2-}$, proposed by Krogmann (48).

Role of the Acid in the Polymerization Reaction

This portion of the thesis describes experiments that were carried out to examine the role of the acid in the polymerization reaction. Krogmann reported

the acid dependence of the polymerization reaction to produce the polymer, $K_{1.6}[Pt(ox)_2]\cdot 2H_2O$ (47, 48), but offered little explanation as to the role of the H^+ in the reaction. Relatively little has been done since Krogmann's work to address the acid dependence. These experiments were designed to examine the H^+ requirement of each of the four solution species, and perhaps provide insight into the role of the acid in the polymerization reaction.

UV-Vis Studies

Utilizing Ce^{4+} and $PtCl_6^{2-}$ as Oxidants Experiments were carried out to examine the effect of the acid concentration on each of each of the four solution species. Experiments were set up with series of solutions each containing a constant concentration of $[Pt(ox)_2]^{2-}$ and a constant concentration of oxidant. Varying concentrations of CF_3SO_3H were added to each of the samples. The spectra were recorded on the UV-Vis. The oxidants used were both $[PtCl_6]^{2-}$ and Ce^{4+}. Both of the oxidants yielded the same results. Figure 38 shows the results of this series of experiments for all concentrations of oxidant used (the oxidant here is $[PtCl_6]^{2-}$). Figures 39 and 40 show the results of the experiment when 0.25 equivalents of Ce^{4+} and 0.25 equivalents of $[PtCl_6]^{2-}$ were added to each solution. It can be seen that the two oxidants give quite comparable results if the results depicted in Figure 39 are compared with the results depicted in Figure 40. It should be noted that the concentration of $[Pt(ox)_2]^{2-}$ used in the $[PtCl_6]^{2-}$ experiment (Figure 40) is 5×10^{-3}M and the concentration of $[Pt(ox)_2]^{2-}$ used in the

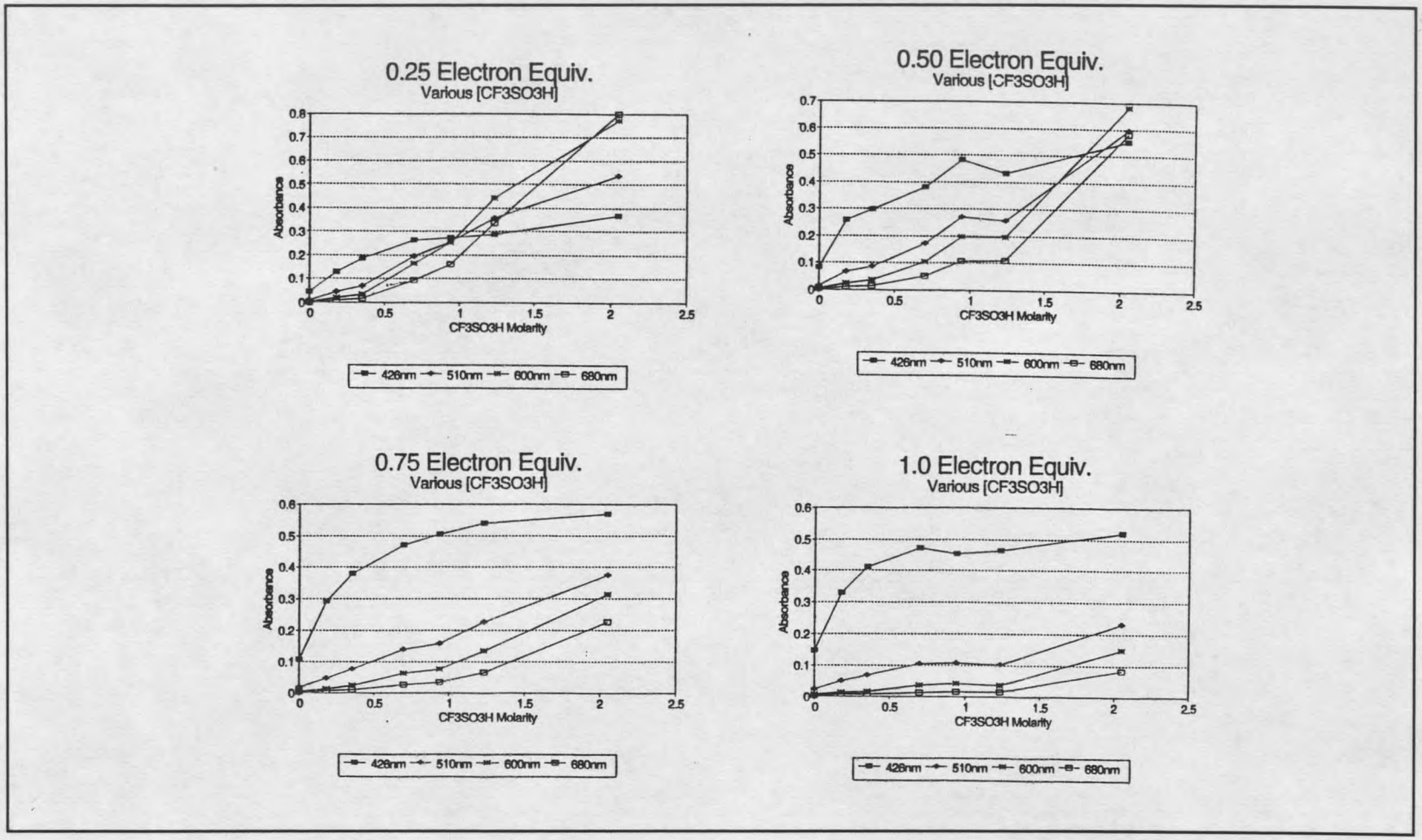

Figure 38. Four experiments are depicted here. In each respective experiment the electron equivalents of oxidant and the concentration of $[Pt(ox)_2]^{2-}$ are held constant and the concentration of CF_3SO_3H is varied. UV-Vis spectra are recorded. Plots here depict the absorbance values at 426 nm, 510 nm, 600 nm and 680 nm versus molarity of CF_3SO_3H. $[PtCl_6]^{2-}$ is the oxidant.

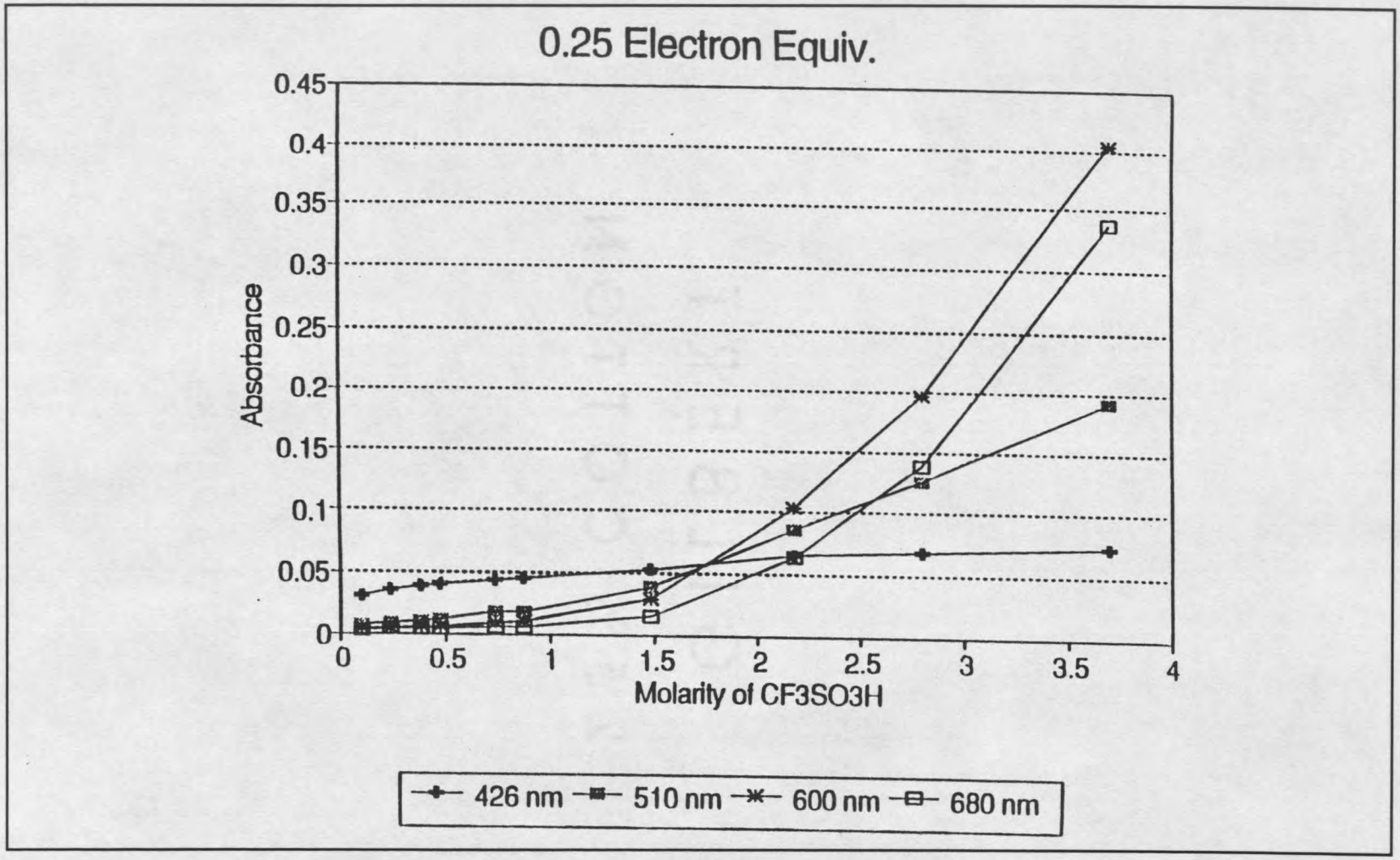

Figure 39. UV-Vis measurements are made of an experiment where 0.25 electron equivalents of oxidant (Ce^{4+}) is added to $[Pt(ox)_2]^{2-}$ and allowed to react in various concentrations of CF_3SO_3H. The absorbances at 426 nm. 510 nm, 600 nm and 680 nm are plotted versus the molarity of CF_3SO_3H.

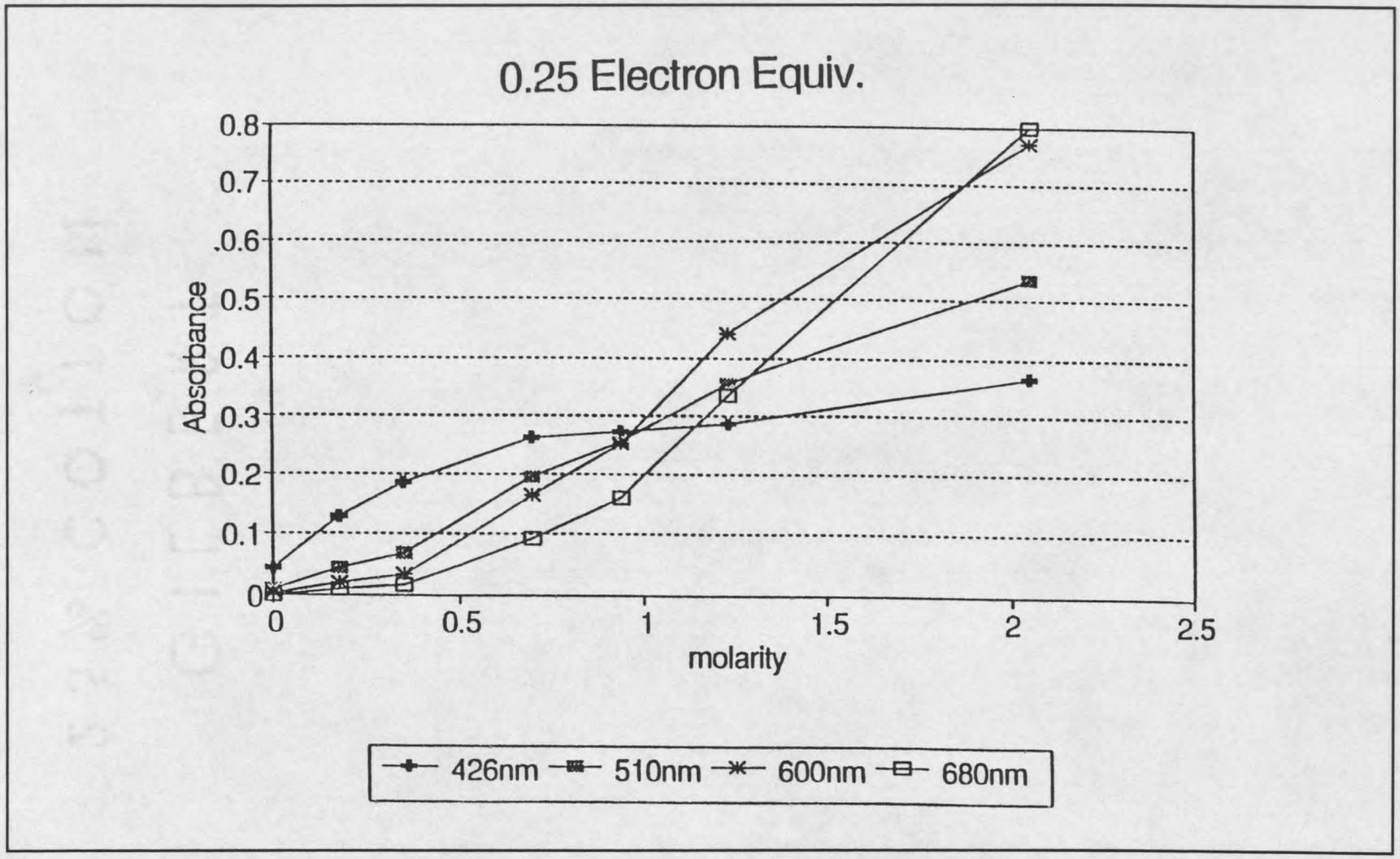

Figure 40. UV-Vis measurements are made of an experiment where 0.25 electron equivalents of oxidant ($[PtCl_6]^{2-}$) is added to $[Pt(ox)_2]^{2-}$ and allowed to react in various concentrations of CF_3SO_3H. The absorbances at 426 nm, 510 nm, 600 nm and 680 nm are plotted versus the molarity of CF_3SO_3H.

Ce^{4+} experiment (Figure 39) is 1 x 10^{-3}M. It is obvious from the results depicted in Figures 39 and 40 that the concentration of acid affects the solution species in the quite different ways. The species absorbing at λ_{max} = 426 nm is not affected significantly by the concentration of acid. This fact is further confirmed by the previously mentioned experiments in which the dimeric $[Pt^{3+}(ox)_2]_2^{2-}$ species (absorbing at λ_{max} = 426 nm) was formed in H_2O. The species absorbing at λ_{max}= 510 nm requires the presence of acid but not to the extent that the species absorbing at λ_{max} = 600 nm and 680 nm require acid. Finally, the acid concentration requirement of the species absorbing at λ_{max} = 600 nm is very nearly the same as that of the species absorbing at λ_{max} = 680 nm. However, in Figure 40 it can be observed that the curve generated by plotting the absorbance at λ_{max} = 680 nm rises somewhat steeper between 1M CF_3SO_3H and 2M CF_3SO_3H than does the curve for the absorbance at λ_{max} = 600 nm. This suggests that the acid dependence of the species absorbing at λ_{max} = 680 nm is slightly greater than the acid dependence of the species absorbing at λ_{max} = 600 nm. Generally speaking the acid dependence of the solution species appears to be:

426nm species < 510nm species < 600nm species < 680nm species

Furthermore, this acid dependence indicates that there must be a term in each of the equilibrium constants for the reactions that form the three species at λ_{max} = 510 nm, 600 nm, 680 nm that includes a $1/[H^+]^n$ term where n is as yet undetermined

for each of the three species, but n (510nm) < n (600nm) < n (680). As mentioned previously, significant overlap of the absorbances precludes calculating the equilibrium constants and the same is true for calculating the $1/[H^+]^n$ term.

It is of interest to note that each of the three species that requires acid also requires the sequential addition of $[Pt(ox)_2]^{2-}$ monomers. It is possible that the proton is somehow required to interact with the $[Pt(ox)_2]^{2-}$ prior to stacking onto the $[Pt^{3+}(ox)_2]_2^{2-}$ dimer. Since the formation of the species absorbing at λ_{max}= 510 nm requires only the addition of one $[Pt(ox)_2]^{2-}$ monomer to the $[Pt^{3+}(ox)_2]_2^{2-}$ dimer the acid requirement for this species would be less than that for the species absorbing at λ_{max}= 600nm which requires the addition of two $[Pt(ox)_2]^{2-}$ monomers. The acid requirement would be the greatest for the species absorbing at λ_{max}= 680 nm since it requires the addition of three $[Pt(ox)_2]^{2-}$ monomers to the $[Pt^{3+}(ox)_2]_2^{2-}$ dimer. Experimental work discussed later verifies that the $[Pt(ox)_2]^{2-}$ monomers are associated with protons. The discussion of the method of proton association with the $[Pt(ox)_2]^{2-}$ monomers, and a discussion of the way the proton may be aiding the stacking of the $[Pt(ox)_2]^{2-}$ monomers onto the $[Pt^{3+}(ox)_2]_2^{2-}$ dimer will occur later in this thesis.

A second possible role for the proton may be to act as the counter balancing cation for the polymeric species. The overall negative charges on each of the four species increases as:

$[Pt^{3+}(ox)_2]_2^{2-}$	<	$[Pt^{2.67+}(ox)_2]_3^{4-}$	<	$[Pt^{2.5+}(ox)_2]_4^{6-}$	<	$[Pt^{2.4+}(ox)_2]_5^{8-}$
(426nm)		(510nm)		(600nm)		(680nm)

It is unlikely that large polyanionic species would be stable in solution due to the repulsion between the negative charges. The presence of protons could act to stabilize the increasing negative charges on each of the polyanionic species. It is reasonable to assume that some kind of counter cationic charge would be necessary to stabilize these species in solution, and the proton would be a good choice for this since it is present in high concentration in the solution. It is probable that the proton is both acting upon the $[Pt(ox)_2]^{2-}$ monomer somehow to enable it to stack (as will be discussed later in this thesis), and acting as a countercation to stabilize the increasing negative charges on the polyanionic solution species.

UV-Vis Studies

Utilizing *trans*-$[Pt(ox)_2(OH_2)_2]$ as Oxidant When *trans*-$[Pt(ox)_2(OH_2)_2]$ was utilized to oxidize $[Pt(ox)_2]^{2-}$ it was found that oxidation could occur only under acidic conditions. An experiment was performed in which the concentration of $[Pt(ox)_2]^{2-}$ was held constant at 6×10^{-3} M and the concentration of the oxidant, $[Pt(ox)_2(OH_2)_2]$, was held constant at 1.0 electron equivalents. The pH of the reaction medium was varied from pH = 4.0 to pH = 0.5. The formation of $[Pt^{3+}(ox)_2]_2^{2-}$ was monitored by the appearance of an absorbance band at 426 nm. Figure 41 depicts the results of this experiment. The formation of the dimeric $[Pt^{3+}(ox)_2]_2^{2-}$ begins to appear at a pH < 2.0. The reported pKa values for *trans*-$[Pt(ox)_2(OH_2)_2]$ are $pKa_1 = 2.3$ and $pKa_2 = 2.83$ (68). It appears that for oxidation

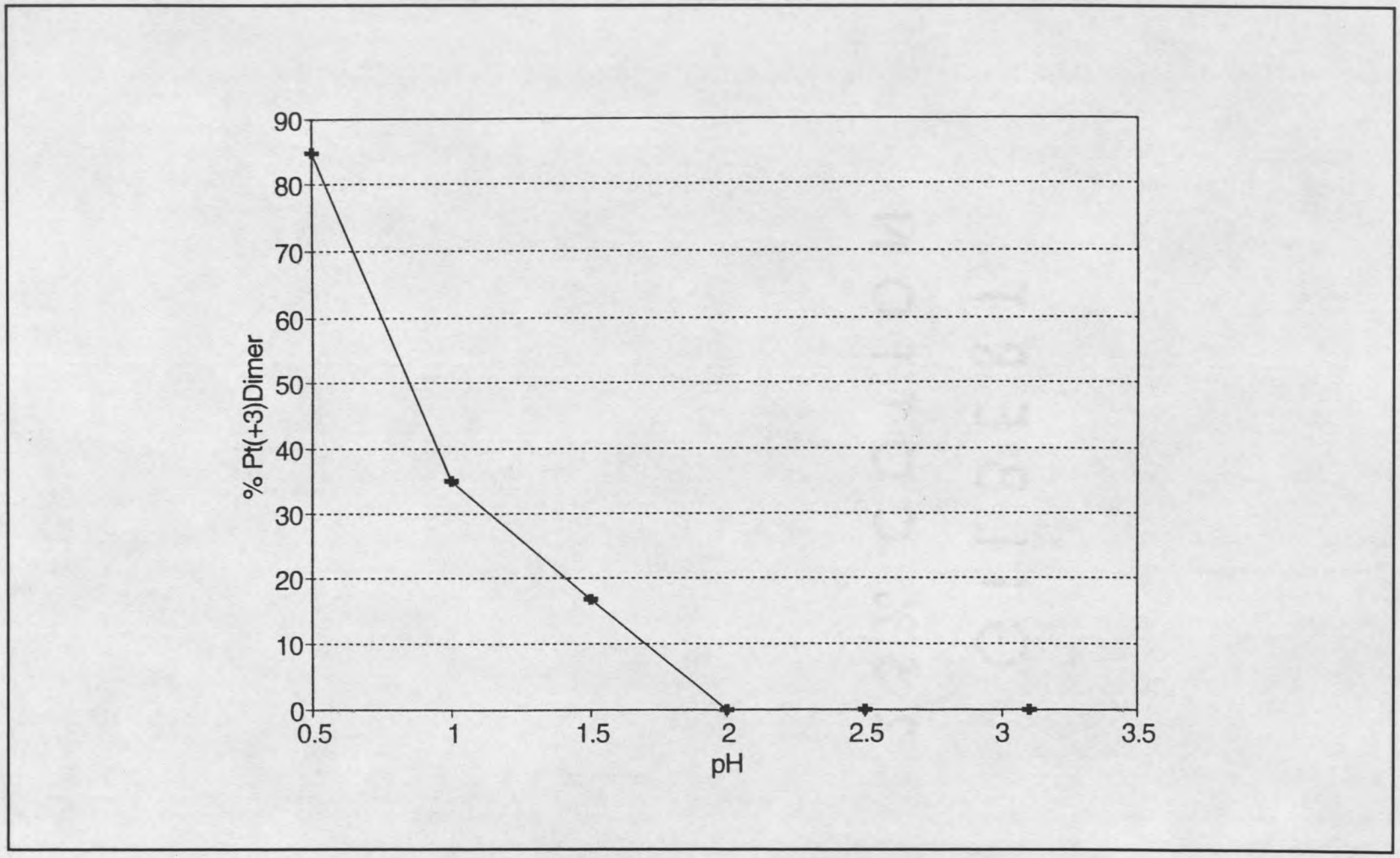

Figure 41. The oxidation of $[Pt(ox)_2]^{2-}$ with 1.0 electron equivalent of *trans*-$[Pt(ox)_2(OH_2)_2]$ is carried out in various pH conditions. The pH is varied by varying the concentration of CF_3SO_3H. The % of $[Pt^{3+}(ox)_2]_2^{2-}$ formed versus the pH of the reaction medium is plotted. The % of $[Pt^{3+}(ox)_2]_2^{2-}$ formed is based upon the absorbance at 426 nm.

to occur H_2O ligands must be present on the Pt^{4+} oxidant, $[Pt(ox)_2(OH_2)_2]$, rather than OH^- since these results clearly indicate that oxidation occurs at very nearly the exact pH at which both ligands are protonated. The presence of the weak-field H_2O ligand must be a requirement for the oxidation/reduction to occur. Similar results have been observed by Wilmarth et al. when comparing the reduction rates of *trans*-$[Pt(CN)_4Br(OH_2)]^-$ and *trans*-$[PtCN)_4Br(OH)]^2$ (70).

pH Studies

Formation of the Polymer An experiment was conducted to determine if any pH changes occurred during the polymerization reaction. pH measurements were made as increasing amounts of oxidant was added to $[Pt(ox)_2]^{2-}$. The reaction was carried out in 0.1M CF_3SO_3H. Figure 42 depicts the results of the pH measurements. It should be noted that lower line in Figure 42 are the results of adding the oxidant alone to the 0.1M CF_3SO_3H (i.e. without $[Pt(ox)_2]^{2-}$ being present). The experimental results show that the Pt(II) monomer, $[Pt(ox)_2]^{2-}$, took up protons. As the oxidation was carried out, the amount of protons associated with the solution species decreased until at 1.0 electron equivalent of oxidant the pH of the reaction mixture was the same as that of the oxidant alone in the 0.1M CF_3SO_3H. These results are in agreement with those observed in the UV-Vis experiment mentioned above.

At 0 electron equivalents of oxidant the uptake of protons was at its maximum. This indicates that the protons are somehow associating with the Pt(II)

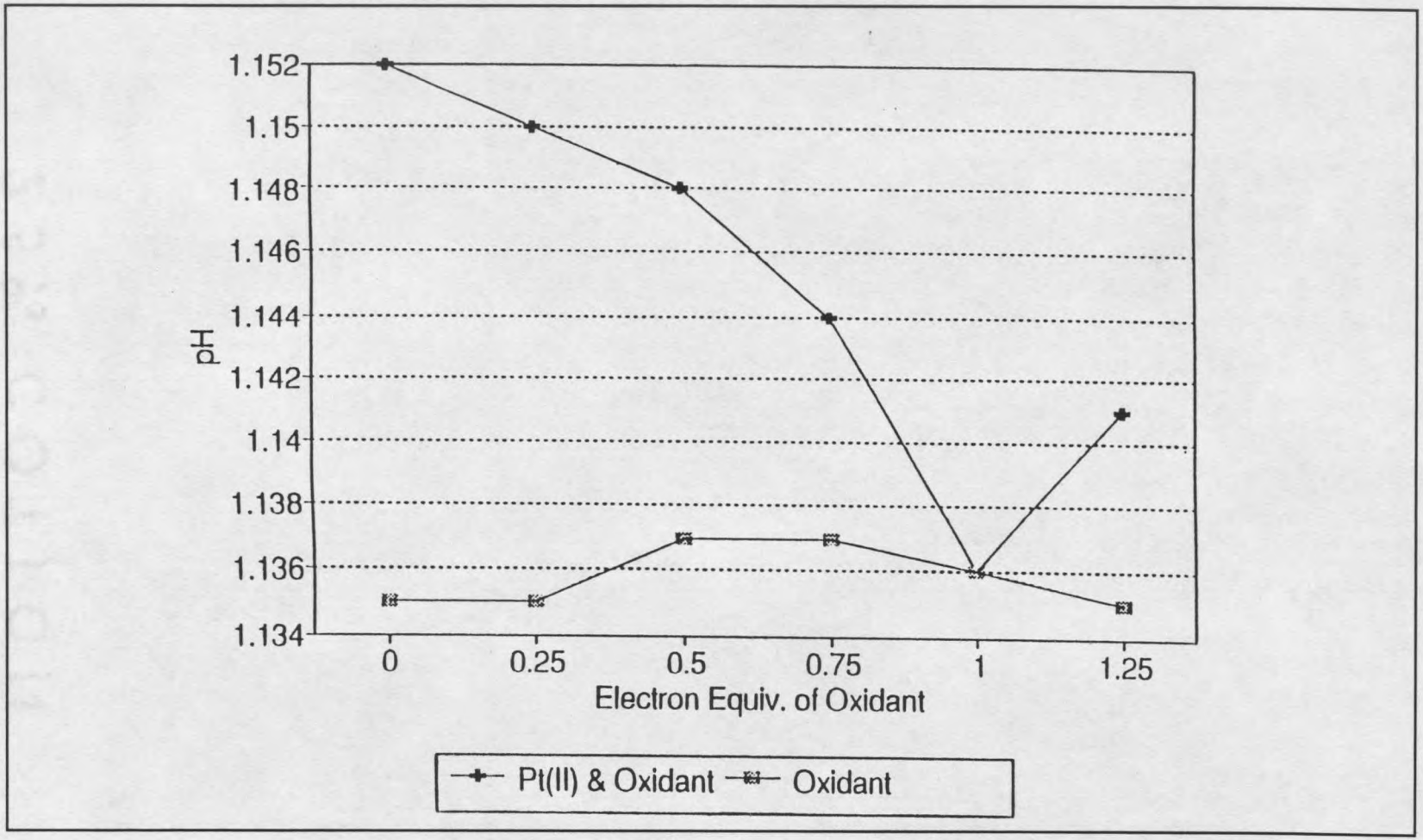

Figure 42. pH measurements are made of the oxidative titration of $[Pt(ox)_2]^{2-}$ in 0.1M CF_3SO_3H. The oxidant is $[PtCl_6]^{2-}$. The upper curve on the plot represents pH measurements versus the electron equivalents of oxidant added to $[Pt(ox)_2]^{2-}$ in 0.1M CF_3SO_3H. The lower curve represents the pH measurements versus the electron equivalents of oxidant added to 0.1M CF_3SO_3H (no $[Pt(ox)_2]^{2-}$ is present).

monomeric species, $[Pt(ox)_2]^{2-}$. Experiments discussed under the FT-IR results will show that the protons are associating with the carbonyl groups of the oxalate ligands bound to the $[Pt(ox)_2]^{2-}$. As oxidant is added to the $[Pt(ox)_2]^{2-}$, protons are released and the pH drops, until at 1.0 electron equivalents of oxidant the pH is that of the background mixture (i.e. oxidant and 0.1M CF_3SO_3H without $[Pt(ox)_2]^{2-}$). At one equivalent of oxidant the dimeric $[Pt^{3+}(ox)_2]_2^{2-}$ species is present. The experimental results indicate that this species does not associate with protons. Previously mentioned results showed that acid is not required for the formation of the $[Pt^{3+}(ox)_2]_2^{2-}$ dimeric species since the dimer can be prepared in neutral media. Furthermore, the UV-Vis measurements mentioned before demonstrated that the acid concentration does not affect the formation of the $[Pt^{3+}(ox)_2]_2^{2-}$ species. The addition of $[Pt(ox)_2]^{2-}$ is not required to form this species as it is to form the other three. The overall results of the pH experiment indicate that proton uptake by the solution Pt species is as follows:

$$Pt^{3+} < Pt^{2.67+} < Pt^{2.5+} < Pt^{2.4+} < Pt^{2+}$$

or:

$$[Pt^{3+}(ox)_2]_2^{2-} < [Pt^{2.67+}(ox)_2]_3^{4-} < [Pt^{2.5+}(ox)_2]_4^{6-} < [Pt^{2.4+}(ox)_2]_5^{8-} < Pt^{2+}(ox)_2]^{2-}$$

These experimental results are consistent with the UV-Vis experiments mentioned previously. These results do verify that the $[Pt(ox)_2]^{2-}$ monomer is associated with protons somehow, and it may be that this association is necessary in order for the

monomeric $[Pt(ox)_2]^{2-}$ species to stack onto the $[Pt^{3+}(ox)_2]_2^{2-}$ dimer. The role of the proton is therefore not limited to acting only as a countercation to the negative charges on the polyanionic species since the negative charge on the $[Pt(ox)_2]^{2-}$ monomer is only -2, the same as that of the $[Pt^{3+}(ox)_2]_2^{2-}$ dimer. There is an association of the proton with the $[Pt(ox)_2]^{2-}$ monomer, and that this association is necessary in the polymerization process.

Furthermore, based upon the pH measurements of this experiment, the relative amount of protons (range) associated with each species were determined. Calculated ranges of protons required for (or amount of H^+ taken up during) the formation of each of the respective solution species is:

				Range
$[Pt^{3+}(ox)_2]_2^{2-}$	+ $[Pt^{2+}(ox)_2]^{2-}$	$\rightleftharpoons$	$[Pt^{2.67+}(ox)_2]_3^{4-}$	(0 to 1.3 mole H^+)
$[Pt^{2.67+}(ox)_2]_3^{4-}$	+ $[Pt^{2+}(ox)_2]^{2-}$	$\rightleftharpoons$	$[Pt^{2.5+}(ox)_2]_4^{6-}$	(1 to 1.5 mole H^+)
$[Pt^{2.5+}(ox)_2]_4^{6-}$	+ $[Pt^{2+}(ox)_2]^{2-}$	$\rightleftharpoons$	$[Pt^{2.4+}(ox)_2]_5^{8-}$	(1.3 to 2 mole H^+)

These ranges are also listed in Table 9 for each of the respective species. It appears the association of these protons may be due to the protonation of the carbonyl group of the oxalate ligands of the $[Pt^{2+}(ox)_2]^{2-}$ complex. This will be discussed further later in this thesis.

Table 9. Calculated ranges of protons required for the formation of each of the respective solution species.

COMPLEX	Proton Range Required
$[Pt^{2.67+}(ox)_2]_3^{4-}$	0 to 1.3 mole H^+
$[Pt^{2.5+}(ox)_2]_4^{6-}$	1 to 1.5 mole H^+
$[Pt^{2.4+}(ox)_2]_5^{8-}$	1.3 to 2 mole H^+

Dissolution of the Polymer (Depolymerization) An experiment was carried out where the polymer, $K_{1.6}[Pt(ox)_2]\cdot 2H_2O$, was dissolved in 0.1M CF_3SO_3H. pH measurements were made of the .1M CF_3SO_3H before and after the addition of polymer. The results of the pH measurements showed that 0.28 moles H^+/ moles Pt (or 1.4 mole H^+ for 5 moles $Pt^{2.4+}$)are taken by the dissolution of the polymer. These results are consistent with those reported above. The number of protons taken up by the dissolved polymer are within the range reported for the $[Pt^{2.4+}(ox)_2]_5^{8-}$ complex in Table 9. It is unclear what the exact role of these protons is, but as mentioned FT-IR results below show that protons are indeed associating with the carbonyl group of the oxalate ligand bound to Pt^{2+}. It is also not unrealistic to presume that these protons may be acting to counterbalance the large polyanionic charges of the solution species.

FT-IR Studies

Oxidative Titrations Oxidative titrations of $[Pt(ox)_2]^{2-}$ were carried out in

1.2M CF_3SO_3D and the stretching frequencies of the C=O and the C-O groups were followed on the FT-IR instrument. The experimental results were consistent with protonation of the C=O of the $[Pt(ox)_2]^{2-}$ oxalate ligand. Table 10 lists the FT-IR results of the oxidative titration. The vibrational energy of the C=O of the oxalate ligands of the $[Pt(ox)_2]^{2-}$ complex decreased under acidic conditions going from 1709 cm^{-1}, 1674 cm^{-1} in D_2O to 1693 cm^{-1}, 1657 cm^{-1} in CF_3SO_3D . The vibrational energy of the C-O of the oxalate ligands of the $[Pt(ox)_2]^{2-}$ complex increased in energy under acidic conditions changing from 1388 cm^{-1} in D_2O to 1411 cm^{-1} in CF_3SO_3D. This result is consistent with protonation of the C=O group of the $[Pt(ox)_2]^{2-}$ species. When the carbonyl is protonated the C=O bond would become more single bond like in character and the C-O would become more double bond like in character as the platinum oxygen bond is weakened (Figure 43). As oxidant is added the C=O bond vibrational energy and the C-O bond vibrational energy eventually return to those of the C=O and C-O bond vibrational energies in D_2O. Deprotonation of the carbonyl must be occurring as an increasing amount of oxidant is added to the protonated $[Pt(ox)_2]^{2-}$ complex in solution. Since the Pt(+3) atom would be expected to bond more tightly to the oxygen of the oxalate ligand, the protonation of the carbonyl on the oxalate ligand of the $[Pt^{3+}(ox)_2]_2^{2-}$ complex would not be as likely. Similarly, the protonation of the oxalate ligand of the Pt(+2.67) species, $[Pt(ox)_2]_3^{4-}$, would occur less than that of the Pt(+2.5) species, $[Pt(ox)_2]_4^{6-}$, and the protonation of the oxalate ligand of the Pt(+2.5) species, $[Pt(ox)_2]_4^{6-}$, would occur less than that of the Pt(+2.4) species,

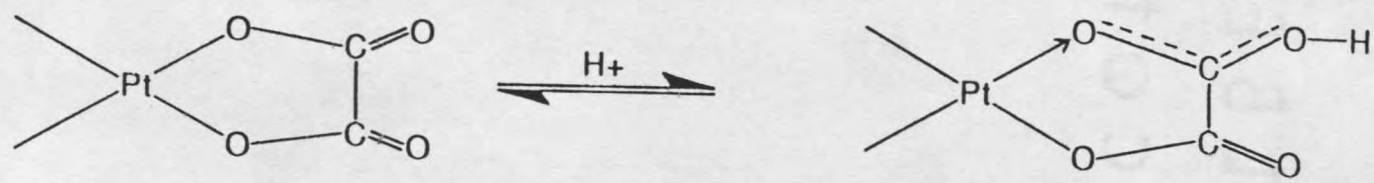

Figure 43. Protonation of the carbonyl group of the oxalate ligand of $[Pt(ox)_2]^{2-}$.

Table 10. FT-IR results of the oxidative titration of $[Pt(ox)_2]^{2-}$ in 1.2M CF_3SO_3D utilizing $[PtCl_6]^{2-}$ as the oxidant.

Reactants	υ C=O (cm^{-1})	υ C-O (cm^{-1})
$[Pt(ox)_2]^{2-}$ **(3)** in D_2O	1709, 1674	1388
(3) + D^+	1693, 1657	1411
(3) + D^+ + .25eq. oxid.	1697, 1664	1407
(3) + D^+ + .5eq oxid.	1712, 1697	1395
(3) + D^+ + .75eq. oxid.	1712, 1697	1395
(3) + D^+ + 1.0eq. oxid.	1712, 1697	1395

$[Pt(ox)_2]_5^{8-}$. Using this argument, the degree of protonation of the oxalate ligand of the respective Pt complexes would follow the order:

$$Pt(+3) < Pt(+2.67) < Pt(+2.5) < Pt(+2.4) < Pt(+2)$$

This order is supported by vibrational frequencies that were observed in this experiment, the results of which are tabulated in Table 10. It is interesting to note at this point that the partially oxidized tetracyanoplatinate salts seem to form without the presence of acid. The cyano ligands are electron withdrawing and it may be that it is necessary for the electron density around the Pt(II) species to be reduced in order for the Pt(II) monomers to stack. Protonation of the carbonyl of the oxalate ligand would also reduce the electron density around the Pt(II) monomer since the Pt-O bond would tend to break or become a more dative type

bond as protonation of the carbonyl occurs. It may be that reduction of the electron density around the Pt(II) atom enables it to react with the oxidized Pt(III) species and form the polymers. It seems likely then, that the role of the proton is twofold. First, the proton is necessary in that it reacts with the Pt(II) monomer, $[Pt(ox)_2]^{2-}$, and reduces the electron density around the Pt^{2+} atom and allows it to stack. Second, the proton may act as a countercation in solution and help to stabilize the polyanionic species that form during the oxidation reaction.

Solution Studies of the Oxidation of $K_2[Pt(mal)_2]\cdot 2H_2O$

This section of the thesis describes attempts to oxidize the $[Pt(mal)_2]^{2-}$ to produce a partially oxidized bis(malonato)platinate polymer. Since the $[Pt(mal)_2]^{2-}$ monomer is very similar to the $[Pt(ox)_2]^{2-}$ it seems reasonable that the partially oxidized bis(malonato)platinate polymer could also be produced. To date, attempts to form this polymer have been unsuccessful (59). Experiments described in this section will provide a possible explanation as to why it has not been possible to produce this polymer.

UV-Vis Studies An experiment was carried out to see if $K_2[Pt(mal)_2]\cdot 2H_2O$ could be oxidized under the same conditions as $K_2[Pt(ox)_2]\cdot 2H_2O$ to form a

partially oxidized bis(malonato)platinate polymer. $K_2[Pt(mal)_2]\cdot 2H_2O$ was dissolved in 1M CF_3SO_3H to a concentration of 8 x 10^{-4} M. 1.0 electron equivalents of Ce^{4+} was then added to the solution containing the $[Pt(mal)_2]^{2-}$. The reaction was followed on the UV-Vis. Figure 44 depicts the results of the UV-Vis scans taken at 2 minute intervals for 20 minutes. Figure 45 is a plot of the absorbance at 426 nm versus time for the reaction. From the results it is apparent that the dimeric Pt(+3) equivalent in this system, $[Pt^{3+}(mal)_2]_2^{2-}$, forms as it does in the bis(oxalato)platinate system. However, the $[Pt^{3+}(mal)_2]_2^{2-}$ is unstable. It disappears rapidly after its formation. It is probably the instability of this $[Pt^{3+}(mal)_2]_2^{2-}$ complex that prevents the polymerization reaction from occurring. If the partially oxidized bis(malonato)platinate polymer is ever to be prepared, the dimeric $[Pt^{3+}(mal)_2]_2^{2-}$ complex must somehow be stabilized. Until this can be done, attempts to prepare the partially oxidized bis(malonato)platinate polymers will most likely be unsuccessful.

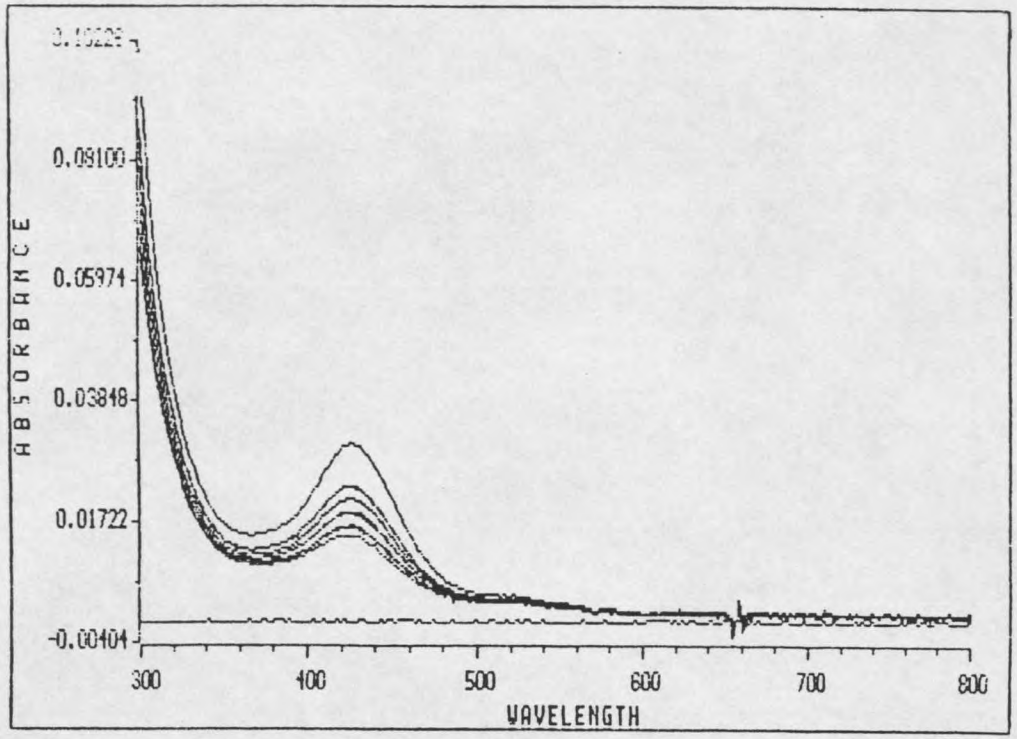

Figure 44. Multiple spectra of the oxidation of $[Pt(mal)_2]^{2-}$ using Ce^{4+} as the oxidant are shown here. The spectra are taken at two minute intervals for 16 minutes after the Ce^{4+} is added to $[Pt(mal)_2]^{2-}$ in CF_3SO_3H. The overlayed spectra depicts the absorbance at 426 nm decreasing with time.

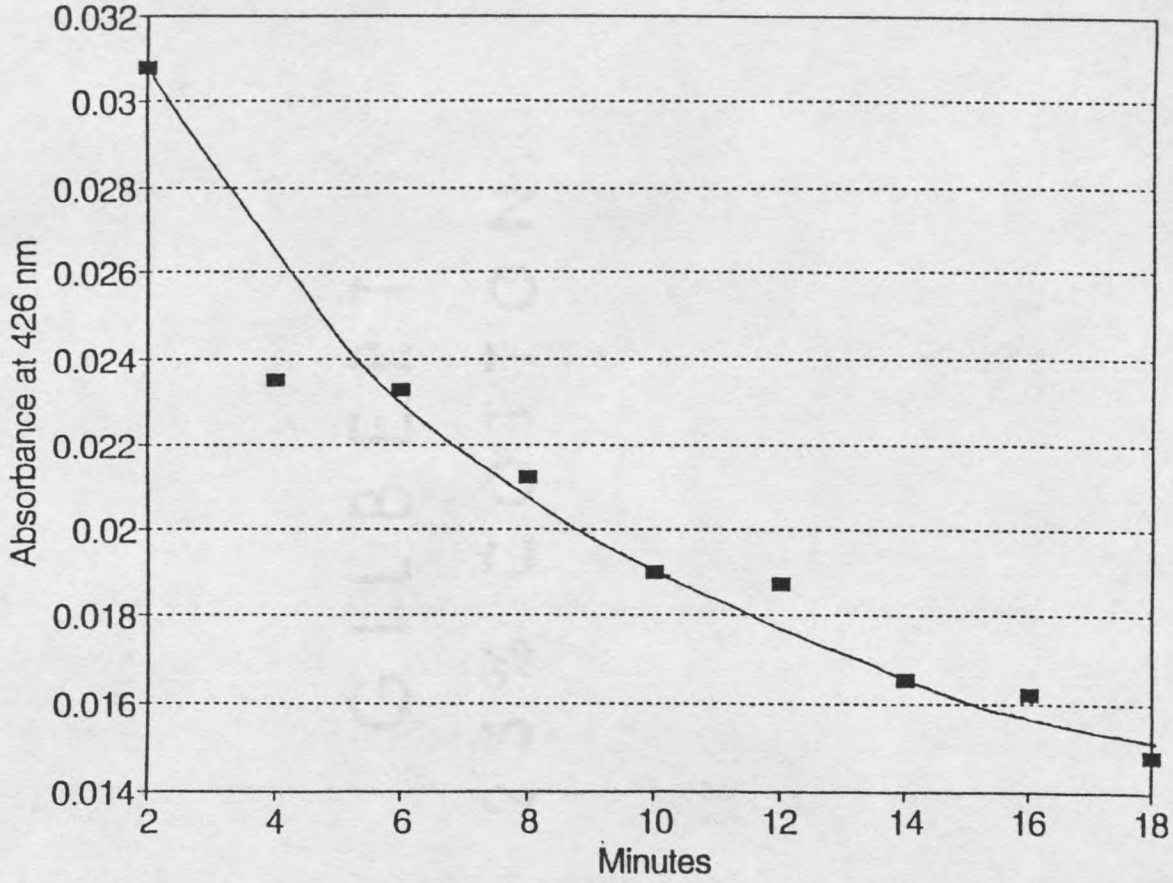

Figure 45. A plot of the UV-Vis absorbance at 426 nm versus time is shown here for the oxidation reaction of $[Pt(mal)_2]^{2-}$ with the oxidant Ce^{4+} in 1M CF_3SO_3H.

SUMMARY

The characterization of the solution chemistry for the reaction to produce the one-dimensional partially oxidized bis(oxalato)platinate polymers has been determined by UV-Vis spectroscopy, FT-IR spectroscopy, ^{195}Pt NMR spectroscopy, and pH measurements. Four distinct solution species form during the polymerization reaction to produce the partially oxidized bis(oxalato)platinate polymers. Those four species contain platinum ions whose average oxidation states are Pt^{3+}, $Pt^{2.67+}$, $Pt^{2.5+}$, and $Pt^{2.4+}$, respectively. The Pt^{3+} complex has been shown to be diamagnetic which means it must be a dimer, tetramer, hexamer, etc. Chemically, the simplest Pt^{3+} complex would be a dimeric species whose most probable chemical formula is $[Pt^{3+}(ox)_2]_2^{2-}$. The $Pt^{2.67+}$ complex, then, would be a trimeric species whose chemical formula is $[Pt^{2.67+}(ox)_2]_3^{4-}$. The $Pt^{2.5+}$ complex would be a tetrameric species whose chemical formula is $[Pt^{2.5+}(ox)_2]_4^{6-}$. And, finally, the $Pt^{2.4+}$ complex would be a pentameric species whose chemical formula is $[Pt^{2.4+}(ox)_2]_5^{8-}$. A reaction scheme has been proposed which shows how each of the species may be formed by the sequential addition of one bis(oxalato)platinate(II) monomer to the dimeric Pt^{3+} complex. In addition an extinction coefficient for $[Pt^{3+}(ox)_2]_2^{2-}$ complex absorbing at 426 nm has been determined. Dissolution of the polymer, $K_{1.6}[Pt(ox)_2]\cdot 2H_2O$, substantiates that the extinction coefficient determined for the $[Pt^{3+}(ox)_2]_2^{2-}$ species absorbing at 426 nm is indeed correct.

Further substantiation for the dimeric $[Pt^{3+}(ox)_2]_2^{2-}$ species came through the dissolution of $K_{1.6}[Pt(ox)_2]\cdot 2H_2O$ polymer in H_2O and subsequent titration with base. The number of protons titrated were consistent with the proposed dimeric structure for the Pt^{3+} solution complex. pK_a values have been determined for $[Pt^{3+}(ox)_2(OH_2)]_2^{2-}$ to be $pK_{a1} = 3.9$ and $pK_{a2} = 5.2$. In addition, ^{195}Pt NMR spectroscopy on the dissolved polymer revealed a ^{195}Pt resonance consistent for a $[Pt^{3+}(ox)_2(OH_2)]_2^{2-}$ complex.

By careful control of pH and concentration an extinction coefficient for the $Pt^{2.67+}$ complex, $[Pt(ox)_2]_3^{4-}$, at 510 nm was determined. Further, determination of a conditional formation constant for the formation of the $Pt^{2.67+}$ complex supported the proposed polymerization reaction scheme. Attempts to isolate the $Pt^{2.5+}$ complex and the $Pt^{2.4+}$ complex were unsuccessful.

The role of the acid in the polymerization reaction was evaluated. It was determined that each of the four solution species required a specific amount of H^+ for their formation. Proton ranges were determined for each of the four complexes. FT-IR spectroscopy revealed that protonation of the carbonyl group on the oxalate ligands is occurring. It was also determined that for the Pt^{4+} complex, *trans*-$[Pt(ox)_2(OH_2)_2]^{2-}$, to act as an oxidant, H_2O ligands, not OH^- ligands, must be present in *trans* positions on the Pt^{4+} complex (i.e. the pH of the reaction must be below the pK_a's for deprotonation of the axial H_2O molecules of the *trans*-$[Pt(ox)_2(OH_2)_2]^{2-}$).

Finally, examination of the $[Pt(mal)_2]^{2-}$ dianion and its potential to form

partially oxidized polymers was evaluated. It was determined that the $[Pt(mal)_2]^{2-}$ complex could indeed be oxidized to form a dimeric Pt^{3+} complex similar to that formed in the polymerization reaction of the partially oxidized bis(oxalato)platinate polymers. However, the Pt^{3+} complex formed in the oxidation of $[Pt(mal)_2]^{2-}$ was not stable, and therefore, attempts to form the partially oxidized bis(malonato)platinate polymers were unsuccessful.

REFERENCES

1. Williams, J.M.; Schultz, A.J.; Underhill, A.E.; Carneiro, K. in Extended Linear Chain Compounds, J.S. Miller, Ed. (plenum Press, New York, 1982), pp. 73-115, and references therein.

2. Toftlund, H. *J. Chem. Soc. Chem. Commun.* 837 (1979).

3. Simonsen, O.; Toftlund, H. *Inorg. Chem.* 20, 4046 (1981).

4. Isci, H. and Mason, W.R. *Inorg. Chem.* 24, 1761 (1985).

5. Krogmann, K. *Angew. Chem. internat. Edit.* 8, 35 (1969), and references therein.

6. Uson, R.; Fornies, J.; Tomas, M.; Menjon, B.; Sunkel, K.; Bau, R. *J. Chem. Soc. Chem. Commun.*, 751 (1984).

7. Blake, A.J.; Gould, R.O.; Hyde, T.L.; Lavery, A.J.; Odulate, M.O.; Schroder, M. *J. Chem. Soc. Chem. Commun.* 118 (1987).

8. Boucher, H.A.; Lawrance, G.A.; Lay, P.A.; Sargeson, A.M.; Bond, A.M.; Sangster, D.F.; Sullivan, J.C. *J. Am. Chem. Soc.*, 105, 4652 (1983).

9. Muraveiskaya, G.S.; Kukina, G.A.; Orlova, V.S.; Evstaf'eva O.N.; Porai-Koshits, M.A. *Doki. Akad. Nauk. SSSR.*, 226, 596 (1976).

10. Appleton, T.G.; Hall, J.R.; Neale, D.W. *Inorg. Chim. Acta* 104, 19 (1985).

11. Harvey, P.D.; Truong, K.D.; Aye, K.T.; Drouin, M.; Bandrauk, A.D. *Inorg. Chem.* 33, 2347 (1994).

12. Newman, R.A.; Martin, D.S.; Dallinger, R.F.; Woodruff, W.H.; Stiegman, A.E.; Che, C-M.; Schaefer, W.P.; Miskowski, V.M., Gray, H.B.; *Inorg. Chem.* 30, 4647 (1991).

13. Nissen. S.C. *B.Sc (Hons) Thesis*, 1991, University of Queensland.

14. Muraveiskaya G.S.; Abashkin, V.E.; Evstaf'eva, N.; Golovaneva, I.F.; Shchelokov, R.N. *Koord. Khim.* 6, 463 (1980).

15. Shin, Y.K.; Miskowski, V.M.; Nocera, D.G. *Inorg. Chem.* 29, 2308 (1990).

16. Arrizabalaga, P.; Castan, P.; Laurent, J.P. *Chem Phys. Let.* 76, 548 (1980).

17. Sperline, R.P.; Dickson, M.K.; Roundhill, D.M. *J. Chem. Soc. Chem. Commun.* 62 (1977).

18. Alexander, K.A.; Bryan, S.A.; Dickson, M.A.; Hedden, D.; Roundhill, D.M. *Inorg. Synth.* 24, 211, (1986).

19. Filomena Dos Remedio Pinto, M.A.; Sadler, P.J.; Neidle, S.; Sanderson, M.R.; Subbiah, A.; Kuroda, R.J. *J. Chem. Soc. Chem. Commun.* 13 (1980).

20. Che C-M; Mak, T.C.W.; Miskowski, V.M.; Gray, H.B. *J. Am. Chem. Soc.* 108, 7840 (1986).

21. Alexander, K.A.; Bryan, S.A.; Fronczek, F.R.; Fultz, W.C.; Rheingold, A.L.; Roundhill, D.M.; Stein, P; Watkins, S.F. *Inorg. Chem.* 24, 2803 (1985).

22. Clark, R.J.H.; Kurmoo, M.; Dawes, H.M.; Hursthouse, M.B. *Inorg. Chem.* 25, 409 (1986).

23. Che, C-M.; Herbstein, F.H.; Schaefer, W.P.; Marsh, R.E.; Gray, H.B. *J. Am. Chem. Soc.* 105, 4604 (1983).

24. Clark, R.J.H. *Chem. Soc. Rev.* 19, 107 (1990).

25. Che, C-M.; Scaefer, W.P.; Gray, H.B. Dickson, M.K.; Stein, P.B.; Roundhill, D.M. *J. Am. Chem. Soc.* 104, 4253 (1982).

26. Hedden, D.; Roundhill, D.M.; Walkinshaw, M.D. *Inorg. Chem.* 24, 3146 (1985).

27. Kuyper, J. Vrieze, K. *Trans. Met. Chem.* 1, 208 (1976).

28. Mathieson, M.T. *B. Sc. (Hons.) Thesis* University of Queensland (1992).

29. Appleton, T. G.; Byriel, K.A.; Hall, J.R.; Kennard, C.H.L.; Mathieson, M.T. *J. Am. Chem. Soc.* 114, 7305 (1992).

30. Cini, R.; Fanizzi, F.P.; Intini, F.P.; Natile, G.; *J. Am. Chem. Soc.* 113, 7805 (1991).

31. Baxter, L.A.M.; Heath, G.A.; Raptis, R.G.; Willis, A.C. *J. Am. Chem. Soc.* 114, 6944 (1992).

32. Davidson, P.J.; Faber, P.J.; Fischer, R.G.(Jr.); Mansy, S.; Peresie, H.J.; Rosenberg, B.; Van Camp, L. *Cancer Chemother. Rep.*, 59, 287 (1975).

33. Rosenberg, B. *Cancer Chemother. Rep.* 59, 589 (1975).

34. Speer, R.J; Ridgeway, H.; Hall, L.M.; Steard, D.P.; Howe, K.E.; Lieberman, D.Z.; Newmann, A.O; Hill, J.M. *Cancer Chemother. Rep.* 59, 629 (1975).

35. Barton, J.K.; Szaldo, D.J.; Rabinowitz, H.W.; Waszczak, J.V.; Lippard, S.J. *J. Am. Chem. Soc.* 101, 1434 (1979).

36. Woollins, J.D.; Kelly, P.F. *Coordination Chem. Rev.* 65, 115 (1985).

37. Matsumoto, K.; Fuwa, K. *J. Am. Chem. Soc.* 104, 897 (1982).

38. Matsumoto, K.; Takahashi, H.; Fuwa, K. *Inorg. Chem.* 22, 4086 (1983).

39. Matsumoto, K; Takahashi, H.; Fuwa, K. *J. Am. Chem. Soc.* 106, 2049 (1984).

40. Trotscher, G.; Micklitz, W.; Schloohorn, H.; Thewalt, U.; Lippert, B. *Inorg. Chem.* 29, 2541 (1990).

41. Mitewa, M.; Gencheva, G. Research on Chemical Intermediates 18, 115 (1992).

42. Sakai,K.; Matsumoto, K. *J. Am. Chem. Soc.* 111, 3074 (1989).

43. Sakai, K.; Matsumoto, K.; Nishio, K. *Chem. Lett.* 0, 1081 (1991).

44. Williams, J.M., et al. in Inorganic Syntheses, Vol. 19 Shriver, D.F. Ed. (John Wiley and Sons, New York, 1979) pp. 1-13.

45. Miller, J.S. in Inorganic Syntheses, Vol. 19 Shriver, D.F. Ed. (John Wiley and Sons, New York, 1979) pp. 13-18, and references therein.

46. Williams, J.M., et al. in Inorganic Syntheses, Vol. 20, Busch, D. H., Ed. (John Wiley and Sons, New York, 1980), pp. 20-31.

47. Dodel, P.; Krogmann, K. *Chem. Ber.* 99, 3402 (1966).

48. Dodel, P.; Krogmann, K. *Chem. Ber. 99*, 3408 (1966).

49. Underhill, A.E.; Watkins, D.M.; Williams, J.M.; Carneiro, K. in Extended Linear Chain Compounds, J.S. Miller, Ed. (Plenum Press, New York, 1982) pp. 119-154, and references therein.

50. Williams, J.M.; Schultz, A.J.; Underhill, A.E.; Carneiro, K. in Extended Linear Chain Compounds, J.S. Miller, Ed. (Plenum Press, New YOrk, 1982) pp. 73-115, and references therein.

51. Browser, L.T. *J. Am. Chem. Soc.* 33, 1566 (1911).

52. Mattes, V.R.; Krogmann, K. *Z. anorg. allg. Chem.* 332, 247 (1964).

53. Dunham, S. O.; Larsen, R.D.; Abbott, E.H. *Inorg. Chem.* 30, 4328 (1991).

54. Rimkus, V.G.; Preetz, W.Z. *Z. anorg. allg. Chem.* 0,73 (1983).

55. Grabowski, A.; Preetz, W.Z. *Z. anorg. allg. Chem.* 0, 101 (1987).

56. Werner, A. *Z. Anorg. Chem.* 12, 51 (1896).

57. Pregosin, P.S. *Coord. Chem. Rev.* 44, 247 (1982).

58. Strobel, H.A.; Heineman, W.R. in Chemical Instrumentation: A Systematic Approach 3rd Edition (John Wiley and Sons, New York, 1989) pp. 252-300 and references therein.

59. Dunham, S.O. Doctoral thesis, Montana State University, Bozeman MT (1992).

60. Felthouse, T.R. *Prog. Inorg. Chem.* 29, 73 (1982).

61. Barton, J.K.; Rabinowitz, H.N.; Szalda, D.J.; Lippard, S.J. *J. Am. Chem. Soc.* 99, 2827 (1977).

62. Barton, J.K.; Caravanna, C.; Lippard, S.J. *J. Am. Chem. Soc.* 107, 7269 (1979).

63. Barton, J.K.; Best, S.A.; Lippard, S.J.; Walton, R.A. *J. Am. Chem. Soc.* 100, 3785 (1978).

64. Barton, J.K.; Lippard, S.J. *Ann. N.Y. Acad. Sci.* 313, 686 (1978).

65. Papavassiliou, G.C *J. Phys. Chem.* 10, 489 (1977).

66. Abraham, R.J.; Fisher, J.; Loftus, P. in Introduction To NMR Spectroscopy (John Wiley and Sons, New York, 1988) pp. 120-121.

67. Schollhorn, H.; Eisenmann P.; Thewalt, U.; Lippert, B. *Inorg. Chem.* 25, 3384 (1986).

68. Hamm, R.E.; Kollrack, R.; Welch, G.L.; Perkins, R.H. *J. Am. Chem. Soc.* 83, 340 (1961).

69. Wienkotter, T.; Sabat, M.; Fusch, G.; Lippert, B. *Inorg. Chem.* 34, 1022 (19950).

70. Wilmarth, W.K.; Fanchiang, Y.T.; Byrd, J.E. *Coord. Chem. Reviews* 51, 141 (1983).